國 立 交 通 大 學

機械工程學系

碩士論文

Ge-Ku-Duffing 系統及 Sprott C, E 系統

的渾沌與渾沌同步

Chaos and Chaos Synchronization of Ge-Ku-Duffing

System and Sprott C, E Systems

研 究 生：李泳厚

指導教授：戈正銘　教授

中華民國九十九年六月

Ge-Ku-Duffing 系統及 Sprott C, E 系統的渾沌與渾沌同步

Chaos and Chaos Synchronization of Ge-Ku-Duffing System and Sprott C, E Systems

研究生：李泳厚   Student: Yong-Hou Li

指導教授：戈正銘   Advisor: Zheng-Ming Ge

國 立 交 通 大 學

機 械 工 程 學 系

碩 士 論 文

A Thesis
Submitted to Department of Mechanical Engineering
College of Engineering
National Chiao Tung University
In Partial Fulfillment of the Requirement
For the Degree of master of science
In
Mechanical Engineering
June 2010
Hsinchu, Taiwan, Republic of China

中 華 民 國 九 十 九 年 六 月

Ge-Ku-Duffing 系統及 Sprott C, E 系統的渾沌與渾沌同步

學生：李泳厚　　　　　　　　　　　　　　　指導教授：戈正銘

國 立 交 通 大 學

機 械 工 程 學 系

摘要

　　本篇論文以相圖、龐卡萊映射圖、李亞普洛夫指數以及分歧圖等數值方法研究新 Ge-Ku-Duffing 系統的渾沌現象。對此系統應用部分區域穩定性理論和實用漸進穩定理論來達成廣義同步；應用主動控制獲得雙重及多重渾沌交織同步。更進一步使用新模糊模型來研究 Sprott C, E 系統的模糊模型和渾沌同步。此外，將探討新模糊邏輯常數控制器應用在投影同步及含有不確定度的渾沌系統。在以上研究中，皆可由相圖和時間歷程圖得到驗證。
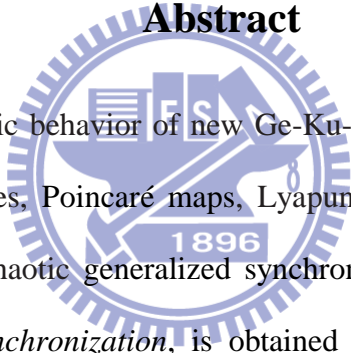
Chaos and Chaos Synchronization of Ge-Ku-Duffing System

and Sprott C, E Systems

Student：Yong-Hou Li　　　　　　　　　　**Advisor：Zheng-Ming Ge**

Department of Mechanical Engineering

National Chiao Tung University

Abstract

In this thesis, the chaotic behavior of new Ge-Ku-Duffing system is studied by phase portraits, time histories, Poincaré maps, Lyapunov exponent and bifurcation diagrams. A new kind of chaotic generalized synchronization, *different translation pragmatical generalized synchronization,* is obtained by pragmatical asymptotical stability theorem and partial region stability theory. New type for chaotic synchronization, *double and multiple symplectic synchronization*, are obtained by active control. A new method, using new fuzzy model, is studied for fuzzy modeling and synchronization of Sprott C, E systems. Moreover, the new fuzzy logic constant controller is studied for projective synchronization and chaotic system with uncertainty. Numerical analyses, such as phase portraits and time histories can be provided to verify the effectiveness of all above studies.

誌　　謝

　　本篇論文得以順利完成，首先要感謝指導教授　戈正銘教授這兩年的耐心指導與教誨。老師在專業領域上的成就以及對學生的有教無類與因材施教，都令學生印象深刻且受益匪淺。在這兩年的相處，老師其達觀的待人處事態度與文學、史學、哲學的涵養，這都開拓了學生不一樣的視野。

　　在交大兩年的研究生活中，我要感謝博士班的張晉銘、李仕宇學長，碩士班的陳聰文、徐瑜韓、陳志銘、張育銘學長，在我研究出現困難時給予我寶貴的指導及意見，同時也要感謝我的同學尚恩、振賓及翔平，除了在學業上的相互討論及幫忙外，在閒暇之餘也一起運動及玩樂，讓兩年的研究生活充滿歡樂與回憶。此外還要謝謝一些默默支持我的好朋友們，無法一一列名，在此一併誌謝。

　　最後要特別感謝我的父親及母親對我的養育及付出，讓我得以一路順利求學，可以不必擔心課業以外的事物，感謝弟弟響芳每當我要返家時，不辭辛勞的到車站接我，另外要謝謝女友莉崴這兩年的陪伴，讓我度過一個愉快的研究生生涯。最後，僅以此論文獻給你們。

CONTENTS

LIST OF FIGURES

Chapter 1

Introduction

Synchronization of chaotic systems has become an important topic since the pioneering work of Pecora and Carroll in 1990 [1]. Furthermore, chaos synchronization has been applied in biological systems [2,3], secure communication [4,5], and many other disciplines. Many methods of synchronization have been proposed, such as linear and nonlinear feedback control[6-16], complete synchronization[17],phase synchronization[18], lag synchronization[19], active control[20-21], generalized synchronization[22-27] and fuzzy control[28-35] and are investigated extensively in the past years.

In this thesis, a new generalized different translation synchronization strategy by partial region stability theory by which the Lyapunov function of error states becomes a simple linear homogeneous function is proposed. The controllers are more simple since they are in lower degree than that of traditional controllers. By pragmatical asymptotical stability theorem, an adaptive control law is derived so that it can be proved strictly that the common null solution of error dynamics and of parameter dynamics is actually asymptotically stable.

Traditional generalized synchronization and symplectic synchronization are special cases of the double symplectic synchronization. Since the symplectic functions are presented on both the right hand side and the left hand side of the equality, it is called "double symplectic synchronization". When the double symplectic functions is extended to a more general form, $\mathbf{G}(\mathbf{x},\mathbf{y},\mathbf{z},...,\mathbf{w},t) = \mathbf{F}(\mathbf{x},\mathbf{y},\mathbf{z},...,\mathbf{w},t)$, it is called "multiple symplectic synchronization". $\mathbf{G}(\mathbf{x},\mathbf{y},\mathbf{z},...,\mathbf{w},t)$ and $\mathbf{F}(\mathbf{x},\mathbf{y},\mathbf{z},...,\mathbf{w},t)$ are given vector functions of $\mathbf{x},\mathbf{y},\mathbf{z},...,\mathbf{w}$ and time. Due to the complexity of the form of the multiple

symplectic synchronization, it may be applied to increase the security of secret communication.

In recent years, fuzzy logic proposed by L. A. Zadeh [36] has received much attention as a powerful tool for the nonlinear control. Among various kinds of fuzzy methods, Takagi-Sugeno fuzzy (T-S fuzzy) system is widely accepted as a useful tool for design and analysis of fuzzy control system [37-42].

In traditional Takagi-Sugeno fuzzy (T-S fuzzy) model, we focus on the whole system. The number of the linear subsystem is decided on how many nonlinear terms should we linearize in original system. As a result, there will be 2^N linear subsystems (according to 2^N fuzzy rules) and $m \times 2^N$ equations in the T-S fuzzy system, where N is the number of minimum nonlinear terms and m is the order of the system. If N is large, the number of linear subsystems in T-S fuzzy system is huge. It becomes more inefficient and complicated. Via the new fuzzy model, a complicated nonlinear system is linearized to a simple form – linear coupling of only two linear subsystems and the numbers of fuzzy rules can be reduced from 2^N to $2 \times N$ (where N is the number of nonlinear terms). The fuzzy equations become much simpler.

In this thesis, a simplest controller, the fuzzy logic constant controller (FLCC) ,which are derived via fuzzy logic design and Lyapunov direct method, are presented for projective synchronization of non-autonomous chaotic systems with deterministic and stochastic uncertainties. Controllers in traditional method by Lyapunov direct method are always nonlinear and complicated. Unlike traditional method, the simplest controllers are proposed via fuzzy logic design and Lyapunov direct method. We propose a new idea to design constant numbers as controllers, while the constant numbers are decided by the upper and lower bounds of the error derivatives. The strength of controllers in our new approach can be adjusted according to the error derivatives. This powerful tool is used for projective synchronization of

2

chaotic systems with uncertainty and stochastic disturbance to show the robustness and effectiveness of FLCC.

This thesis is organized as follows. Chapter 2 gives the dynamic equations of new Ge-Ku-Duffing system and its chaotic behaviors are studied. In Chapter 3, a new generalized different translation synchronization strategy by partial region stability theory and pragmatical asymptotical stability theorem are presented. In Chapter 4 and Chapter 5, double and multiple symplectic synchronization for Ge-Ku-Duffing system are presented. In Chapter 6, a new fuzzy model is used to simulate and synchronize two different chaotic systems are presented. In Chapter 7, a simplest controller, the fuzzy logic constant controller (FLCC) ,which are derived via fuzzy logic design and Lyapunov direct method, are presented for projective synchronization of non-autonomous chaotic systems with deterministic and stochastic uncertainties. In Chapter 8, conclusions are drawn.
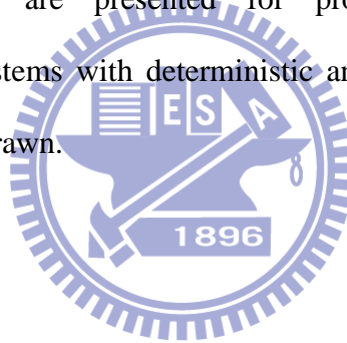
Chapter 2

Chaos of a New Ge-Ku-Duffing System

2.1 Preliminary

In this Chapter, the chaotic behaviors of a new Ge-ku-Duffing system is studied numerically by phase portraits, time histories, Poincaré maps, Lyapunov exponents, and bifurcation diagrams.

2.2 Description of New Ge-Ke-Duffing System

Ge and Ku[43] gave a chaotic system formed by simple pendulum with its pivot rotating about an axis as Fig 2.1. This chaotic system is

$$\dot{x}_1 = x_2,$$
$$\dot{x}_2 = -ax_2 - \sin x_1 \left[b_1 \left(c_1 + \cos x_1 \right) + d \sin \omega t \right], \tag{2.1}$$

where a, b_1, c_1, d are parameters. Combining the Ge-Ku system with Duffing equation

$$\dot{x}_3 = x_4,$$
$$\dot{x}_4 = -x_3 - x_3^3 - fx_4 + g \cos \Omega t, \tag{2.2}$$

after simplification $\sin x_1 = x_1, \cos x_1 = 1 - \dfrac{x_1^2}{2},$ and substitution $\sin \omega t = x_3, \cos \Omega t = x_1$ and addition of coupling terms, we get the Ge-Ku-Duffing system

$$\dot{x}_1 = x_2,$$
$$\dot{x}_2 = -ax_2 - x_1 \left[b \left(c - x_1^2 \right) + dx_3 \right], \tag{2.3}$$
$$\dot{x}_3 = -x_3 - x_3^3 - fx_2 + gx_1,$$

where a, b, c, d, f, g are parameters.

2.3 Computational Analysis of a New Ge-Ku-Duffing System

For numerical analysis of computation, this system exhibits chaos when the parameters of system are $a = 0.1, b = 11, c = 40, d = 54, f = 6, g = 30$ and the initial

states of system are $x_1(0) = 2, x_2(0) = 2.4, x_3(0) = 5$. The bifurcation diagram by changing damping parameter f is shown in Fig. 2.2. Its corresponding Lyapunov exponents are shown in Fig. 2.3. The phase portraits, time histories, and Poincaré maps of the systems are showed in Fig. 2.4~Fig. 2.8.When $f=4.4$, period 1 phenomena are shown in Fig. 2.4. When $f=5$, period 2 phenomena are shown in Fig. 2.5. When $f=5.3$, period 4 phenomena are shown in Fig. 2.6. When $f=5.33$, period 8 phenomena are shown in Fig. 2.7.When $f=6$, the chaotic behaviors are given in Fig. 2.8.
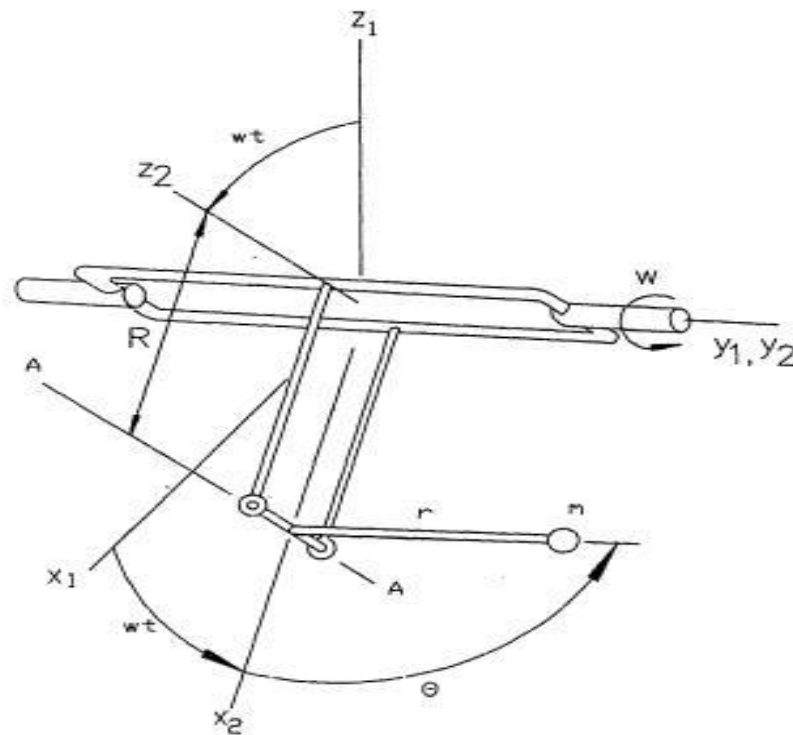
Fig 2.1. The pendulum on rotating arm
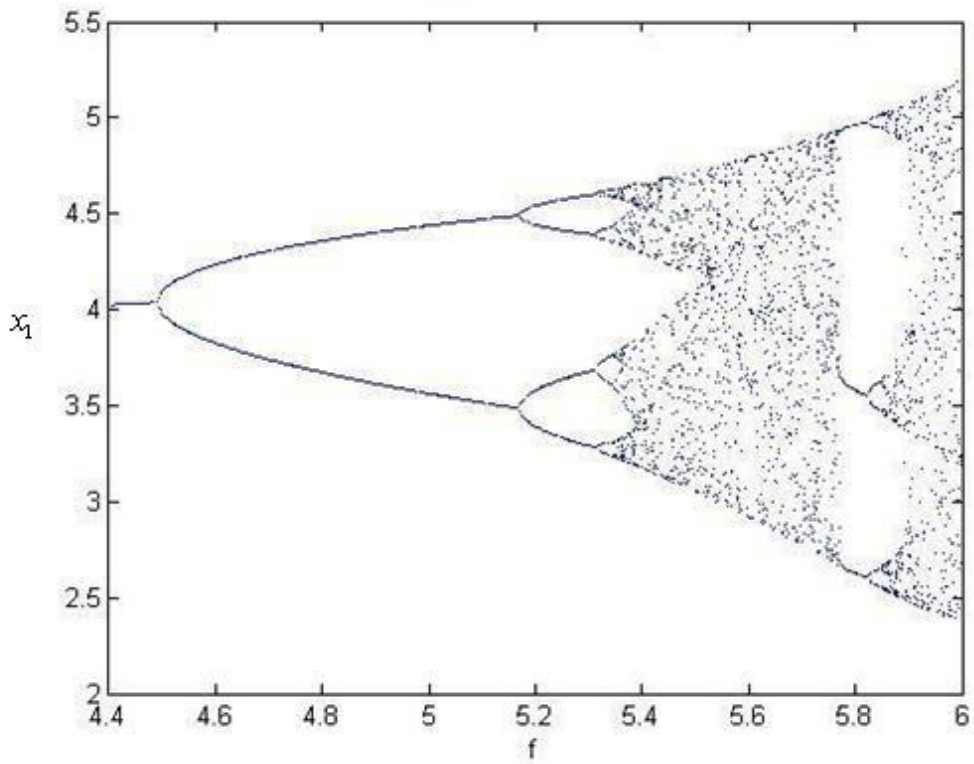
Fig. 2.2 The bifurcation diagram for new Ge-Ku-Duffing system.
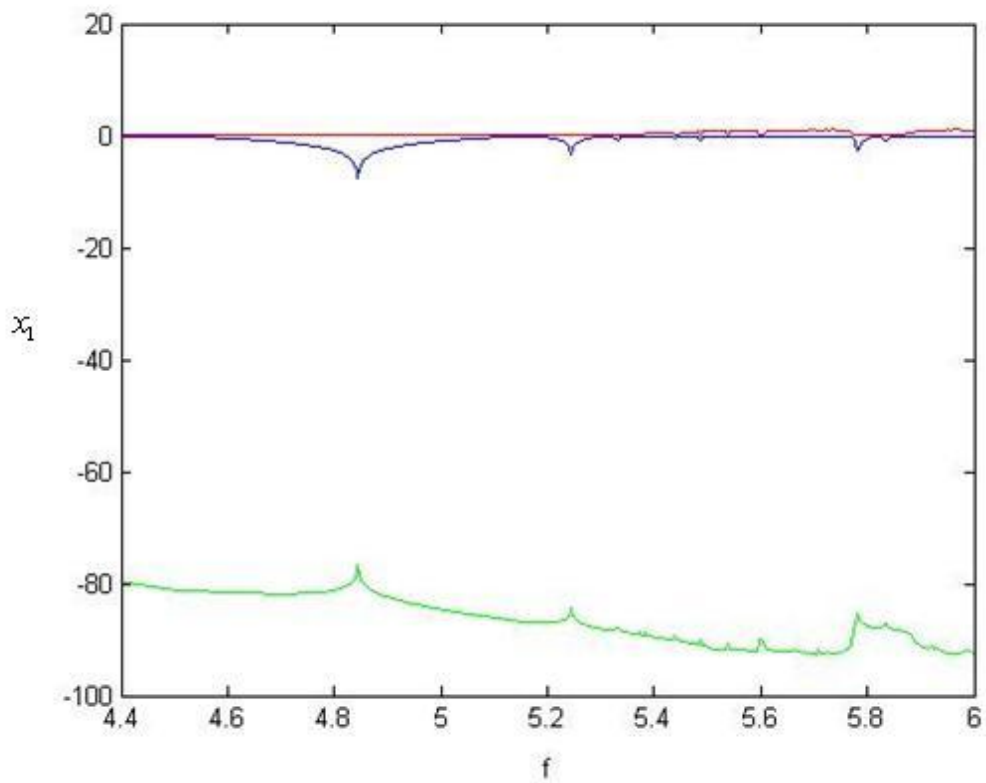
Fig. 2.3 The Lyapunov exponents for new Ge-Ku-Duffing system
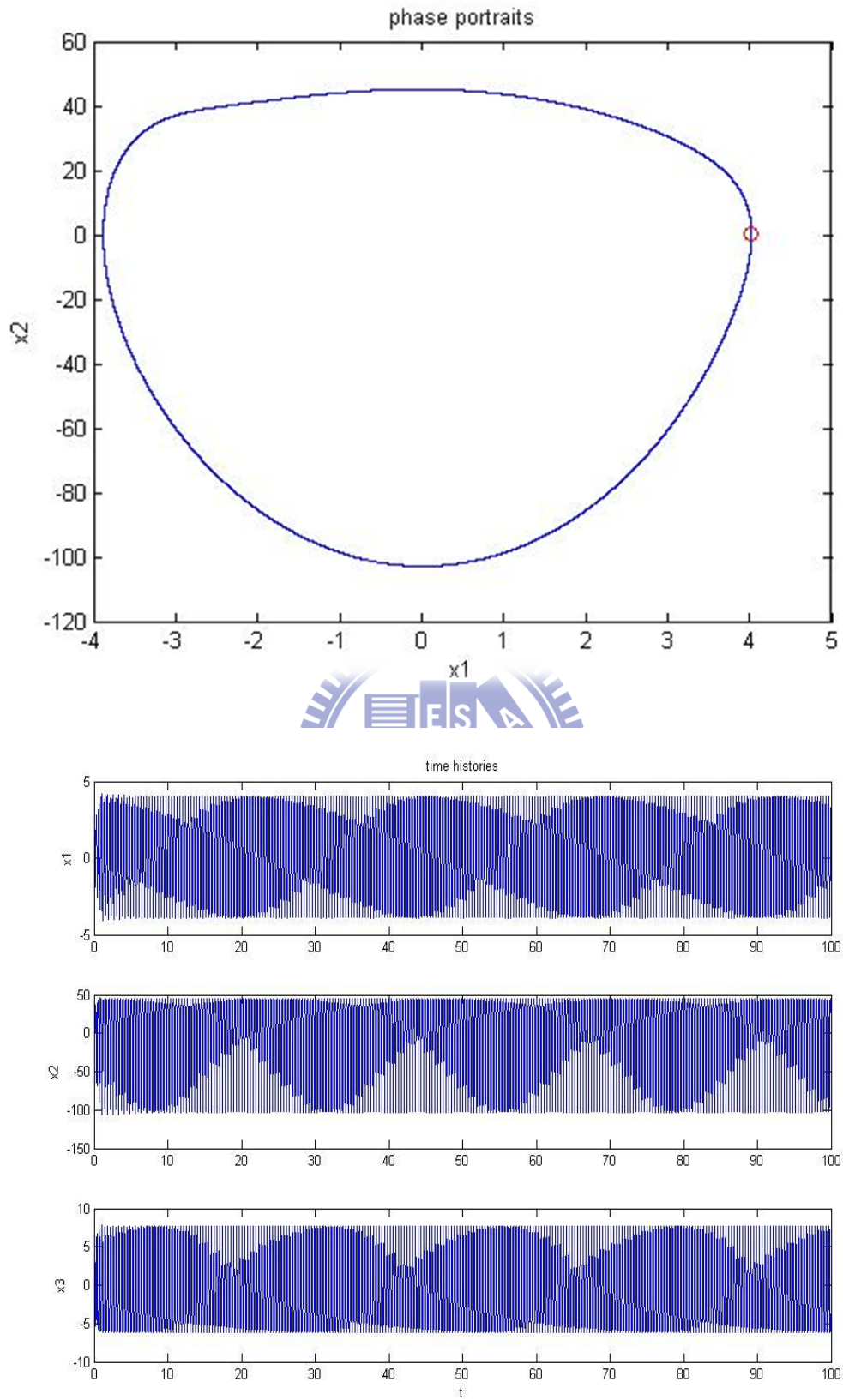
Fig. 2.4 Phase portrait, Poincaré maps, and time histories for new Ge-Ku-Duffing system with $f = 4.4$ (period 1).
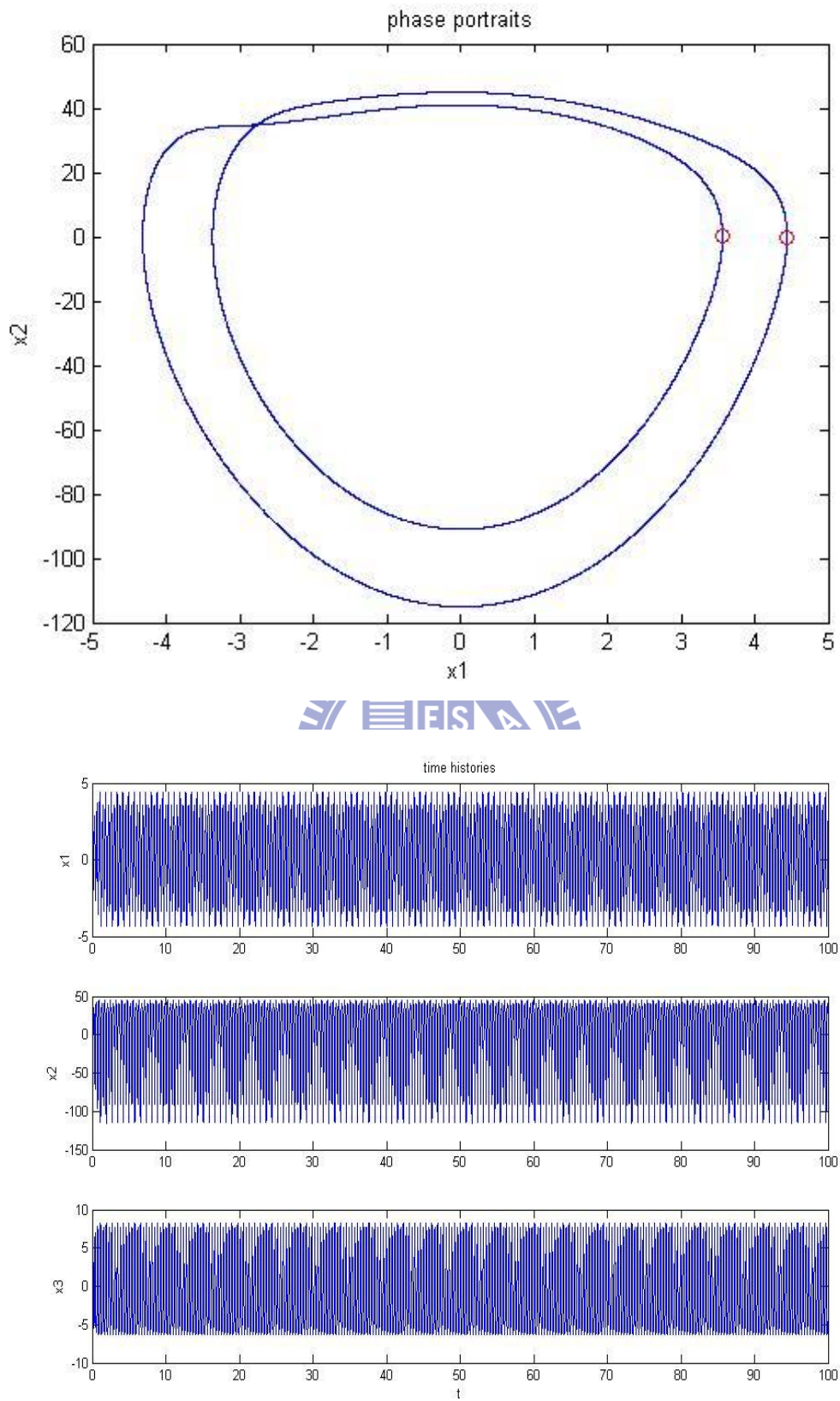
Fig. 2.5 Phase portrait, Poincaré maps, and time histories for new Ge-Ku-Duffing system with $f = 5$ (period 2).
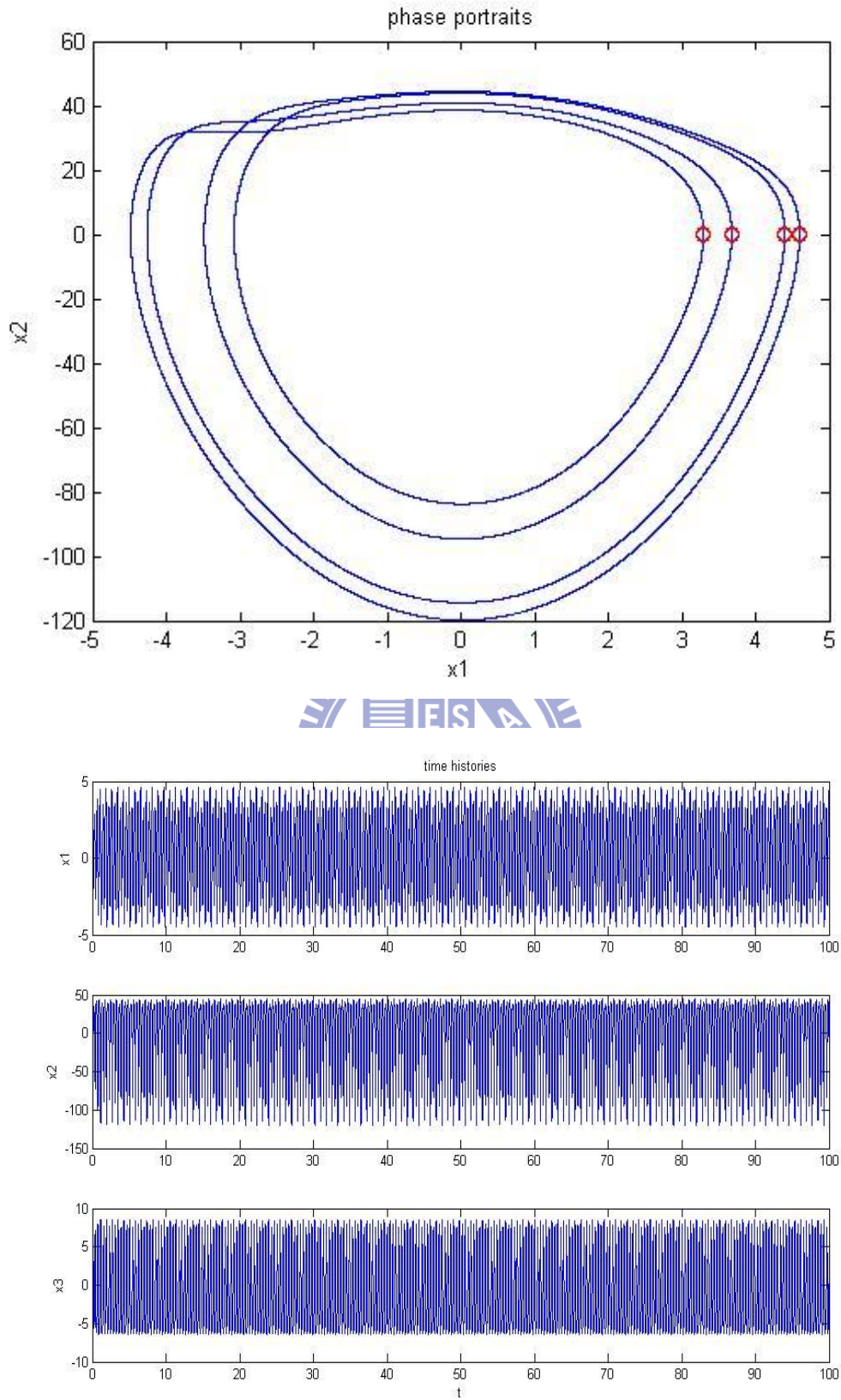
Fig. 2.6 Phase portrait, Poincaré maps, and time histories for new Ge-Ku-Duffing system with $f = 5.3$ (period 4).
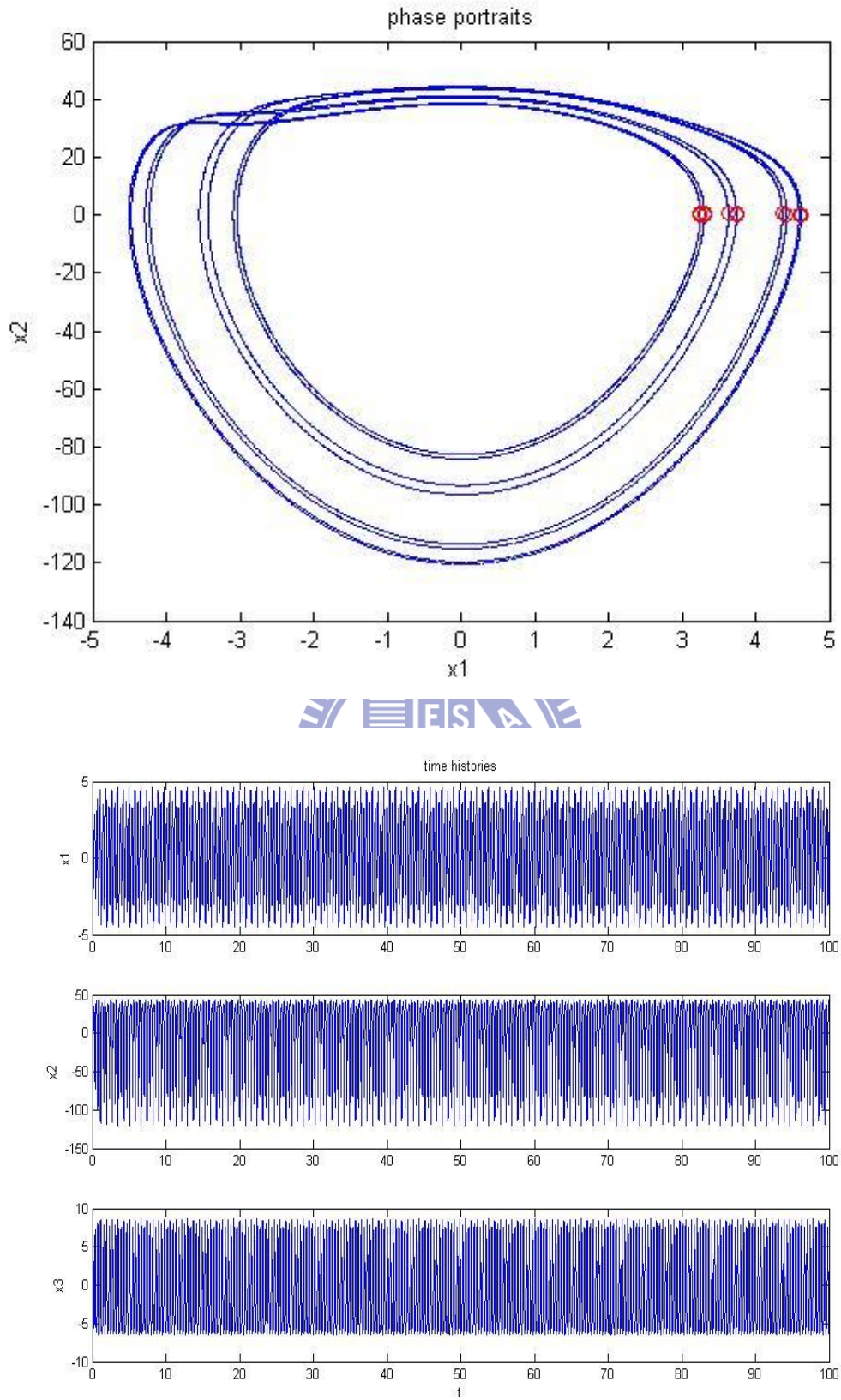
Fig. 2.7 Phase portrait, Poincaré maps, and time histories for new Ge-Ku-Duffing system with *f =5.33* (period 8).
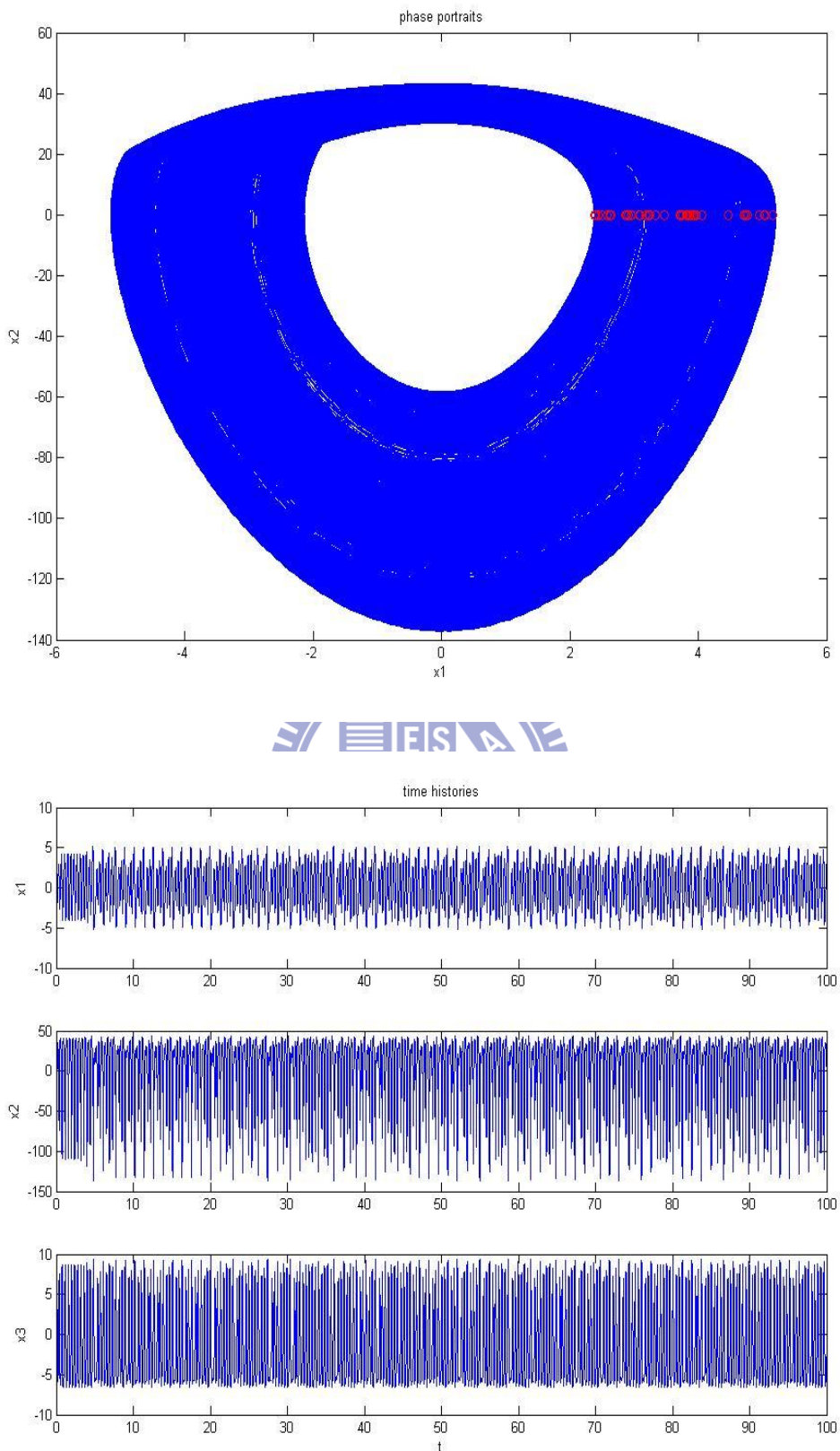
Fig. 2.8 Phase portrait, Poincaré maps, and time histories for new Ge-Ku-Duffing system with $f = 6$ (chaos).

Chapter 3

Using Partial Region Stability Theory for Different

Translation Pragmatical Generalized Synchronization

3.1 Preliminary

In this Chapter, a new generalized different translation synchronization strategy by partial region stability theory is proposed. By using partial regional stability theory, the Lyapunov function becomes a simple linear homogeneous function of error states and the controllers are more simple since they are in lower degree than that of traditional controllers while the tranditional Lyapunov function is a quadratic form of error states.

3.2 The Scheme of Different Translation Pragmatical Generalized Synchronization by Partial Region Theory

There are two identical nonlinear dynamical systems, and the master system synchronizes the slave system. The master system is given by

$$\dot{x} = Ax + f(x, B) \tag{3.1}$$

The master system after the origin of x-coordinate system is translated to $(k_1, k_1, ..., k_1)$ is

$$\dot{x}' = Ax' + f(x', B) \tag{3.1'}$$

where $x' = [x'_1, x'_2, \cdots x'_n]^T = x - k_1 = [x_1 - k_1, x_2 - k_1, ..., x_n - k_1]^T \in R^n$ denotes a state vector, where $k_1 = [k_1, k_1, ..., k_1]$ is a constant vector with positive component k_1 as shown in Fig 3.1. A is an $n \times n$ uncertain constant coefficient matrix, f is a nonlinear vector function, and B is a vector of uncertain constant coefficients in f. The slave system is given by

$$\dot{y} = \hat{A}y + f(y, \hat{B}) + u(t) \tag{3.2}$$

The slave system after the origin of y-coordinate system is translated to $(k_2, k_2, ..., k_2)$ is

$$\dot{y}' = \hat{A}y' + f(y', \hat{B}) + u(t) \tag{3.2'}$$

where $y' = [y'_1, y'_2, \cdots y'_n]^T = y - k_2 = [y_1 - k_2, y_2 - k_2, ..., y_n - k_2]^T \in R^n$ denotes a state vector, where k_2 is a constant vector with constant component k_2 as shown in Fig 3.2. $\hat{A}$ is an $n \times n$ estimated coefficient matrix, $\hat{B}$ is a vector of estimated coefficients in f, and $u(t) = [u_1(t), u_2(t), ...u_n(t)]^T \in R^n$ is a control input vector.

Our goal is to design a controller $u(t)$ so that the state vector of the translated slave system (3.2') asymptotically approaches the state vector of the translated master system (3.1') plus a given nonchaotic or chaotic vector function $F(t) = [F_1(t), F_2(t), \cdots, F_n(t)]^T$:

$$y' = G(x') = x' + F(t). \tag{3.3}$$

The synchronization can be accomplished when $t \to \infty$, the limit of the error vector $e(t) = [e_1, e_2, \cdots e_n]^T$ approaches zero:

$$\lim_{t \to \infty} e = 0 \tag{3.4}$$

where

$$e = x' - y' + F(t) \tag{3.5}$$

From Eq. (3.5) we have

$$\dot{e} = \dot{x}' - \dot{y}' + \dot{F}(t) \tag{3.6}$$

$$\dot{e} = Ax' - \hat{A}y' + f(x', B) - f(y', \hat{B}) + \dot{F}(t) - u(t). \tag{3.7}$$

where k_1 and k_2 are chosen to guarantee that the error dynamics always occurs

13

in first quadrant of e coordinate system.

A Lyapnuov function $V(e, \tilde{A}_c, \tilde{B}_c)$ is chosen as a positive definite function in first quadrant of e coordinate system by stability theory in partial region as shown in Appendix A:

$$V(e, \tilde{A}_c, \tilde{B}_c) = e + \tilde{A}_c + \tilde{B}_c \qquad (3.8)$$

where $\tilde{A}_c = A - \hat{A}$, $\tilde{B}_c = B - \hat{B}$, $\tilde{A}_c$ and $\tilde{B}_c$ are two column matrices whose elements are all the elements of matrix $\tilde{A}_c$ and of column matrix $\tilde{B}_c$, respectively. Its derivative along any solution of the differential equation system consisting of Eq. (3.7) and updated parameter differential equations for $\tilde{A}_c$ and $\tilde{B}_c$ is

$$\dot{V}(e, \tilde{A}_c, \tilde{B}_c) = Ax' - \hat{A}y' + f(x', B) - f(y', \hat{B}) + \dot{F}(t) - u(t) + \dot{\tilde{A}}_c + \dot{\tilde{B}}_c$$

(3.9)

where $u(t)$, $\dot{\tilde{A}}_c$, and $\dot{\tilde{B}}_c$ are chosen so that $\dot{V} = Ce$, C is a diagonal negative definite matrix, and $\dot{V}$ is a negative semi-definite function of e and parameter differences $\tilde{A}_c$ and $\tilde{B}_c$.

In this Chapter, a new Ge-ku-Duffing system is used as an example. By pragmatical asymptotically stability theorem in Appendix B, the Lyapunov function used is a simple linear homogeneous function of states and the controllers are simpler because they in lower order than the that of traditional controllers. In many papers[44-48], traditional Lyapunov stability theorem and Babalat lemma are used to prove the error vector approaches zero, as time approaches infinity. But the question, why the estimated parameters also approach to the uncertain parameters, remains no answer. By pragmatical asymptotical stability theorem, the question can be answered strictly.

3.3 Different Translation Pragmatical Synchronization of New Ge-Ku-Duffing Chaotic System

Case 1.

The following chaotic system are two translated Ge-Ku-Duffings system of which the origins are translated to $(x_1, x_2, x_3) = (250, 250, 250)$, $(y_1, y_2, y_3) = (50, 50, 50)$ to guarantee the error dynamics always happens in the first quadrant of e coordinate system. The translated master system and slave system are:

$$\begin{cases} \dfrac{dx_1}{dt} = (x_2 - 250) \\[2mm] \dfrac{dx_2}{dt} = -a(x_2 - 250) - (x_1 - 250)[b(c - (x_1 - 250)^2) + d(x_3 - 250)] \\[2mm] \dfrac{dx_3}{dt} = -(x_3 - 250) - (x_3 - 250)^3 - f(x_2 - 250) + g(x_1 - 250) \end{cases} \qquad (3.10)$$

$$\begin{cases} \dfrac{dy_1}{dt} = (y_2 - 50) + u_1 \\[2mm] \dfrac{dy_2}{dt} = -\hat{a}(y_2 - 50) - (y_1 - 50)[\hat{b}(\hat{c} - (y_1 - 50)^2) + \hat{d}(y_3 - 50)] + u_2 \\[2mm] \dfrac{dy_3}{dt} = -(y_3 - 50) - (y_3 - 50)^3 - \hat{f}(y_2 - 50) + \hat{g}(y_1 - 50) + u_3 \end{cases} \qquad (3.11)$$

Let initial states be $x_1(0) = 2, x_2(0) = 2.4, x_3(0) = 5$, $y_1(0) = 2, y_2(0) = 2.4, y_3(0) = 5$ and system parameters $a = 0.1, b = 11, c = 40,\ d = 54, f = 6, g = 30$. The generalized synchronization error vector is

$$e = x - y + F(t) = x - y + \cos(t) \qquad (3.12)$$

We find that the error dynamic without controllers always exists in first quadrant as shown in Fig. 3.3.

Our goal is $\lim\limits_{t \to \infty} e_i = 0$. We obtain the error dynamics :

$$\begin{cases} \dot{e}_1 = (x_2 - 250) - (y_2 - 50) - \sin(t) - u_1 \\[1mm] \dot{e}_2 = -a(x_2 - 250) - (x_1 - 250)[b(c - (x_1 - 250)^2) + d(x_3 - 250)] \\[1mm] \qquad + \hat{a}(y_2 - 50) + (y_1 - 50)[\hat{b}(\hat{c} - (y_1 - 50)^2) + \hat{d}(y_3 - 50)] - \sin(t) - u_2 \\[1mm] \dot{e}_3 = -(x_3 - 250) - (x_3 - 250)^3 - f(x_2 - 250) + g(x_1 - 250) + (y_3 - 50) \\[1mm] \qquad + (y_3 - 50)^3 + \hat{f}(y_2 - 50) - \hat{g}(y_1 - 50) - \sin(t) - u_3 \end{cases} \qquad (3.13)$$

where $\tilde{a}=a-\hat{a}$, $\tilde{b}=b-\hat{b}$, $\tilde{c}=c-\hat{c}$, $\tilde{d}=d-\hat{d}$, $\tilde{f}=f-\hat{f}$ and $\tilde{g}=g-\hat{g}$ are estimates of uncertain parameters a, b, c, d, f and g respectively.

Using different translation pragmatical synchronization by partial region stability theory, we can choose a Lyapunov function in the form of a positive definite function in first quadrant:

$$V = e_1 + e_2 + e_3 + \tilde{a} + \tilde{b} + \tilde{c} + \tilde{d} + \tilde{f} + \tilde{g} \tag{3.14}$$

The time derivative of V is

$$
\begin{aligned}
\dot{V} &= \dot{e}_1 + \dot{e}_2 + \dot{e}_3 + \dot{\tilde{a}} + \dot{\tilde{b}} + \dot{\tilde{c}} + \dot{\tilde{d}} + \dot{\tilde{f}} + \dot{\tilde{g}} \\
&= (x_2 - 250) - (y_2 - 50) - \sin(t) - u_1 \\
&\quad - a(x_2 - 250) - (x_1 - 250)[b(c - (x_1 - 250)^2) + d(x_3 - 250)] \\
&\quad + \hat{a}(y_2 - 50) + (y_1 - 50)[\hat{b}(\hat{c} - (y_1 - 50)^2) + \hat{d}(y_3 - 50)] - \sin(t) - u_2 \\
&\quad - (x_3 - 250) - (x_3 - 250)^3 - f(x_2 - 250) + g(x_1 - 250) + (y_3 - 50) \\
&\quad + (y_3 - 50)^3 + \hat{f}(y_2 - 50) - \hat{g}(y_1 - 50) - \sin(t) - u_3 \\
&\quad + \dot{\tilde{a}} + \dot{\tilde{b}} + \dot{\tilde{c}} + \dot{\tilde{d}} + \dot{\tilde{f}} + \dot{\tilde{g}}
\end{aligned}
\tag{3.15}
$$

Choose

$$
\begin{cases}
u_1 = (x_2 - 250) - (y_2 - 50) - \sin(t) - \tilde{a}e_1 - \tilde{b}e_1 + e_1 \\
u_2 = -a(x_2 - 250) - (x_1 - 250)[b(c - (x_1 - 250)^2) + d(x_3 - 250)] + \hat{a}(y_2 - 50) \\
\quad + (y_1 - 50)[\hat{b}(\hat{c} - (y_1 - 50)^2) + \hat{d}(y_3 - 50)] - \sin(t) - \tilde{c}e_2 - \tilde{d}e_2 + e_2 \\
u_3 = -(x_3 - 250) - (x_3 - 250)^3 - f(x_2 - 250) + g(x_1 - 250) + (y_3 - 50) \\
\quad + (y_3 - 50)^3 + \hat{f}(y_2 - 50) - \hat{g}(y_1 - 50) - \sin(t) - \tilde{f}e_3 - \tilde{g}e_3 + e_3
\end{cases}
\tag{3.16}
$$

$$
\begin{cases}
\dot{\tilde{a}} = -\tilde{a}e_1 \\
\dot{\tilde{b}} = -\tilde{b}e_1 \\
\dot{\tilde{c}} = -\tilde{c}e_2 \\
\dot{\tilde{d}} = -\tilde{d}e_2 \\
\dot{\tilde{f}} = -\tilde{f}e_3 \\
\dot{\tilde{g}} = -\tilde{g}e_3
\end{cases}
\tag{3.17}
$$

We obtain

$$\dot{V} = -e_1 - e_2 - e_3 \qquad \leq 0$$

(3.18)

which is negative semi-definite function of $e_1, e_2, e_3, \tilde{a}, \tilde{b}, \tilde{c}, \tilde{d}, \tilde{f}$ and $\tilde{g}$. The Lyapunov

asymptotical stability theorem is not satisfied. We cannot obtain that common origin of error dynamics (3.13) and parameter dynamics (3.17) is asymptotically stable. By pragmatical asymptotically stability theorem , D is a 9-manifold, $n = 9$ and the number of error state variables $p = 3$. When $e_1 = e_2 = e_3 = 0$ and $\tilde{a}, \tilde{b}, \tilde{c}, \tilde{d}, \tilde{f}, \tilde{g}$ take arbitrary values, $\dot{V} = 0$, so X is of 6 dimensions, $m = n - p = 9 - 3 = 6$, $m + 1 < n$ is satisfied. According to the pragmatical asymptotically stability theorem, error vector e approaches zero and the estimated parameters also approach the uncertain parameters. The equilibrium point is pragmatically asymptotically stable. Under the assumption of equal probability, it is actually asymptotically stable. The simulation results are shown in Figs. 3.4~3.6.

Case 2.

The following chaotic system are two translated Ge-Ku-Duffings system of which the origin is translated to $(x_1, x_2, x_3) = (250, 250, 250)$, $(y_1, y_2, y_3) = (50, 50, 50)$ to guarantee the error dynamics always happens in the first quadrant of e coordinate system. The translated master system and slave system are:

$$
\begin{cases}
\dfrac{dx_1}{dt} = (x_2 - 250) \\[2mm]
\dfrac{dx_2}{dt} = -a(x_2 - 250) - (x_1 - 250)[b(c - (x_1 - 250)^2) + d(x_3 - 250)] \\[2mm]
\dfrac{dx_3}{dt} = -(x_3 - 250) - (x_3 - 250)^3 - f(x_2 - 250) + g(x_1 - 250)
\end{cases} \tag{3.19}
$$

$$
\begin{cases}
\dfrac{dy_1}{dt} = (y_2 - 50) + u_1 \\[2mm]
\dfrac{dy_2}{dt} = -\hat{a}(y_2 - 50) - (y_1 - 50)[\hat{b}(\hat{c} - (y_1 - 50)^2) + \hat{d}(y_3 - 50)] + u_2 \\[2mm]
\dfrac{dy_3}{dt} = -(y_3 - 50) - (y_3 - 50)^3 - \hat{f}(y_2 - 50) + \hat{g}(y_1 - 50) + u_3
\end{cases} \tag{3.20}
$$

Let initial states be $x_1(0) = 2, x_2(0) = 2.4, x_3(0) = 5$, $y_1(0) = 2, y_2(0) = 2.4, y_3(0) = 5$ and system parameters $a = 0.1, b = 11, c = 40$, $d = 54, f = 6, g = 30$. The generalized synchronization error vector is

$$
e = x - y + F(t) \tag{3.21}
$$

where $F(t) = [\dot{z}_1, \dot{z}_2, \dot{z}_3]^T$ is the state vector of Ge-Ku Mathieu system:

$$
\begin{cases}
\dfrac{dz_1}{dt} = z_2 \\[2mm]
\dfrac{dz_2}{dt} = -kz_2 - z_1\left[m\left(r - z_1^2\right) + sz_2 z_3 \right] \\[2mm]
\dfrac{dz_3}{dt} = -\left(n + hz_1\right)z_3 + lz_2 + pz_1 z_3
\end{cases}
\tag{3.22}
$$

We find that the error dynamic without controllers always exists in first quadrant as shown in Fig. 3.7.

This system exhibits chaos when the parameters of system are $k = -0.6$, $m = 5$, $r = 11$, $s = 0.3, n = 8, h = 10, l = 0.5, p = 0.2$ and the initial states of system are $z_1(0) = 0.01$, $z_2(0) = 0.01$, $z_3(0) = 0.01$, its phase portrait as shown in Fig. 3.8. Our goal is $\lim\limits_{t \to \infty} e_i = 0$. We obtain the error dynamics becomes:

$$
\begin{cases}
\dot{e}_1 = (x_2 - 250) - (y_2 - 50) + z_2 - u_1 \\
\dot{e}_2 = -a(x_2 - 250) - (x_1 - 250)[b(c - (x_1 - 250)^2) + d(x_3 - 250)] \\
\quad + \hat{a}(y_2 - 50) + (y_1 - 50)[\hat{b}(\hat{c} - (y_1 - 50)^2) + \hat{d}(y_3 - 50)] - kz_2 \\
\quad - z_1\left[m\left(r - z_1^2\right) + sz_2 z_3 \right] - u_2 \\
\dot{e}_3 = -(x_3 - 250) - (x_3 - 250)^3 - f(x_2 - 250) + g(x_1 - 250) + (y_3 - 50) \\
\quad + (y_3 - 50)^3 + \hat{f}(y_2 - 50) - \hat{g}(y_1 - 50) - (n + hz_1)z_3 + lz_2 + pz_1 z_3 - u_3
\end{cases}
\tag{3.23}
$$

where $\tilde{a} = a - \hat{a}$, $\tilde{b} = b - \hat{b}$, $\tilde{c} = c - \hat{c}$, $\tilde{d} = d - \hat{d}$, $\tilde{f} = f - \hat{f}$ and $\tilde{g} = g - \hat{g}$ are estimates of uncertain parameters a, b, c, d, f and g respectively.

Using different translation pragmatical synchronization by partial region stability theory, we can choose a Lyapunov function in the form of a positive definite function in first quadrant:

$$
V = e_1 + e_2 + e_3 + \tilde{a} + \tilde{b} + \tilde{c} + \tilde{d} + \tilde{f} + \tilde{g}
\tag{3.24}
$$

The time derivative of V is

$$\dot{V} = \dot{e}_1 + \dot{e}_2 + \dot{e}_3 + \dot{\tilde{a}} + \dot{\tilde{b}} + \dot{\tilde{c}} + \dot{\tilde{d}} + \dot{\tilde{f}} + \dot{\tilde{g}}$$
$$= (x_2 - 250) - (y_2 - 50) + z_2 - u_1$$
$$- a(x_2 - 250) - (x_1 - 250)[b(c - (x_1 - 250)^2) + d(x_3 - 250)]$$
$$+ \hat{a}(y_2 - 50) + (y_1 - 50)[\hat{b}(\hat{c} - (y_1 - 50)^2) + \hat{d}(y_3 - 50)] - kz_2$$
$$- z_1 \left[m(r - z_1^2) + sz_2 z_3 \right] - u_2 \qquad (3.25)$$
$$- (x_3 - 250) - (x_3 - 250)^3 - f(x_2 - 250) + g(x_1 - 250) + (y_3 - 50)$$
$$+ (y_3 - 50)^3 + \hat{f}(y_2 - 50) - \hat{g}(y_1 - 50) - (n + hz_1)z_3 + lz_2 + pz_1 z_3 - u_3$$
$$+ \dot{\tilde{a}} + \dot{\tilde{b}} + \dot{\tilde{c}} + \dot{\tilde{d}} + \dot{\tilde{f}} + \dot{\tilde{g}}$$

Choose

$$\begin{cases} u_1 = (x_2 - 250) - (y_2 - 50) + z_2 - \tilde{a}e_1 - \tilde{b}e_1 + e_1 \\ u_2 = -a(x_2 - 250) - (x_1 - 250)[b(c - (x_1 - 250)^2) + d(x_3 - 250)] \\ \qquad + \hat{a}(y_2 - 50) + (y_1 - 50)[\hat{b}(\hat{c} - (y_1 - 50)^2) + \hat{d}(y_3 - 50)] - kz_2 \\ \qquad - z_1 \left[m(r - z_1^2) + sz_2 z_3 \right] - \tilde{c}e_2 - \tilde{d}e_2 + e_2 \\ u_3 = -(x_3 - 250) - (x_3 - 250)^3 - f(x_2 - 250) + g(x_1 - 250) + (y_3 - 50) \\ \qquad + (y_3 - 50)^3 + \hat{f}(y_2 - 50) - \hat{g}(y_1 - 50) - (n + hz_1)z_3 + lz_2 + pz_1 z_3 \\ \qquad - \tilde{f}e_3 - \tilde{g}e_3 + e_3 \end{cases} \qquad (3.26)$$

$$\begin{cases} \dot{\tilde{a}} = -\tilde{a}e_1 \\ \dot{\tilde{b}} = -\tilde{b}e_1 \\ \dot{\tilde{c}} = -\tilde{c}e_2 \\ \dot{\tilde{d}} = -\tilde{d}e_2 \\ \dot{\tilde{f}} = -\tilde{f}e_3 \\ \dot{\tilde{g}} = -\tilde{g}e_3 \end{cases} \qquad (3.27)$$

We obtain

$$\dot{V} = -e_1 - e_2 - e_3 \qquad \le 0$$

(3.28)

which is negative semi-definite function of $e_1, e_2, e_3, \tilde{a}, \tilde{b}, \tilde{c}, \tilde{d}, \tilde{f}$ and $\tilde{g}$. The Lyapunov asymptotical stability theorem is not satisfied. We cannot obtain that common origin of error dynamics (3.23) and parameter dynamics (3.27) is asymptotically stable. By pragmatical asymptotically stability theorem , D is a 9-manifold, $n = 9$ and the

number of error state variables $p = 3$. When $e_1 = e_2 = e_3 = 0$ and $\tilde{a}, \tilde{b}, \tilde{c}, \tilde{d}, \tilde{f}, \tilde{g}$ take arbitrary values, $\dot{V} = 0$, so X is of 6 dimensions, $m = n - p = 9 - 3 = 6$, $m + 1 < n$ is satisfied. According to the pragmatical asymptotically stability theorem, error vector e approaches zero and the estimated parameters also approach the uncertain parameters. The equilibrium point is pragmatically asymptotically stable. Under the assumption of equal probability, it is actually asymptotically stable. The simulation results are shown in Figs. 3.9~3.11.

Case 3.

The following chaotic system are two translated Ge-Ku-Duffings system of which the origin is translated to $(x_1, x_2, x_3) = (250, 250, 250)$, $(y_1, y_2, y_3) = (50, 50, 50)$ to guarantee the error dynamics always happens in the first quadrant of e coordinate system. The translated master system and slave system are:

$$\begin{cases} \dfrac{dx_1}{dt} = (x_2 - 250) \\ \dfrac{dx_2}{dt} = -a(x_2 - 250) - (x_1 - 250)[b(c - (x_1 - 250)^2) + d(x_3 - 250)] \\ \dfrac{dx_3}{dt} = -(x_3 - 250) - (x_3 - 250)^3 - f(x_2 - 250) + g(x_1 - 250) \end{cases} \tag{3.29}$$

$$\begin{cases} \dfrac{dy_1}{dt} = (y_2 - 50) + u_1 \\ \dfrac{dy_2}{dt} = -\hat{a}(y_2 - 50) - (y_1 - 50)[\hat{b}(\hat{c} - (y_1 - 50)^2) + \hat{d}(y_3 - 50)] + u_2 \\ \dfrac{dy_3}{dt} = -(y_3 - 50) - (y_3 - 50)^3 - \hat{f}(y_2 - 50) + \hat{g}(y_1 - 50) + u_3 \end{cases} \tag{3.30}$$

Let initial states be $x_1(0) = 2, x_2(0) = 2.4, x_3(0) = 5$, $y_1(0) = 2, y_2(0) = 2.4, y_3(0) = 5$ and system parameters $a = 0.1, b = 11, c = 40$, $d = 54, f = 6, g = 30$.

The generalized synchronization error vector is

$$e = x - y + F(t) \tag{3.31}$$

where $F(t) = [\dot{z}_1, \dot{z}_2, \dot{z}_3]^T$ is the state vector of *Rössler* system:

$$\begin{cases} \dfrac{dz_1}{dt} = -(z_2 + z_3) \\[2mm] \dfrac{dz_2}{dt} = z_1 + kz_2 \\[2mm] \dfrac{dz_3}{dt} = m + z_1 z_3 - rz_3 \end{cases} \tag{3.32}$$

We find that the error dynamic without controllers always exists in first quadrant as shown in Fig. 3.12.

This system exhibits chaos when the parameters of system are $k = 0.15$, $m = 0.2$, $r = 10$ and the initial states of system are $z_1(0) = 2$, $z_2(0) = 2.4$, $z_3(0) = 5$, its phase portraits and time histories as shown in Fig. 3.13. Our goal is $\lim\limits_{t \to \infty} e_i = 0$. We obtain the error dynamics :

$$\begin{cases} \dot{e}_1 = (x_2 - 250) - (y_2 - 50) - (z_2 + z_3) - u_1 \\ \dot{e}_2 = -a(x_2 - 250) - (x_1 - 250)[b(c - (x_1 - 250)^2) + d(x_3 - 250)] \\ \qquad + \hat{a}(y_2 - 50) + (y_1 - 50)[\hat{b}(\hat{c} - (y_1 - 50)^2) + \hat{d}(y_3 - 50)] + z_1 \\ \qquad + kz_2 - u_2 \\ \dot{e}_3 = -(x_3 - 250) - (x_3 - 250)^3 - f(x_2 - 250) + g(x_1 - 250) + (y_3 - 50) \\ \qquad + (y_3 - 50)^3 + \hat{f}(y_2 - 50) - \hat{g}(y_1 - 50) + m + z_1 z_3 - rz_3 - u_3 \end{cases} \tag{3.33}$$

where $\tilde{a} = a - \hat{a}$, $\tilde{b} = b - \hat{b}$, $\tilde{c} = c - \hat{c}$, $\tilde{d} = d - \hat{d}$, $\tilde{f} = f - \hat{f}$ and $\tilde{g} = g - \hat{g}$ are estimates of uncertain parameters a, b, c, d, f and g respectively.

Using different translation pragmatical synchronization by partial region stability theory, we can choose a Lyapunov function in the form of a positive definite function in first quadrant:

$$V = e_1 + e_2 + e_3 + \tilde{a} + \tilde{b} + \tilde{c} + \tilde{d} + \tilde{f} + \tilde{g} \tag{3.34}$$

The time derivative of V is

$$\begin{aligned} \dot{V} &= \dot{e}_1 + \dot{e}_2 + \dot{e}_3 + \dot{\tilde{a}} + \dot{\tilde{b}} + \dot{\tilde{c}} + \dot{\tilde{d}} + \dot{\tilde{f}} + \dot{\tilde{g}} \\ &= (x_2 - 250) - (y_2 - 50) - (z_2 + z_3) - u_1 \\ &\quad - a(x_2 - 250) - (x_1 - 250)[b(c - (x_1 - 250)^2) + d(x_3 - 250)] \\ &\quad + \hat{a}(y_2 - 50) + (y_1 - 50)[\hat{b}(\hat{c} - (y_1 - 50)^2) + \hat{d}(y_3 - 50)] + z_1 \\ &\quad + kz_2 - u_2 \\ &\quad - (x_3 - 250) - (x_3 - 250)^3 - f(x_2 - 250) + g(x_1 - 250) + (y_3 - 50) \\ &\quad + (y_3 - 50)^3 + \hat{f}(y_2 - 50) - \hat{g}(y_1 - 50) + m + z_1 z_3 - rz_3 - u_3 \\ &\quad + \dot{\tilde{a}} + \dot{\tilde{b}} + \dot{\tilde{c}} + \dot{\tilde{d}} + \dot{\tilde{f}} + \dot{\tilde{g}} \end{aligned} \tag{3.35}$$

Choose

$$
\begin{cases}
u_1 = (x_2 - 250) - (y_2 - 50) + z_2 - \tilde{a}e_1 - \tilde{b}e_1 + e_1 \\
u_2 = -a(x_2 - 250) - (x_1 - 250)[b(c - (x_1 - 250)^2) + d(x_3 - 250)] \\
\quad + \hat{a}(y_2 - 50) + (y_1 - 50)[\hat{b}(\hat{c} - (y_1 - 50)^2) + \hat{d}(y_3 - 50)] + z_1 \\
\quad + kz_2 - \tilde{c}e_2 - \tilde{d}e_2 + e_2 \\
u_3 = -(x_3 - 250) - (x_3 - 250)^3 - f(x_2 - 250) + g(x_1 - 250) + (y_3 - 50) \\
\quad + (y_3 - 50)^3 + \hat{f}(y_2 - 50) - \hat{g}(y_1 - 50) + m + z_1z_3 - rz_3 - \tilde{f}e_3 - \tilde{g}e_3 + e_3
\end{cases}
\tag{3.36}
$$

$$
\begin{cases}
\dot{\tilde{a}} = -\tilde{a}e_1 \\
\dot{\tilde{b}} = -\tilde{b}e_1 \\
\dot{\tilde{c}} = -\tilde{c}e_2 \\
\dot{\tilde{d}} = -\tilde{d}e_2 \\
\dot{\tilde{f}} = -\tilde{f}e_3 \\
\dot{\tilde{g}} = -\tilde{g}e_3
\end{cases}
\tag{3.37}
$$

We obtain

$$
\dot{V} = -e_1 - e_2 - e_3 \qquad \le 0
$$

(3.38)
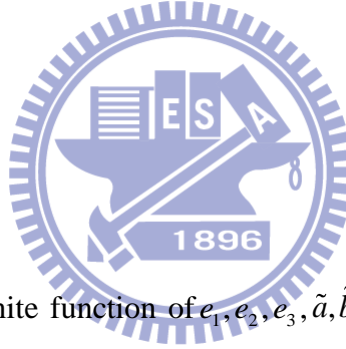
which is negative semi-definite function of $e_1, e_2, e_3, \tilde{a}, \tilde{b}, \tilde{c}, \tilde{d}, \tilde{f}$ and $\tilde{g}$. The Lyapunov

asymptotical stability theorem is not satisfied. We cannot obtain that common origin

of error dynamics (3.33) and parameter dynamics (3.37) is asymptotically stable. By

pragmatical asymptotically stability theorem , D is a 9-manifold, $n = 9$ and the

number of error state variables $p = 3$. When $e_1 = e_2 = e_3 = 0$ and $\tilde{a}, \tilde{b}, \tilde{c}, \tilde{d}, \tilde{f}, \tilde{g}$ take

arbitrary values, $\dot{V} = 0$, so X is of 6 dimensions, $m = n - p = 9 - 3 = 6$, $m + 1 < n$ is

satisfied. According to the pragmatical asymptotically stability theorem, error vector e

approaches zero and the estimated parameters also approach the uncertain parameters.

The equilibrium point is pragmatically asymptotically stable. Under the assumption of

equal probability, it is actually asymptotically stable. The simulation results are shown

in Figs. 3.14~3.16.

Fig. 3.1 Coordinate translation
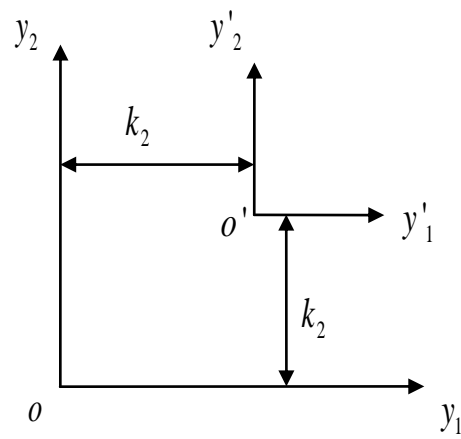
Fig. 3.2 Coordinate translation
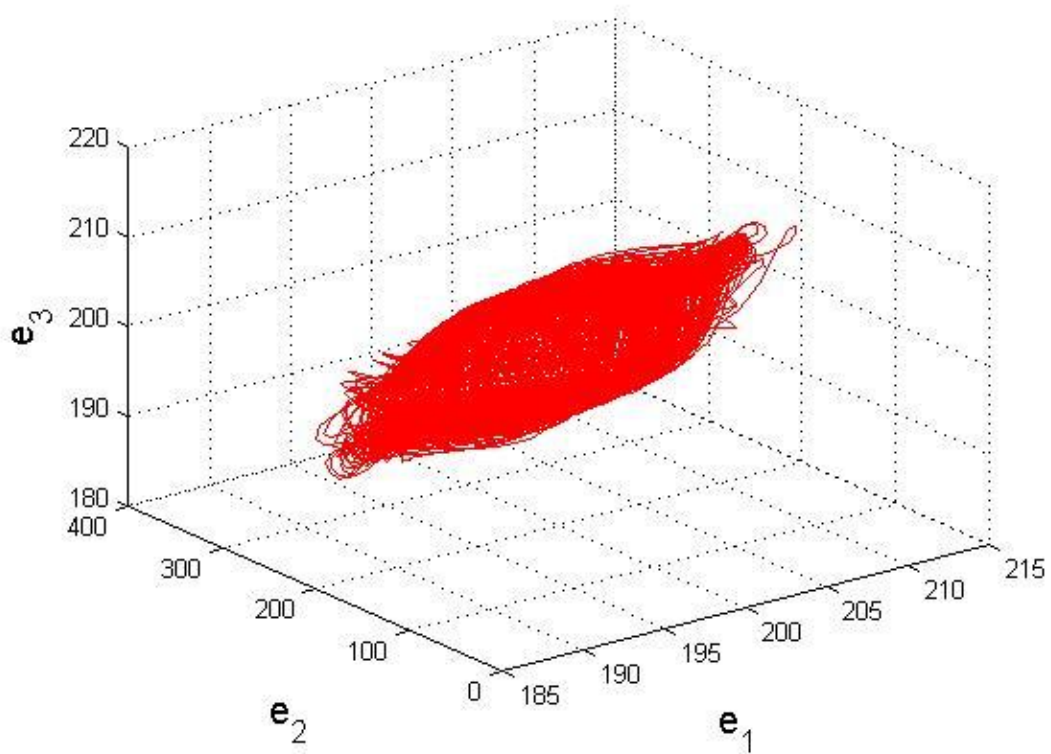
Fig. 3.3 Phase portrait of the error dynamics for Case 1.
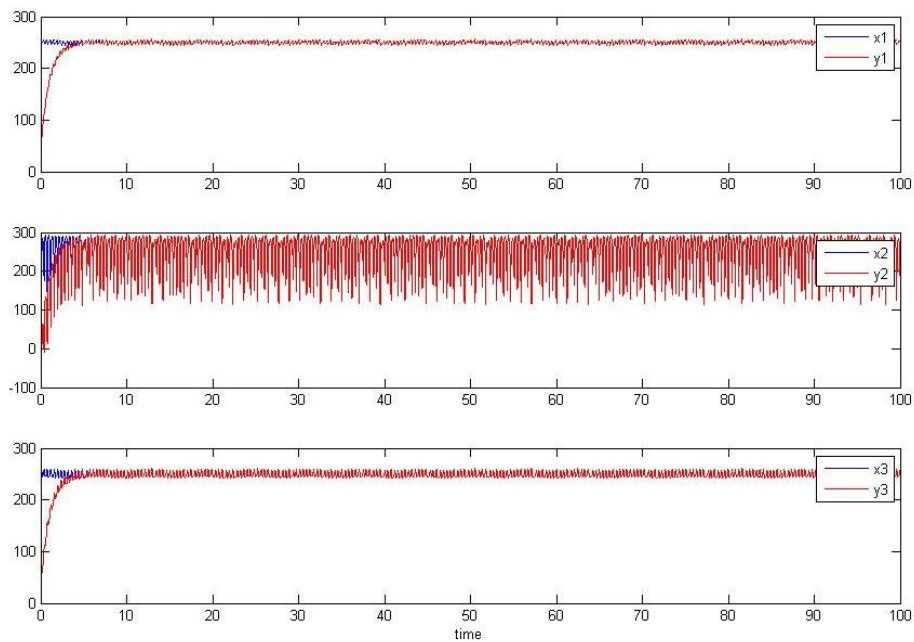
Fig. 3.4 Time histories of x_i, y_i for Case 1.
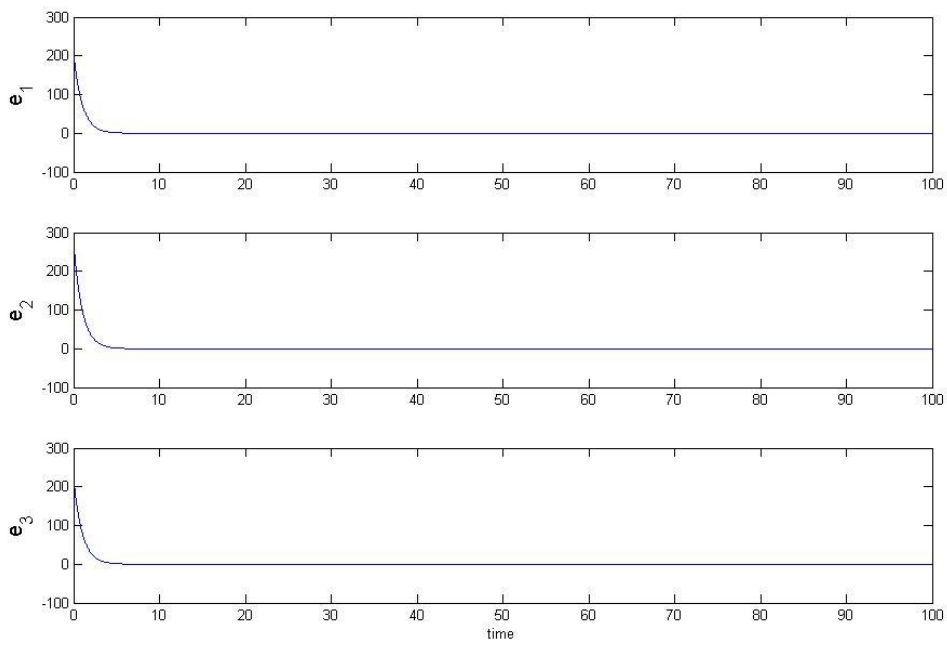
Fig. 3.5 Time histories of errors for Case 1.
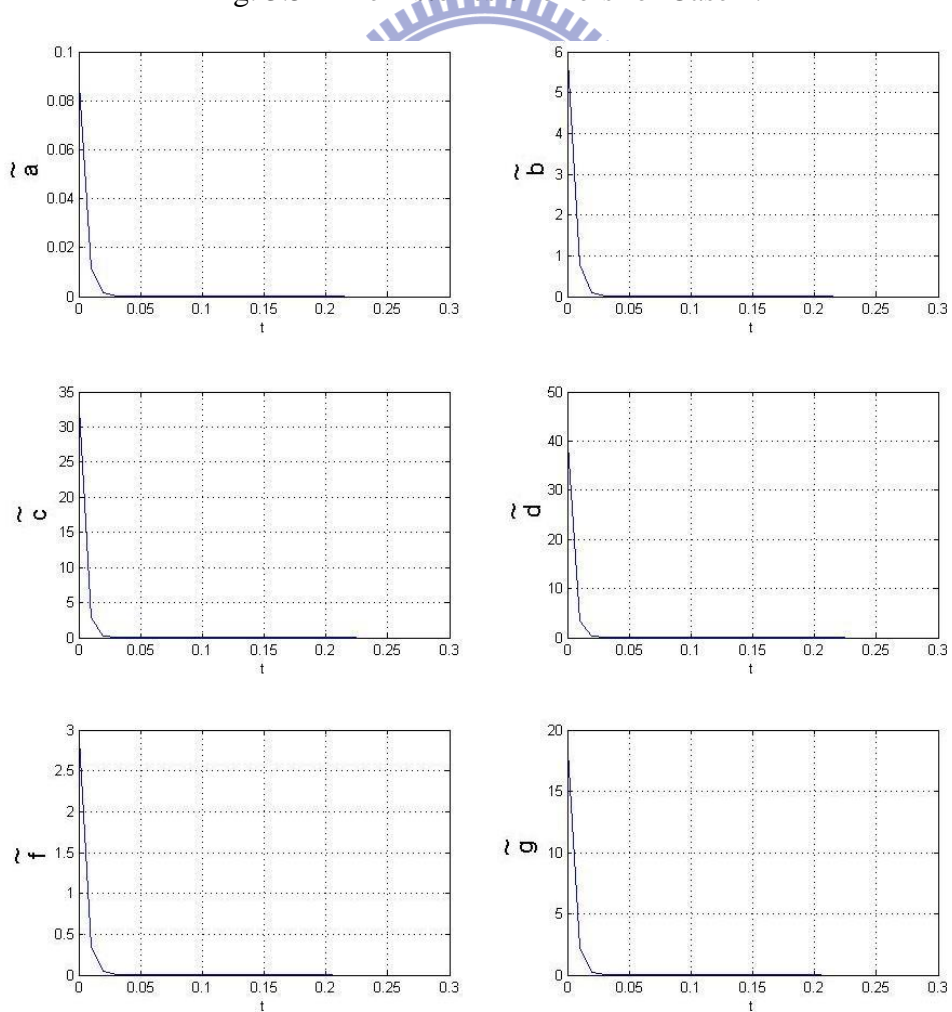
Fig. 3.6 Time histories of the parameter errors for Case 1.

25
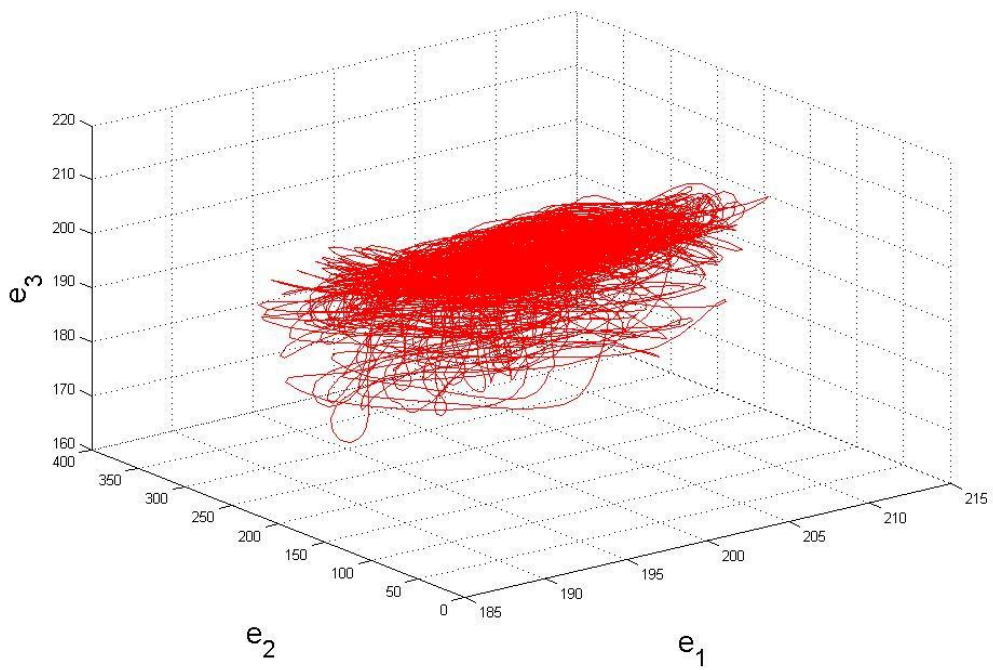
Fig. 3.7 Phase portrait of the error dynamics for Case 2.
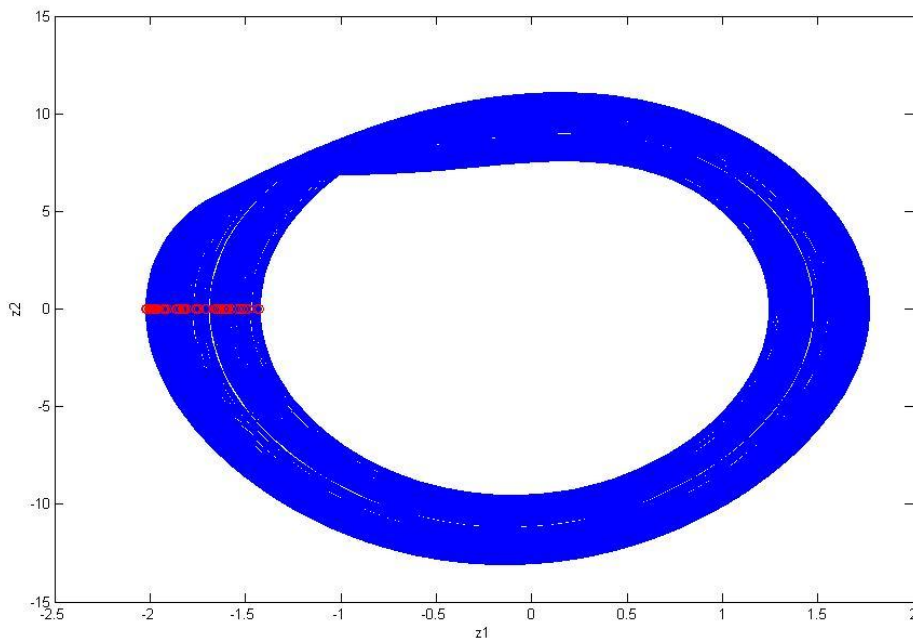
Fig. 3.8 The chaotic attractor of the Ge-Ku-Mathieu system.
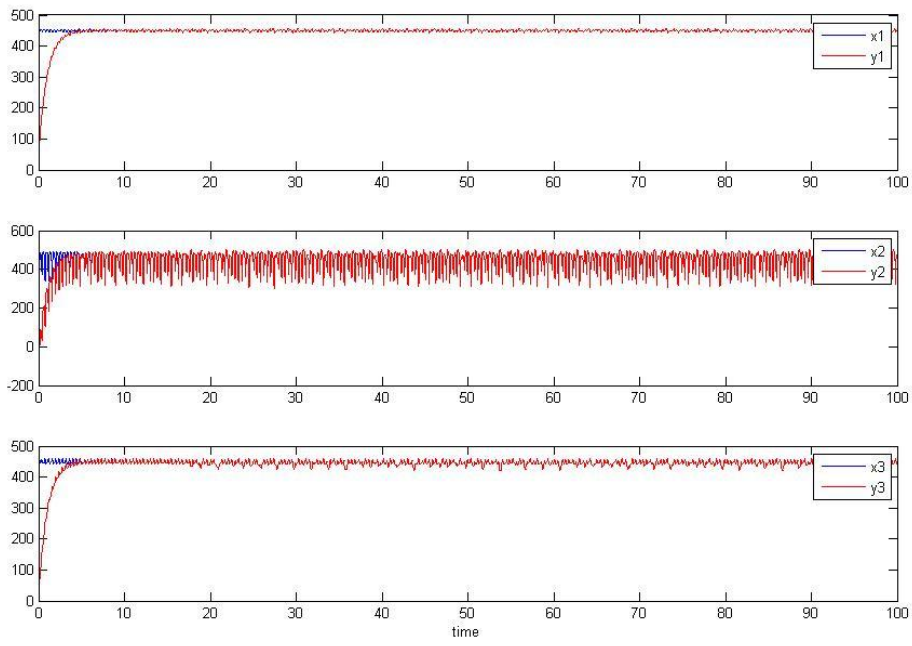
Fig. 3.9 Time histories of x_i, y_i for Case 2.
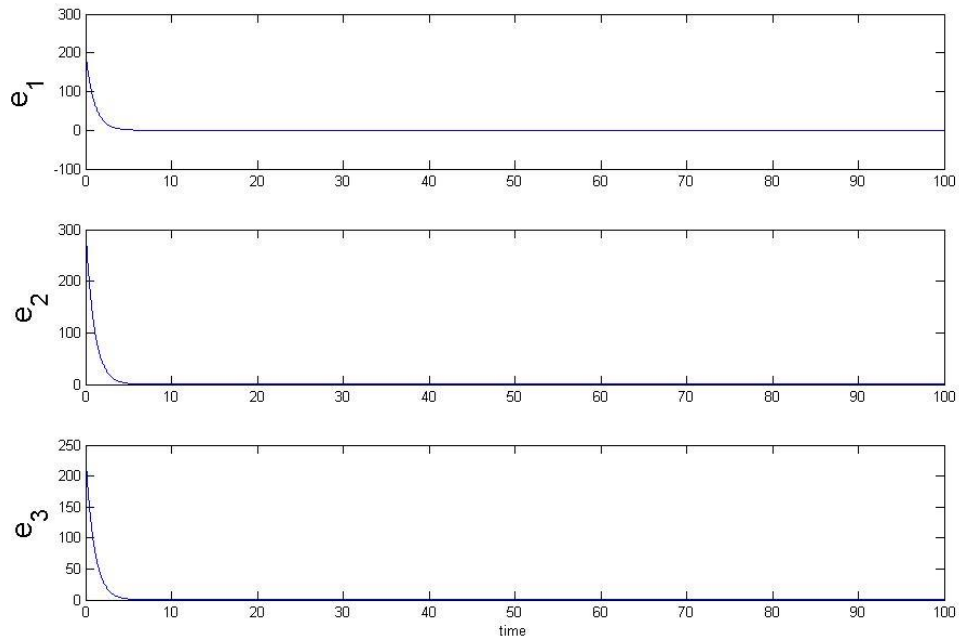
Fig. 3.10 Time histories of errors for Case 2.
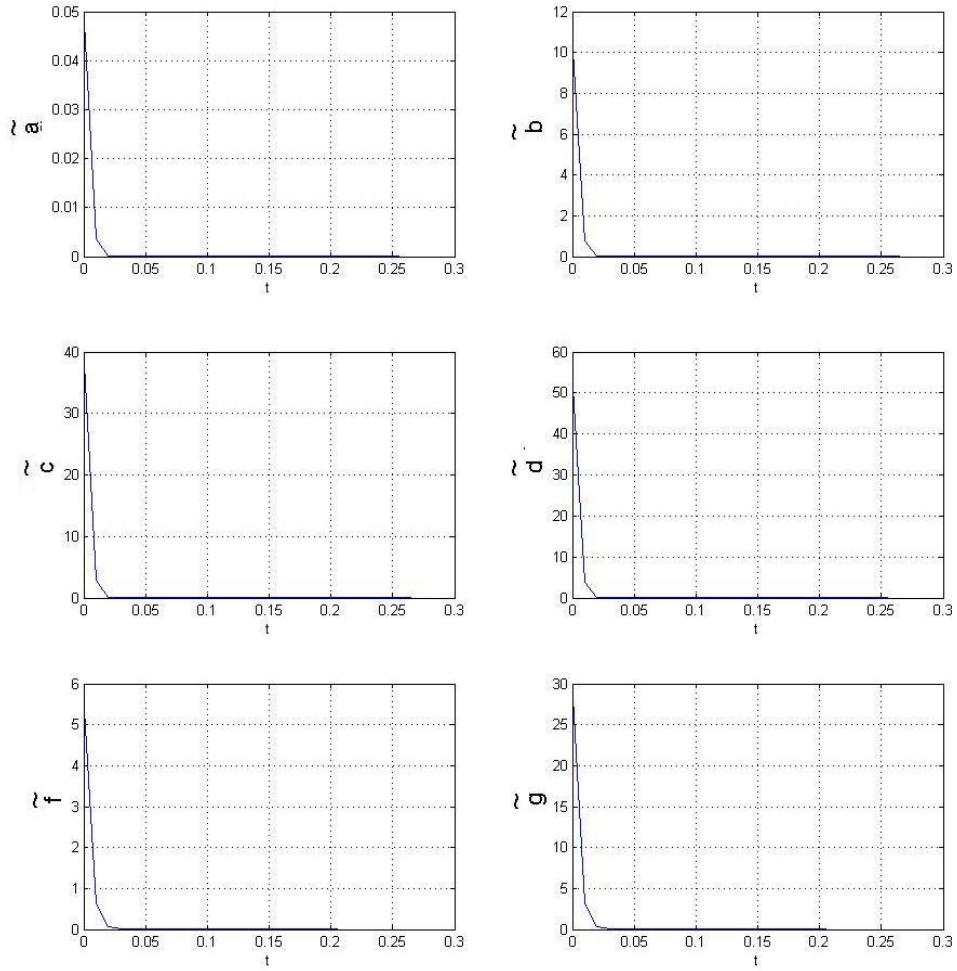
Fig. 3.11 Time histories of the parameter errors for Case 2.
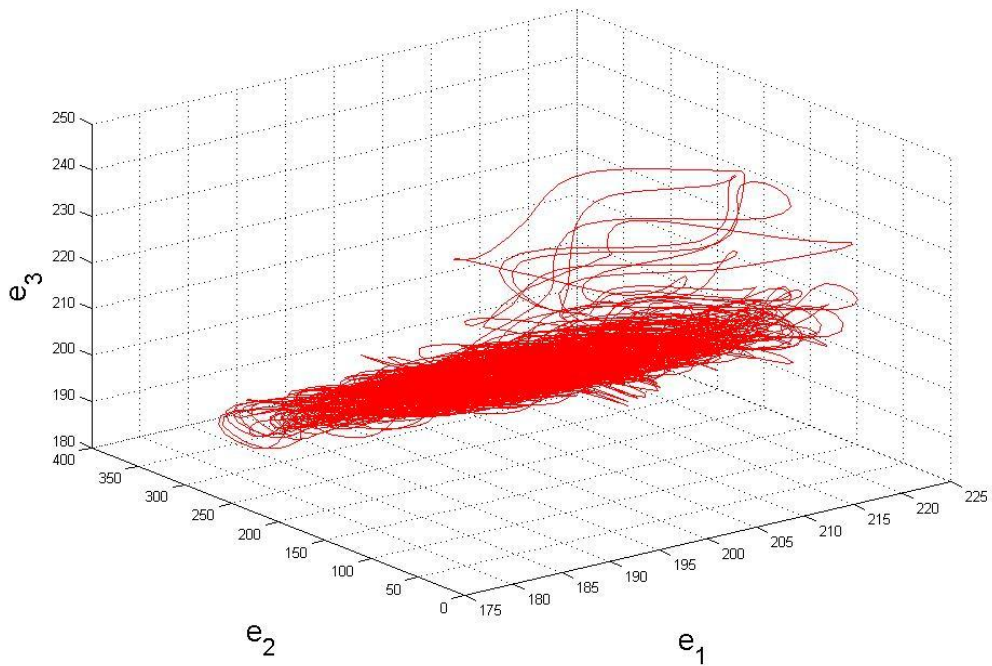
Fig. 3.12 Phase portrait of the error dynamic for Case 3.
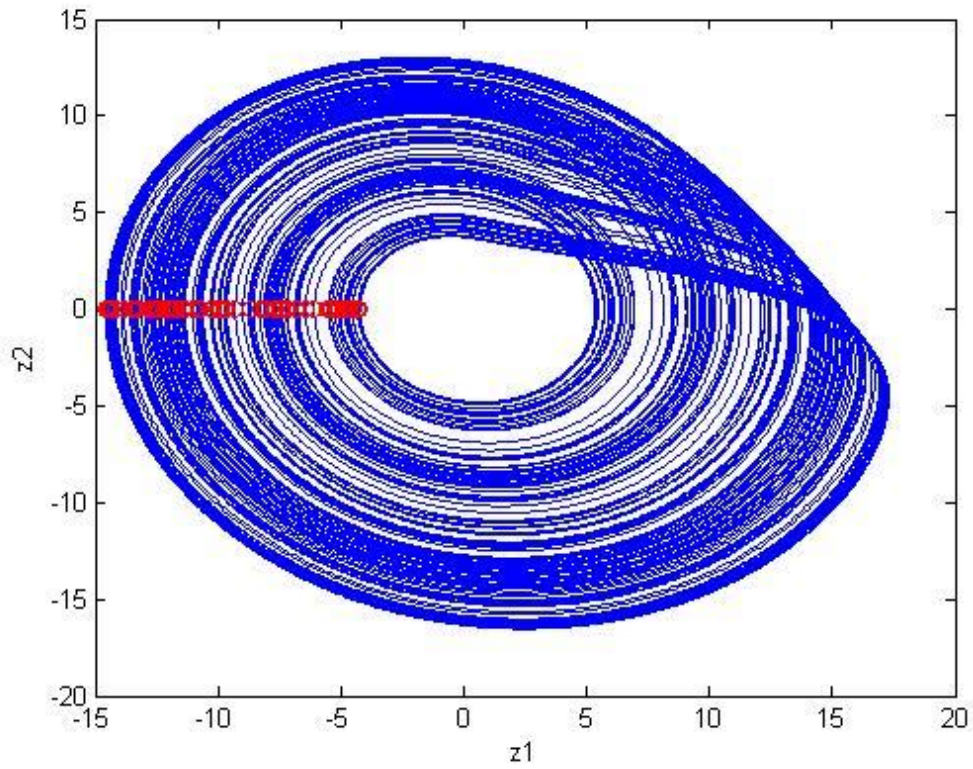
Fig. 3.13 The chaotic attractor of the *Rössler* system.
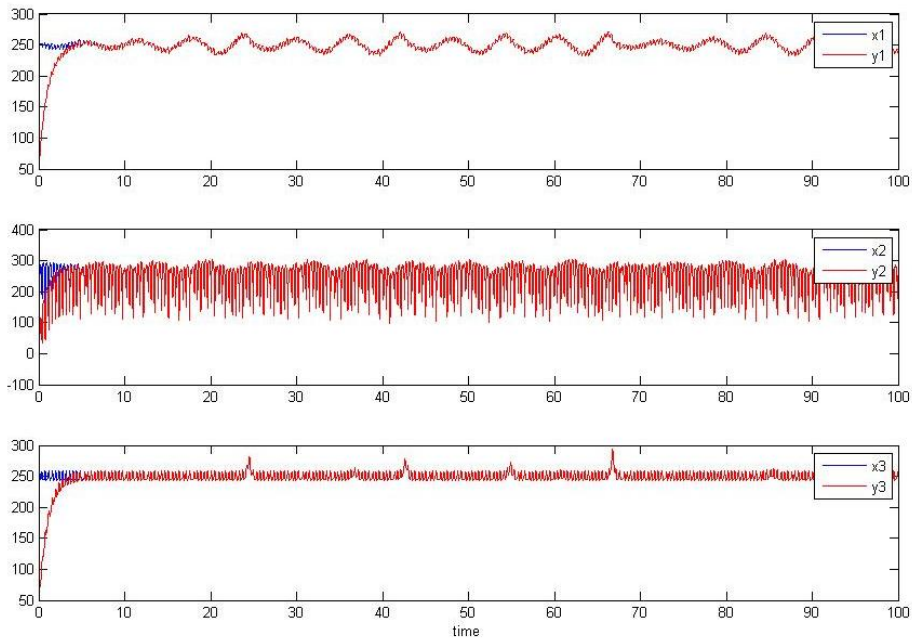
Fig. 3.14 Time histories of x_i, y_i for Case 3.
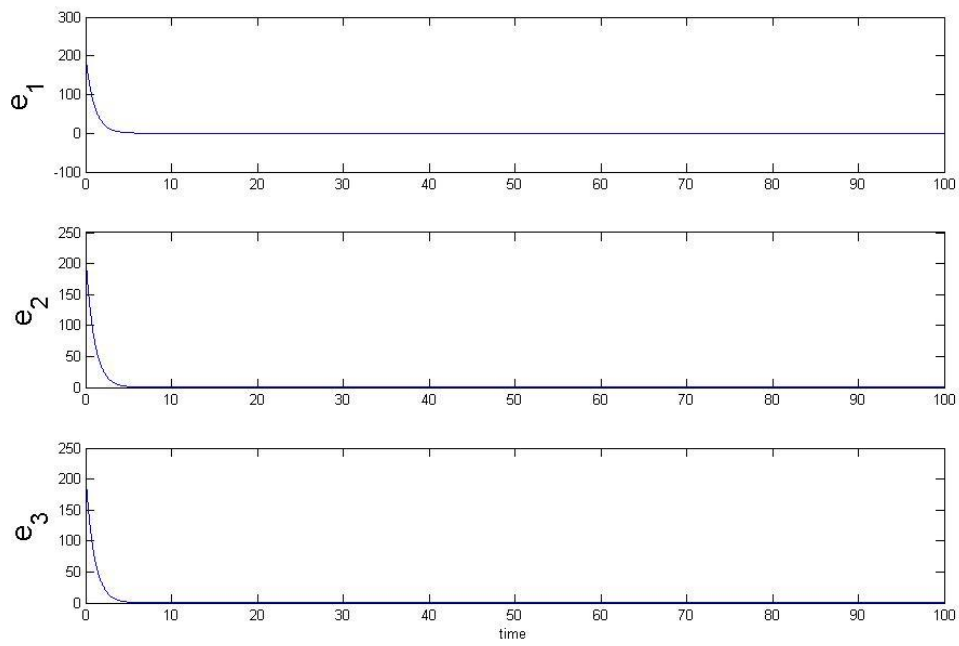
Fig. 3.15 Time histories of errors for Case 3.
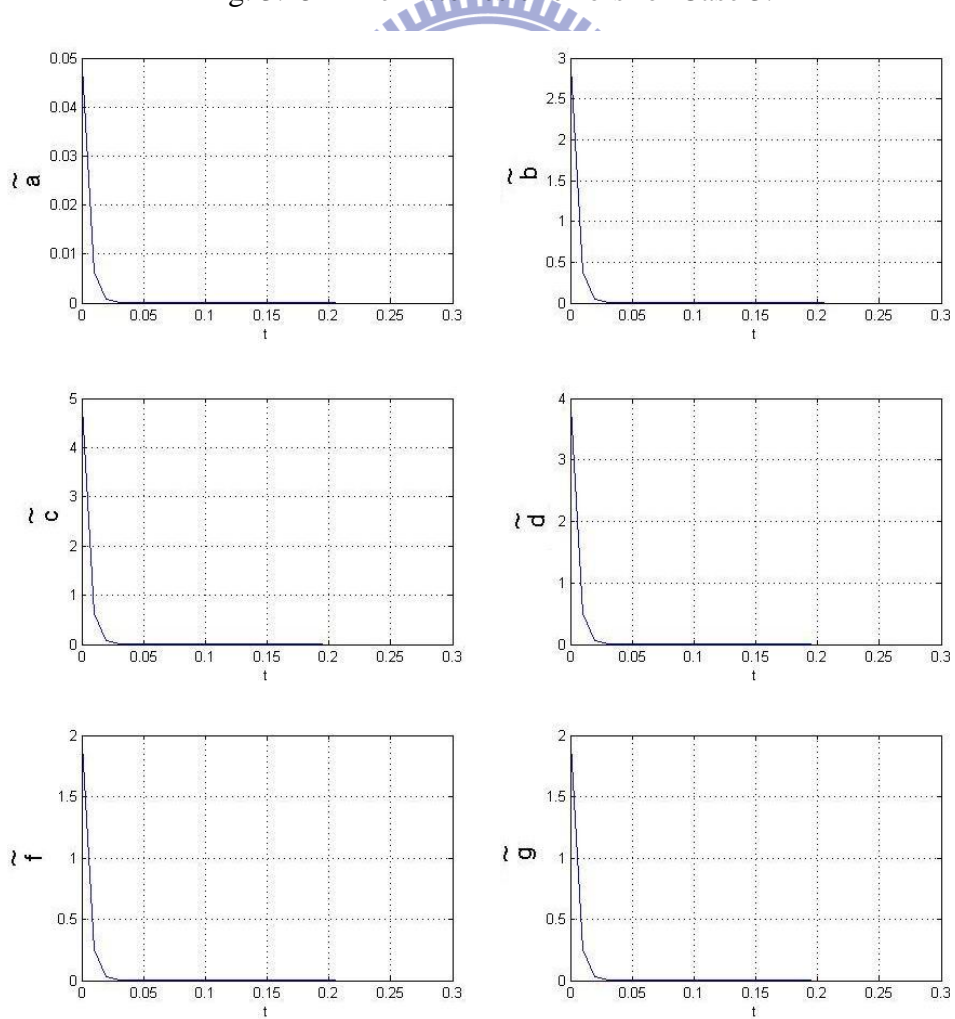
Fig. 3.16 Time histories of the parameter errors for Case 3.

30

Chapter 4

Double Symplectic Synchronization

for Ge-Ku-Duffing System

4.1 Preliminary

In this Chapter, a new double symplectic synchronization $\mathbf{G}(x, y, t) = \mathbf{F}(x, y, t)$ is studied, where x, y are state vectors of Partner A and Partner B, respectively, $\mathbf{G}(x, y, t)$ and $\mathbf{F}(x, y, t)$ are given vector functions of x, y and time. Since the symplectic functions are presented on both the right hand side and the left hand side of the equality, it is called "double symplectic synchronization". When $\mathbf{G}(x, y, t) = y$, the double symplectic synchronization is reduced to the symplectic synchronization.Due to the complexity of the form of the double symplectic synchronization, it may be applied to increase the security of secret communication.
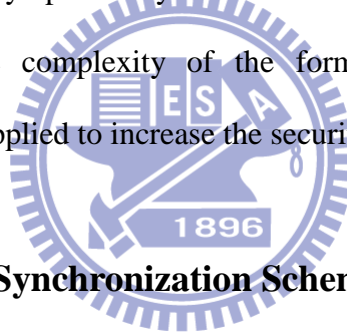
4.2 Double Symplectic Synchronization Scheme

Consider two different nonlinear chaotic systems, Partner A and Partner B, described by

$$\dot{x} = \mathbf{f}(x, t) , \tag{4.1}$$

$$\dot{y} = \mathbf{C}(t)y + \mathbf{g}(y, t) + \mathbf{u} , \tag{4.2}$$

where $x = [x_1, x_2, \ldots, x_n]^{\mathrm{T}} \in R^n$ and $y = [y_1, y_2, \ldots, y_n]^{\mathrm{T}} \in R^n$ are the state vectors of Partner A and Partner B, $\mathbf{C} \in R^{n \times n}$ is a given matrix, $\mathbf{f}$ and $\mathbf{g}$ are continuous nonlinear vector functions, and $\mathbf{u}$ is the controller vector. Our goal is to design the controller $\mathbf{u}$ such that $\mathbf{G}(x, y, t)$ asymptotically approaches $\mathbf{F}(x, y, t)$. For simplicity let $\mathbf{G}(x, y, t) = x + y$ and $\mathbf{F}$ is a continuous nonlinear vector function.

31

Property 1 [49]: An $m \times n$ matrix A of real elements defines a linear mapping $y = Ax$ from R^n into R^m, and the induced p-norm of A for $p = 1$, 2, and ∞ is given by

$$\|A\|_1 = \max_j \sum_{i=1}^m |a_{ij}|, \quad \|A\|_2 = \left[\lambda_{\max}(A^{\mathrm{T}}A) \right]^{1/2}, \quad \|A\|_\infty = \max_i \sum_{j=1}^n |a_{ij}|. \tag{4.3}$$

The useful property of induced matrix norms for real matrix A is as follow:

$$\|A\|_2 \le \sqrt{\|A\|_1 \|A\|_\infty} \,. \tag{4.4}$$

Theorem : For chaotic systems Partner A (4.1) and Partner B (4.2), if the controller $\mathbf{u}$ is designed as

$$\begin{aligned}
\mathbf{u} = (\mathbf{I} - \mathbf{D}_y\mathbf{F})^{-1}[\mathbf{D}_x\mathbf{F}\mathbf{f}(x,t) + \mathbf{D}_y\mathbf{F}(\mathbf{C}(t)y + \mathbf{g}(y,t)) + \mathbf{D}_t\mathbf{F} - \mathbf{f}(x,t) - \mathbf{g}(y,t) \\
+ \mathbf{C}(t)(x - \mathbf{F}) - \mathbf{K}(x + y - \mathbf{F})],
\end{aligned} \tag{4.5}$$

where $\mathbf{D}_x\mathbf{F}$, $\mathbf{D}_y\mathbf{F}$, $\mathbf{D}_t\mathbf{F}$ are the Jacobian matrices of $\mathbf{F}(x, y, t)$, $\mathbf{K} = \mathrm{diag}(k_1, k_2, \ldots, k_m)$, and satisfies

$$\frac{\min(k_i)}{\|\mathbf{C}(t)\|} > 1, \tag{4.6}$$

then the double symplectic synchronization will be achieved.

Proof: Define the error vectors as

$$\mathbf{e} = x + y - \mathbf{F}(x, y, t), \tag{4.7}$$

then the following error dynamics can be obtained by introducing the designed controller

$$\begin{aligned}
\frac{d\mathbf{e}}{dt} = \dot{\mathbf{e}} &= \dot{x} + \dot{y} - \mathbf{D}_x\mathbf{F}\dot{x} - \mathbf{D}_y\mathbf{F}\dot{y} - \mathbf{D}_t\mathbf{F} \\
&= \mathbf{f}(x,t) + \mathbf{C}(t)y + \mathbf{g}(y,t) - \mathbf{D}_x\mathbf{F}\mathbf{f}(x,t) - \mathbf{D}_y\mathbf{F}(\mathbf{C}(t)y + \mathbf{g}(y,t)) - \mathbf{D}_t\mathbf{F} \\
&\quad + (\mathbf{I} - \mathbf{D}_y\mathbf{F})\mathbf{u} \\
&= (\mathbf{C}(t) - \mathbf{K})\mathbf{e}.
\end{aligned} \tag{4.8}$$

Choose a positive definite Lyapunov function of the form

$$V(t) = \frac{1}{2}\mathbf{e}^{\mathrm{T}}\mathbf{e}. \tag{4.9}$$

Taking the time derivative of $V(t)$ along the trajectory of Eq. (4.8), we have

$$\begin{aligned}
\dot{V}(t) &= \mathbf{e}^{\mathrm{T}}\dot{\mathbf{e}} \\
&= \mathbf{e}^{\mathrm{T}}\mathbf{C}(t)\mathbf{e} - \mathbf{e}^{\mathrm{T}}\mathbf{K}\mathbf{e} \\
&\leq \|\mathbf{C}(t)\| \cdot \|\mathbf{e}\|^{2} - \min(k_{i})\|\mathbf{e}\|^{2} \\
&= (\|\mathbf{C}(t)\| - \min(k_{i}))\|\mathbf{e}\|^{2}.
\end{aligned} \tag{4.10}$$

Let $M = \min(k_{i}) - \|\mathbf{C}(t)\| > 0$, then $\dot{V}(t) \leq -M\|\mathbf{e}\|^{2} = -2MV(t)$. Therefore, it can be

obtained that

$$V(t) \leq V(0)e^{-2Mt} \tag{4.11}$$

and $\lim\limits_{t\to\infty}\int_{0}^{t}|V(\xi)|d\xi$ is bounded. Besides, $V(t)$ is uniformly continuous. According

to Barbalat's lemma [27], the conclusion can be drawn that $\lim\limits_{t\to\infty}V(t) = 0$, i.e.

$\lim\limits_{t\to\infty}\|\mathbf{e}(t)\| = 0$. Thus, the double symplectic synchronization can be achieved

asymptotically.

4.3 Synchronization of Two Different New Chaotic Systems

Case 1.

Consider a new Ge-Ku Mathieu(GKM) system[43] as Partner A described by

$$\begin{aligned}
\dot{x}_{1} &= x_{2}, \\
\dot{x}_{2} &= -ax_{2} - x_{1}\left[b\left(c - x_{1}^{2}\right) + dx_{2}x_{3}\right], \\
\dot{x}_{3} &= -\left(g + hx_{1}\right)x_{3} + lx_{2} + px_{1}x_{3},
\end{aligned} \tag{4.12}$$

where $a = -0.6, b = 5, c = 11, d = 0.3, g = 8, h = 10, l = 0.5, p = 0.2$, and the initial

conditions are $x_{1}(0) = 0.01$, $x_{2}(0) = 0.01$, $x_{3}(0) = 0.01$. Eq. (4.12) can be rewritten

in the form of Eq. (2.1), where $\mathbf{f}(x,t) = \begin{bmatrix} x_2 \\ -ax_2 - x_1 \left[b\left(c - x_1^2 \right) + dx_2 x_3 \right] \\ -\left(g + hx_1 \right) x_3 + lx_2 + px_1 x_3 \end{bmatrix}$. The chaotic

attractor of the new Ge-Ku-Mathieu system is shown in Fig. 4.1.

The controlled a new Ge-Ku-Duffing(GKD) system[43] is considered as Partner B described by

$$
\begin{aligned}
\dot{y}_1 &= y_2 + u_1, \\
\dot{y}_2 &= -ky_2 - y_1 \left[m\left(r - y_1^2 \right) + sy_3 \right] + u_2, \\
\dot{y}_3 &= -y_3 - y_3^3 - ny_2 + wy_1 + u_3,
\end{aligned}
\tag{4.13}
$$

where $k = 0.1, m = 11, r = 40, s = 54, n = 6, w = 30$, $\mathbf{u} = \left[u_1, u_2, u_3 \right]^{\mathrm{T}}$ is the controller,

and the initial conditions are $y_1(0) = 2$, $y_2(0) = 2.4$, $y_3(0) = 5$. The chaotic attractor

of the uncontrolled new GKD system is shown in Fig. 4.2. The Lyapunov exponents

and the bifurcation diagram of the uncontrolled new GKD system are shown in Fig.

4.3 and Fig. 4.4. Eq. (4.13) can be rewritten in the form of Eq. (4.2), where

$\mathbf{C}(t) = \begin{bmatrix} 0 & 1 & 0 \\ -mr & -k & 0 \\ w & -n & -1 \end{bmatrix}$ and $\mathbf{g}(y,t) = \begin{bmatrix} 0 \\ my_1^3 - sy_1 y_3 \\ -y_3^3 \end{bmatrix}$. By applying *Property 1*, it can

be derived that $\left\| \mathbf{C}(t) \right\|_1 = mr - w$, $\left\| \mathbf{C}(t) \right\|_\infty = mr + k$, and

$\left\| \mathbf{C}(t) \right\|_2 \leq \sqrt{(mr - w)(mr + k)} = \sqrt{180441}$. Then $\left\| \mathbf{C}(t) \right\| = 424$ is estimated.

Define $\mathbf{F}(x, y, t) = \begin{bmatrix} x_1 y_1^2 \\ x_2 y_2^2 \\ x_3 y_3^2 \end{bmatrix}$, and our goal is to achieve the double symplectic

synchronization $x + y = \mathbf{F}(x, y, t)$. According to the Theorem , the inequality

$\dfrac{\min(k_i)}{\left\| \mathbf{C}(t) \right\|} > 1$ must be satisfied. It can be obtained that $\min(k_i) > 424$. Thus we

choose $\mathbf{K} = \begin{bmatrix} k_1 & 0 & 0 \\ 0 & k_2 & 0 \\ 0 & 0 & k_3 \end{bmatrix} = \begin{bmatrix} 425 & 0 & 0 \\ 0 & 426 & 0 \\ 0 & 0 & 427 \end{bmatrix}$ and design the controller as

$$u_1 = -(x_2 + y_2 - x_2 y_1^2 - 2x_1 y_1 y_2 + x_1 + y_1 - x_1 y_1^2),$$

$$
\begin{aligned}
u_2 = -\{ &(-ax_2 - x_1(b(c - x_1^2) + dx_2 x_3) + (-ky_2 - y_1(m(r - y_1^2) + sy_3)) \\
&- (-ax_2 - x_1(b(c - x_1^2) + dx_2 x_3))y_2^2 - 2x_2 y_2(-ky_2 - y_1(m(r - y_1^2) + sy_3)) \\
&+ x_2 + y_2 - x_2 y_2^2 \}
\end{aligned}
$$

$$
\begin{aligned}
u_3 = -\{ &-(g + hx_1)x_3 + lx_2 + px_1 x_3 + (-y_3 - y_3^3 - ny_2 + wy_1) \\
&- (-(g + hx_1)x_3 + lx_2 + px_1 x_3)y_3^2 - 2x_3 y_3(-y_3 - y_3^3 - ny_2 \\
&+ wy_1) + x_3 + y_3 - x_3 y_3^2 \}
\end{aligned}
$$

When the double symplectic synchronization is achieved, the phase portrait of the controlled new GKD system and the time histories of the state errors and the time histories of $x_i + y_i$ and $x_i y_i^2$ are shown in Fig. 4.5 and Fig. 4.6 and Fig. 4.7, respectively.
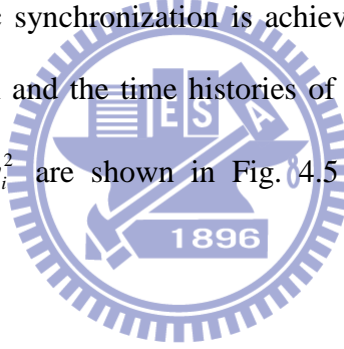
Case 2.

Consider a new Ge-Ku-van der Pol(GKv)system[43] as Partner A described by

$$
\begin{aligned}
\dot{x}_1 &= x_2, \\
\dot{x}_2 &= -ax_2 - x_3\left[b\left(c - x_1^2\right) + dx_3\right], \\
\dot{x}_3 &= -gx_3 - h\left(1 - x_3^2\right)x_2 + lx_1,
\end{aligned}
\tag{4.14}
$$

where $a = 0.08, b = -0.35, c = 100.56, d = -1000.02, g = 0.61, h = 0.08, l = 0.01$ and the initial condition is $x_1(0) = 0.01, x_2(0) = 0.01, x_3(0) = 0.01$. Eq. (3.14) can be

rewritten in the form of Eq. (4.1), where $\mathbf{f}(x,t) = \begin{bmatrix} x_2 \\ -ax_2 - x_3\left[b\left(c - x_1^2\right) + dx_3\right] \\ -gx_3 - h\left(1 - x_3^2\right)x_2 + lx_1 \end{bmatrix}$. The

chaotic attractor of the new Ge-Ku-van der Pol system is shown in Fig. 4.8.

The controlled Ge-Ku-Duffing(GKD) system is considered as Partner B described by

$$\dot{y}_1 = y_2 + u_1,$$
$$\dot{y}_2 = -ky_2 - y_1\left[m\left(r - y_1^2\right) + sy_3\right] + u_2, \qquad (4.15)$$
$$\dot{y}_3 = -y_3 - y_3^3 - ny_2 + wy_1 + u_3,$$

where $k = 0.1, m = 11, r = 40, s = 54, n = 6, w = 30$, $\mathbf{u} = [u_1, u_2, u_3]^T$ is the controller, and the initial condition is $y_1(0) = 2$, $y_2(0) = 2.4$, $y_3(0) = 5$. Eq.(4.15) can be rewritten in the form of Eq. (4.2), where $\mathbf{C}(t) = \begin{bmatrix} 0 & 1 & 0 \\ -mr & -k & 0 \\ w & -n & -1 \end{bmatrix}$ and

$$\mathbf{g}(y,t) = \begin{bmatrix} 0 \\ my_1^3 - sy_1 y_3 \\ -y_3^3 \end{bmatrix}.$$ By applying *Property 1*, it is derived that $\|\mathbf{C}(t)\|_1 = mr - w$, $\|\mathbf{C}(t)\|_\infty = mr + k$, and $\|\mathbf{C}(t)\|_2 \leq \sqrt{(mr - w)(mr + k)} = \sqrt{180441}$. Then $\|\mathbf{C}(t)\| = 424$ is estimated.

Define $\mathbf{F}(\mathbf{x}, \mathbf{y}, t) = \begin{bmatrix} x_1 y_1^2 \\ x_2 y_2^2 \\ x_3 y_3^2 \end{bmatrix}$, and our goal is to achieve the double symplectic synchronization $x + y = \mathbf{F}(x, y, t)$. According to the Theorem , the inequality $\dfrac{\min(k_i)}{\|\mathbf{C}(t)\|} > 1$ has to be satisfied. It can be obtained that $\min(k_i) > 424$. Thus we choose

$$\mathbf{K} = \begin{bmatrix} k_1 & 0 & 0 \\ 0 & k_2 & 0 \\ 0 & 0 & k_3 \end{bmatrix} = \begin{bmatrix} 425 & 0 & 0 \\ 0 & 426 & 0 \\ 0 & 0 & 427 \end{bmatrix}$$ and design the controller as

$$u_1 = x_2 + y_2 - x_2 y_1^2 - 2x_1 y_1 y_2 + x_1 + y_1 - x_1 z_1^2,$$

$$u_2 = -\{-ax_2 - x_3(b(c - x_1^2) + dx_3) + (-ky_2 - y_1(m(r - y_1^2) + sy_3))$$
$$- (-ax_2 - x_3(b(c - x_1^2) + dx_3))y_2^2 - 2x_2y_2(-ky_2 - y_1(m(r - y_1^2) + sy_3))$$
$$+ x_2 + y_2 - x_2y_2^2$$

$$u_3 = -\{-gx_3 + h(1 - x_3^2)x_2 + lx_1 - y_3 - y_3^3 - ky_2 + wy_1$$
$$- (-gx_3 + h(1 - x_3^2)x_2 + lx_2)y_3^2 - 2x_3y_3(-y_3 - y_3^3 - ky_2 + wy_1)$$
$$+ x_3 + y_3 - x_3y_3^2\}$$

When the double symplectic synchronization is achieved, the phase portrait of the controlled Ge-Ku-Duffing system and the time histories of the state errors and the time histories of $x_i + y_i$ and $x_iy_i^2$ are shown in Fig. 4.9 and Fig. 4.10 and Fig. 4.11, respectively.

Case 3.

Consider a new Double Ge-Ku system as Partner A described by

$$\dot{x}_1 = x_2,$$
$$\dot{x}_2 = -ax_2 - x_1\left[b\left(c - x_1^2\right) + dx_3\right], \qquad (4.16)$$
$$\dot{x}_3 = -ax_3 - x_3\left[b\left(c - x_3^2\right) + ex_1\right],$$

where $a = -0.5, b = -1.4, c = 1.9, d = 54, e = 6.2$ and the initial conditions are

$x_1(0) = 0.01, x_2(0) = 0.01, x_3(0) = 0.01$. Eq. (3.16) can be rewritten in the form of

Eq.(3.1), where $\mathbf{f}(x,t) = \begin{bmatrix} x_2 \\ -ax_2 - x_1\left[b\left(c - x_1^2\right) + dx_3\right] \\ -ax_3 - x_3\left[b\left(c - x_3^2\right) + ex_1\right] \end{bmatrix}$. The chaotic attractor of the

new Double Ge-Ku system is shown in Fig. 4.12.

The controlled Ge-Ku-Duffing system is considered as Partner B described by

$$\dot{y}_1 = y_2 + u_1,$$
$$\dot{y}_2 = -ky_2 - y_1\left[m\left(r - y_1^2\right) + sy_3\right] + u_2, \qquad (4.17)$$
$$\dot{y}_3 = -y_3 - y_3^3 - ny_2 + wy_1 + u_3,$$

where $k = 0.1, m = 11, r = 40, s = 54, n = 6, w = 30$, $\mathbf{u} = [u_1, u_2, u_3]^T$ is the controller,

and the initial conditions are $y_1(0) = 2$, $y_2(0) = 2.4$, $y_3(0) = 5$. Eq. (4.17) can be

rewritten in the form of Eq. (4.2), where $\mathbf{C}(t) = \begin{bmatrix} 0 & 1 & 0 \\ -mr & -k & 0 \\ w & -n & -1 \end{bmatrix}$ and

$\mathbf{g}(y,t) = \begin{bmatrix} 0 \\ my_1^3 - sy_1y_3 \\ -y_3^3 \end{bmatrix}$. By applying *Property 1*, it is derived that $\left\| \mathbf{C}(t) \right\|_1 = mr - w$,

$\left\| \mathbf{C}(t) \right\|_\infty = mr + k$, and $\left\| \mathbf{C}(t) \right\|_2 \le \sqrt{(mr - w)(mr + k)} = \sqrt{180441}$. Then $\left\| \mathbf{C}(t) \right\| = 424$ is

estimated.

Define $\mathbf{F}(x, y, t) = \begin{bmatrix} x_1 y_1^2 \\ x_2 y_2^2 \\ x_3 y_3^2 \end{bmatrix}$, and our goal is to achieve the double symplectic

synchronization $x + y = \mathbf{F}(x, y, t)$. According to the Theorem , the inequality

$\dfrac{\min(k_i)}{\left\| \mathbf{C}(t) \right\|} > 1$ has to be satisfied. It can be obtained that $\min(k_i) > 424$. Thus we

choose

$\mathbf{K} = \begin{bmatrix} k_1 & 0 & 0 \\ 0 & k_2 & 0 \\ 0 & 0 & k_3 \end{bmatrix} = \begin{bmatrix} 425 & 0 & 0 \\ 0 & 426 & 0 \\ 0 & 0 & 427 \end{bmatrix}$ and design the controller as

$u_1 = -\{x_2 + y_2 - x_2 y_1^2 - 2x_1 y_1 y_2 + x_1 + y_1 - x_1 y_1^2\}$,

$u_2 = -\{-ax_2 - x_1(b(c - x_1^2) + dx_3) - ky_2 - y_1(m(r - y_1^2) + sy_3)$
$\quad - (-ax_2 - x_1(b(c - x_1^2) + dx_3))y_2^2 - 2x_2 y_2(-ky_2 - y_1(m(r - y_1^2) + sy_3))$
$\quad + x_2 + y_2 - x_2 y_2^2\}$

$u_3 = -\{-ax_3 - x_3(b(c - x_3^2) + ex_1) - y_3 - y_3^3 - ny_2 + wy_1$
$\quad - (-ax_3 - x_3(b(c - x_3^2) + ex_1))y_3^2 - 2x_3 y_3(-y_3 - y_3^3 - ny_2 + wy_1)$
$\quad + x_3 + y_3 - x_3 y_3^2\}$

When the double symplectic synchronization is achieved, the phase portrait of the

controlled Ge-Ku-Duffing system and the time histories of the state errors and the

time histories of $x_i + y_i$ and $x_i y_i^2$ are shown in Fig. 4.13 and Fig. 4.14 and Fig. 4.15, respectively.
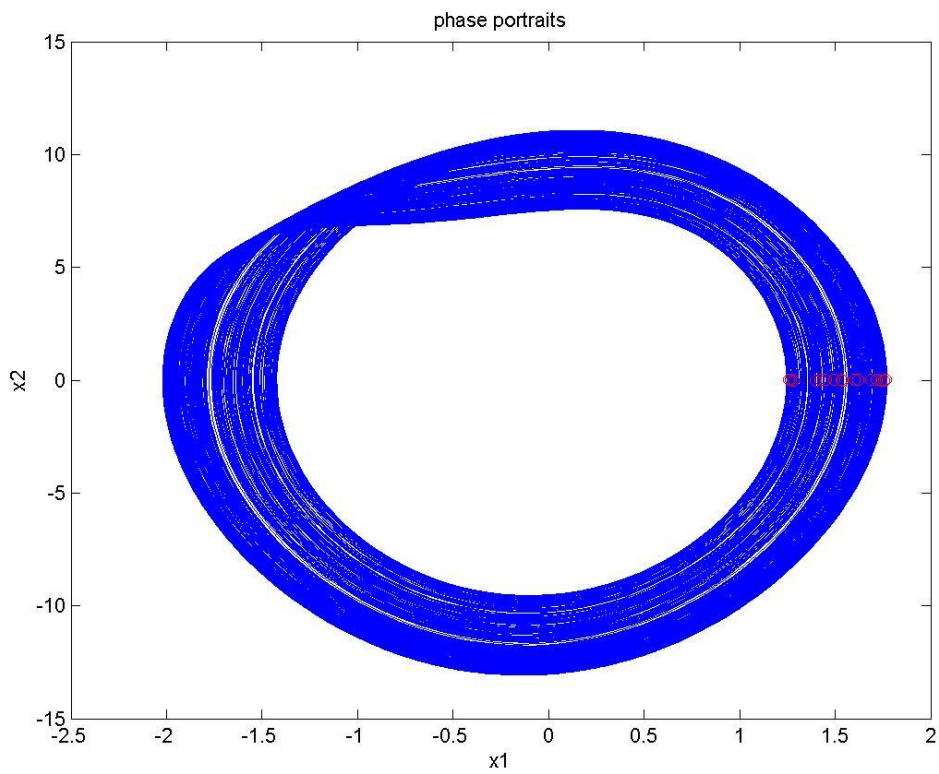
Fig. 4.1 The chaotic attractor of a new Ge-Ku-Mathieu system.
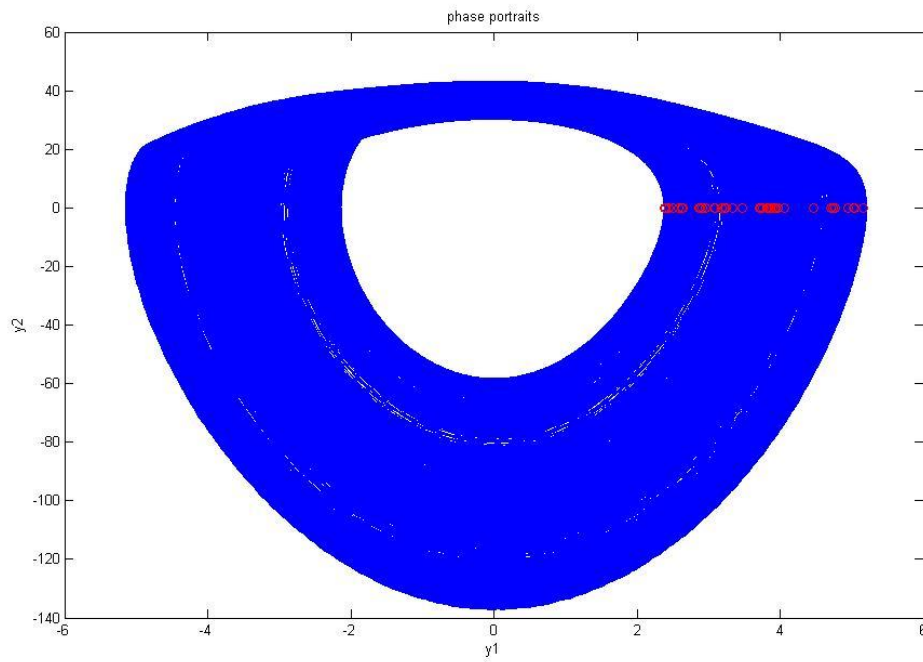
Fig. 4.2 The chaotic attractor of a uncontrolled new Ge-Ku-Duffing system.
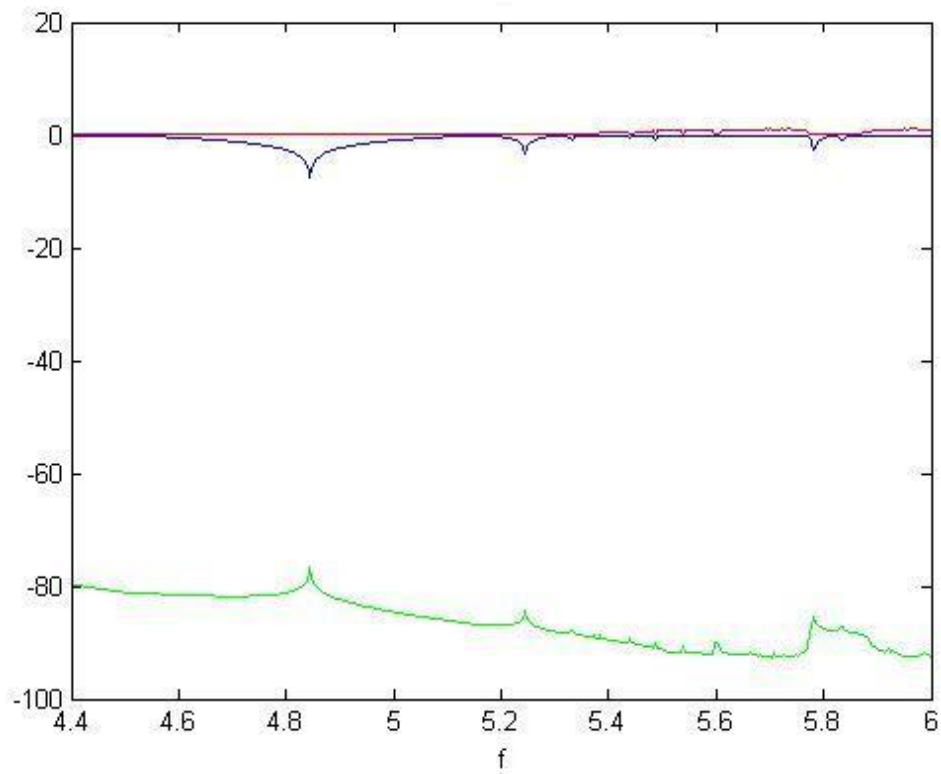
Fig. 4.3 The Lyapunov exponents of a uncontrolled new Ge-Ku-Duffing system.
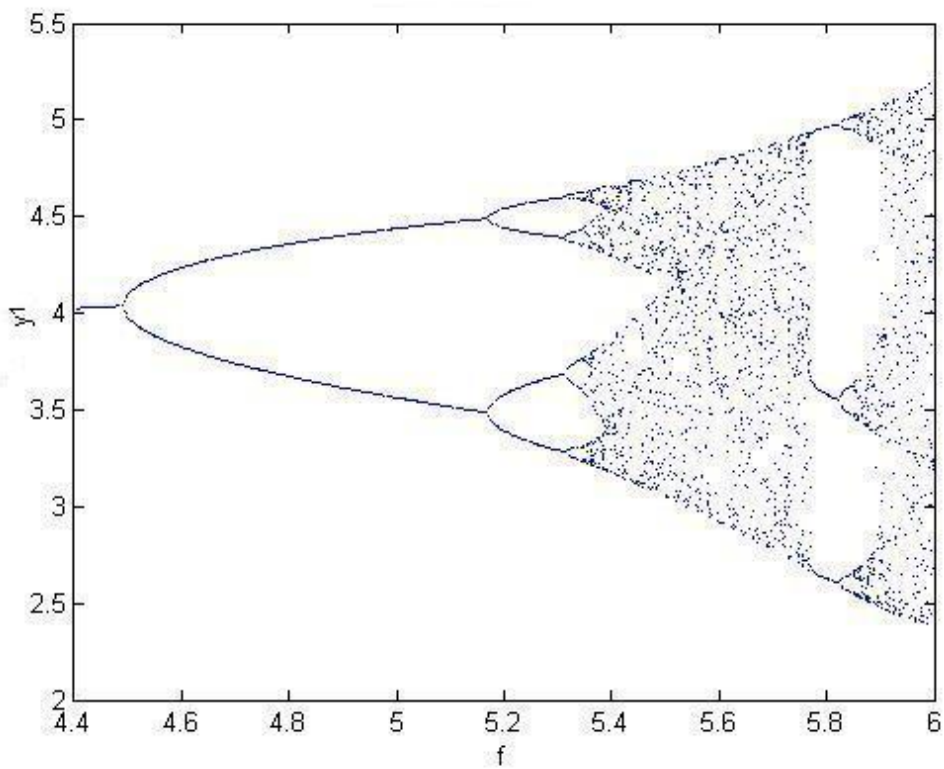
Fig. 4.4 The bifurcation diagram of a uncontrolled new Ge-Ku-Duffing system.
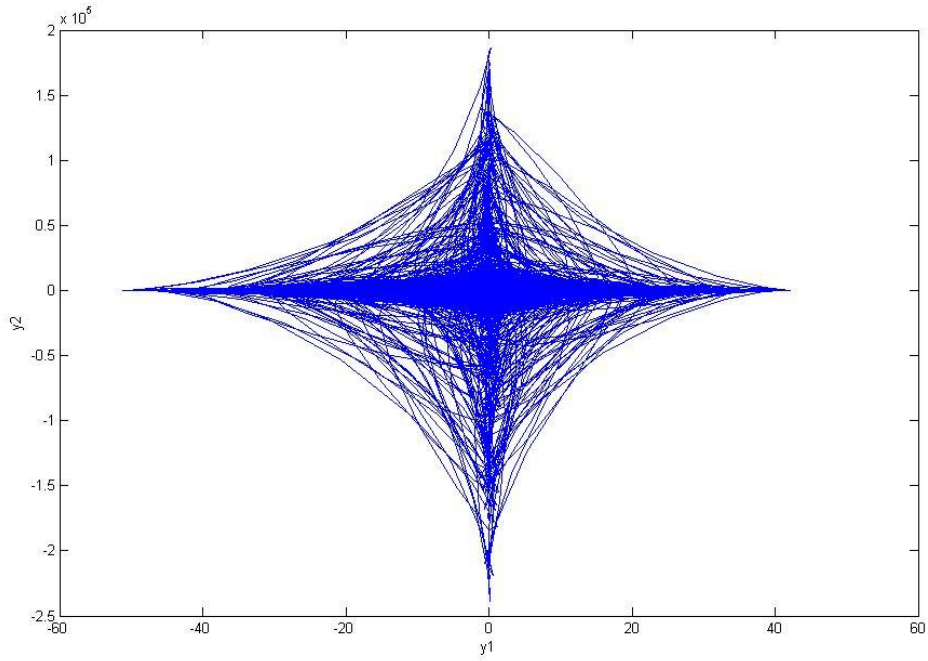
Fig. 4.5 Phase portrait of a controlled new Ge-Ku-Duffing system for Case 1.
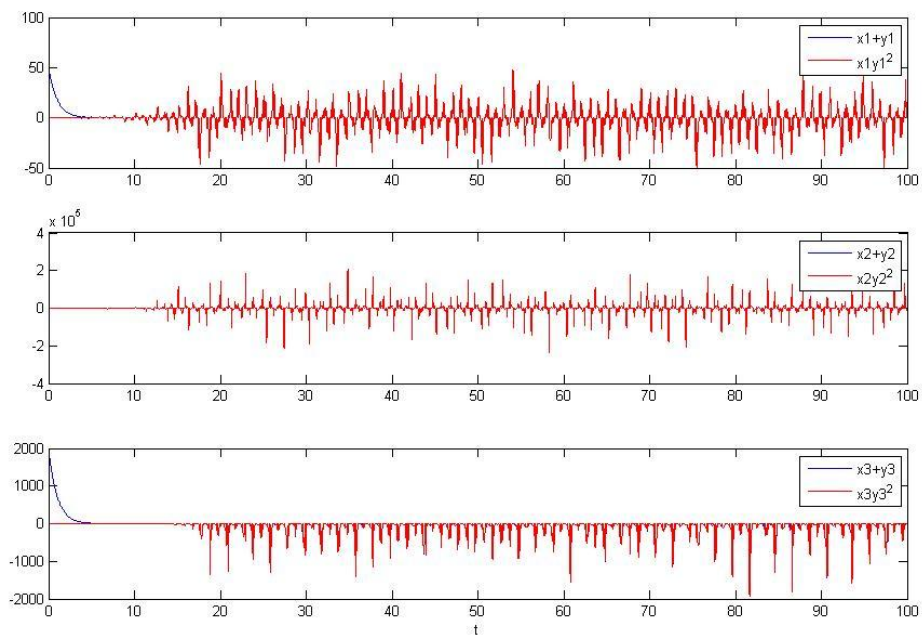
Fig. 4.6 Time histories of $x_i + y_i$ and $x_i y_i^2$ for Case 1.
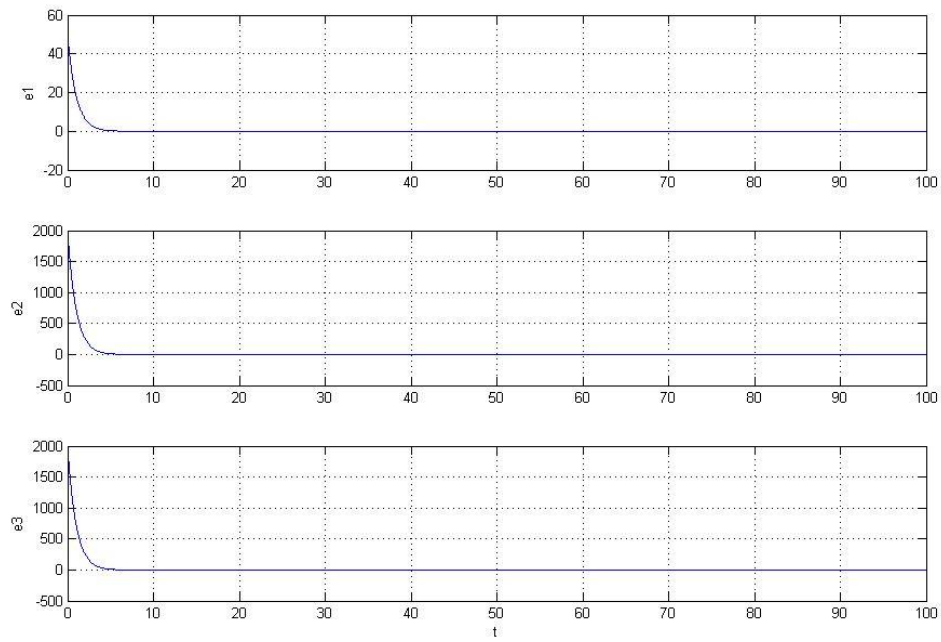
Fig. 4.7 Time histories of the state errors for Case 1.
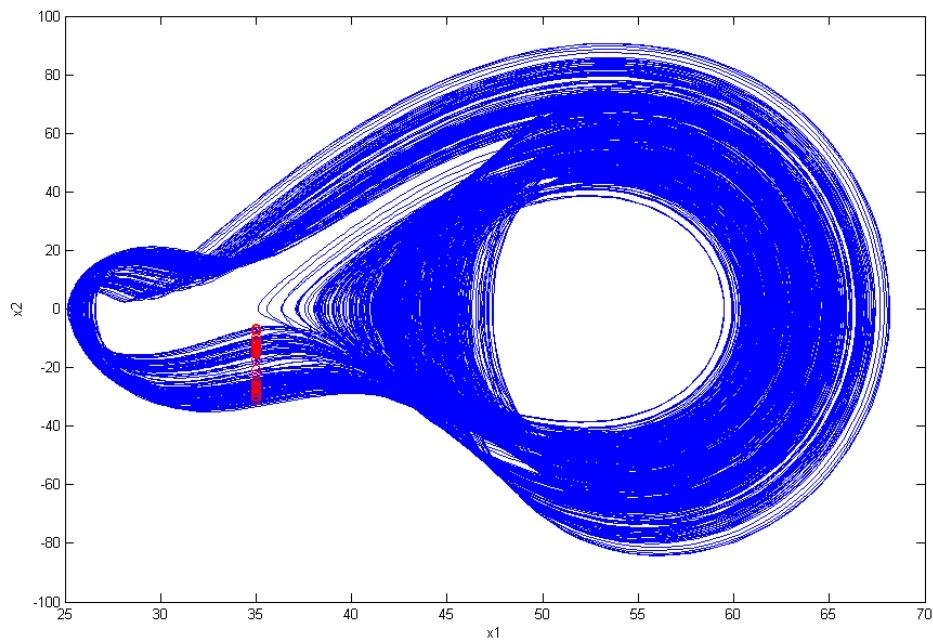
Fig. 4.8 The chaotic attractor of a new Ge-Ku-van der Pol system.
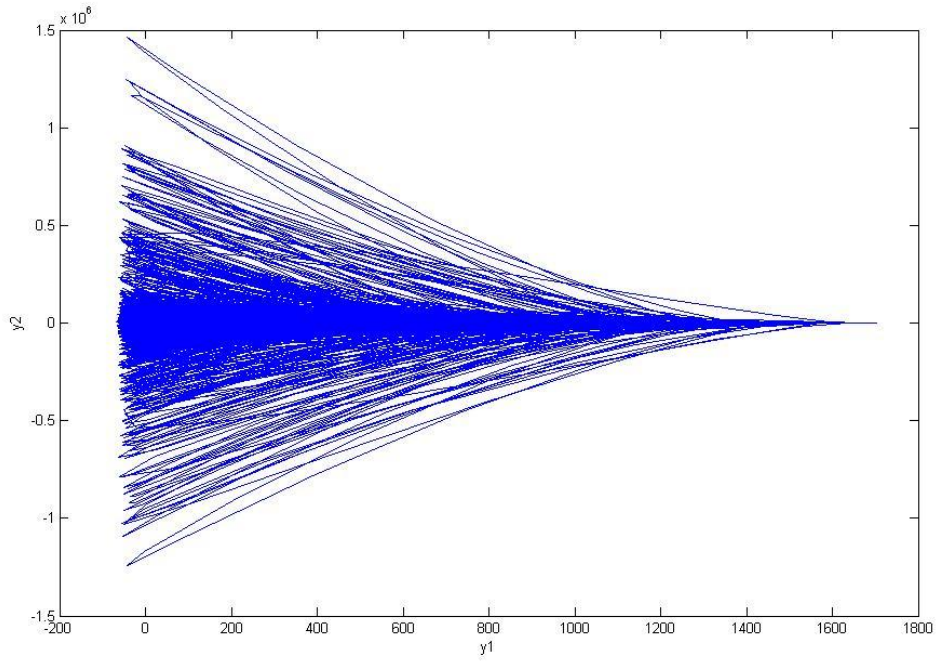
Fig. 4.9 Phase portrait of the controlled Ge-Ku-Duffing system for Case 2.
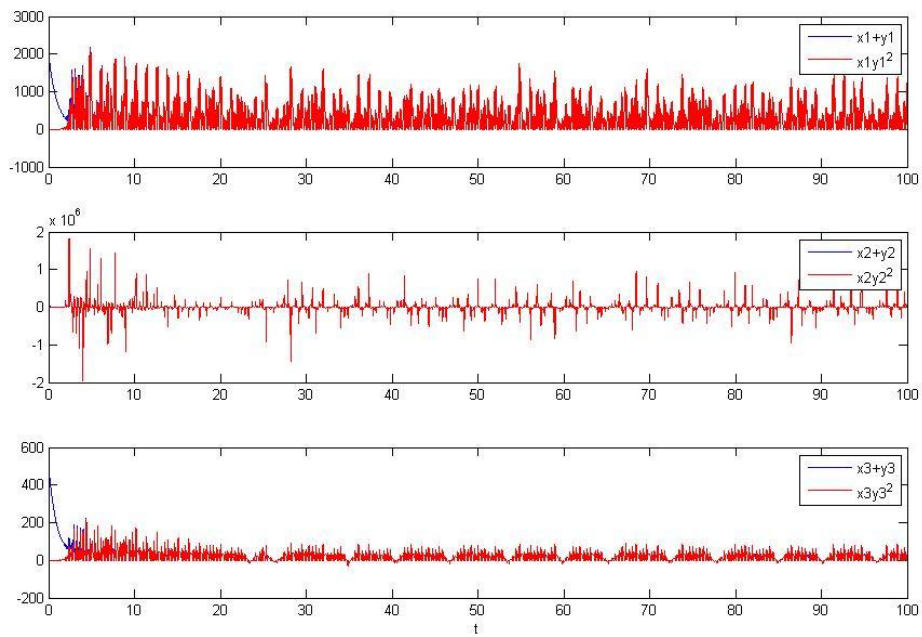
Fig. 4.10 Time histories of $x_i + y_i$ and $x_i y_i^2$ for Case 2.
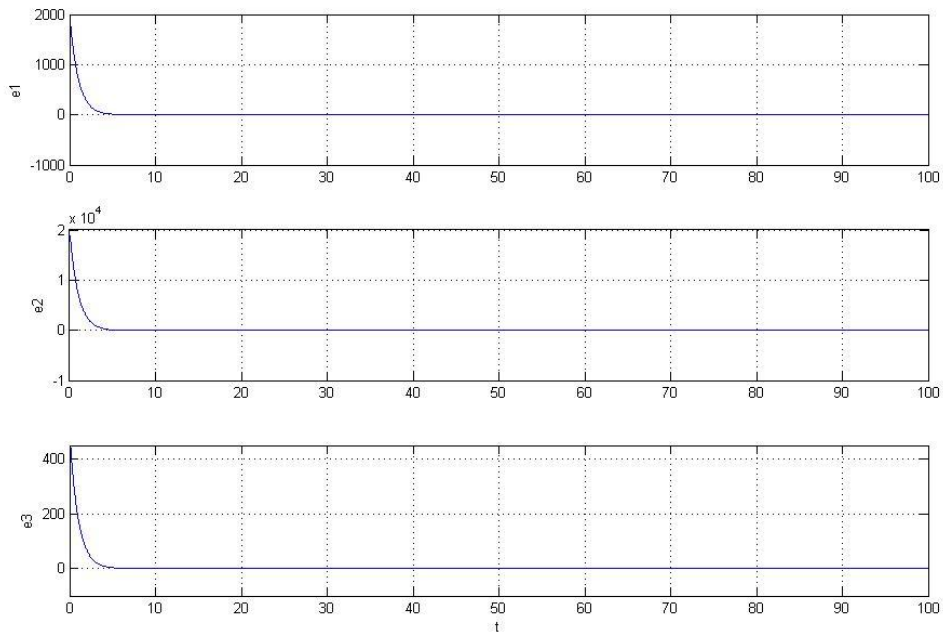
Fig. 4.11 Time histories of the state errors for Case 2.
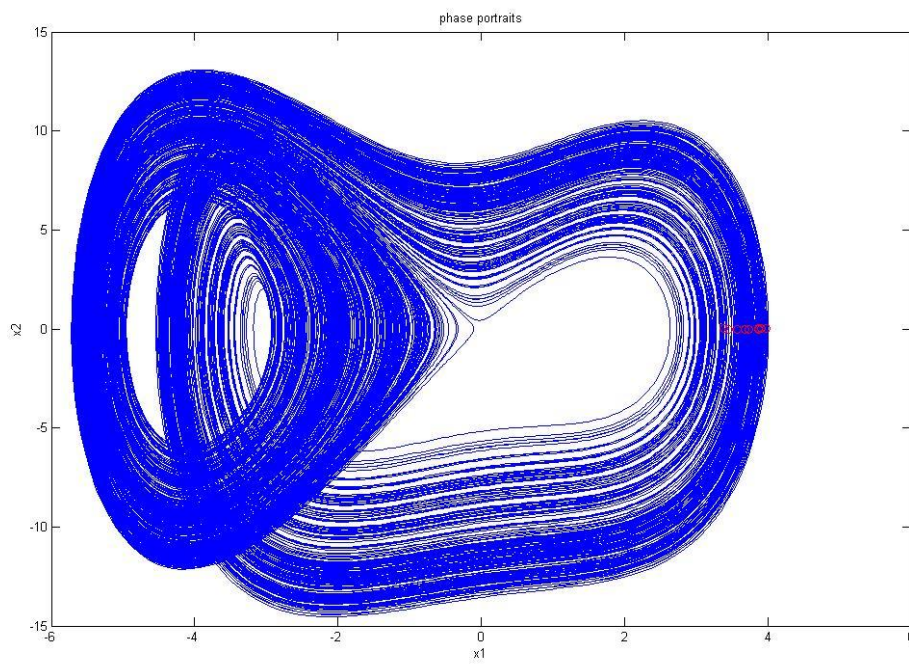
Fig. 4.12 The chaotic attractor of a new Double Ge-Ku system.
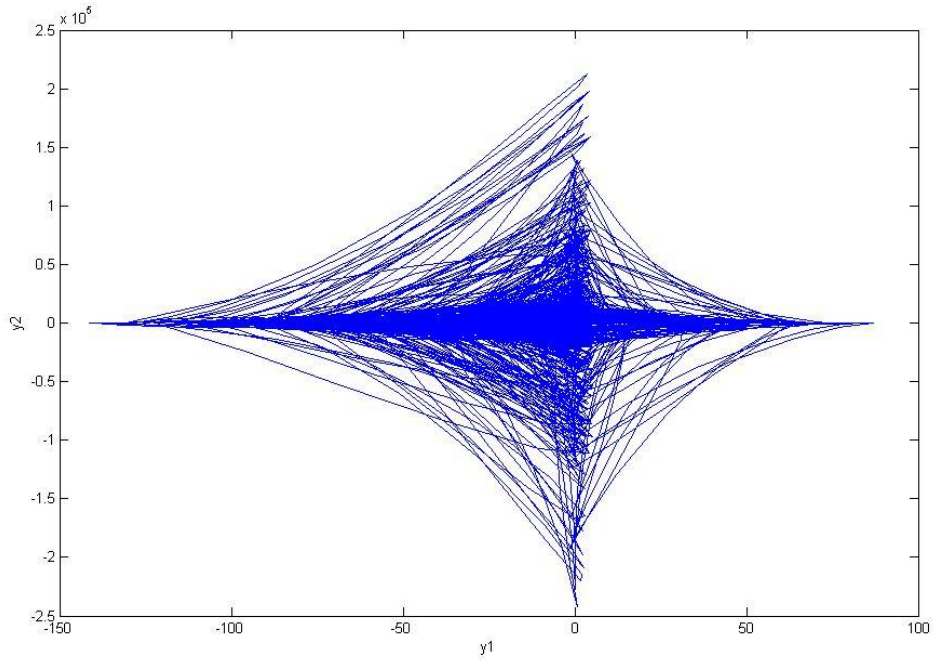
Fig. 4.13 Phase portrait of the controlled Ge-Ku-Duffing system for Case 3.
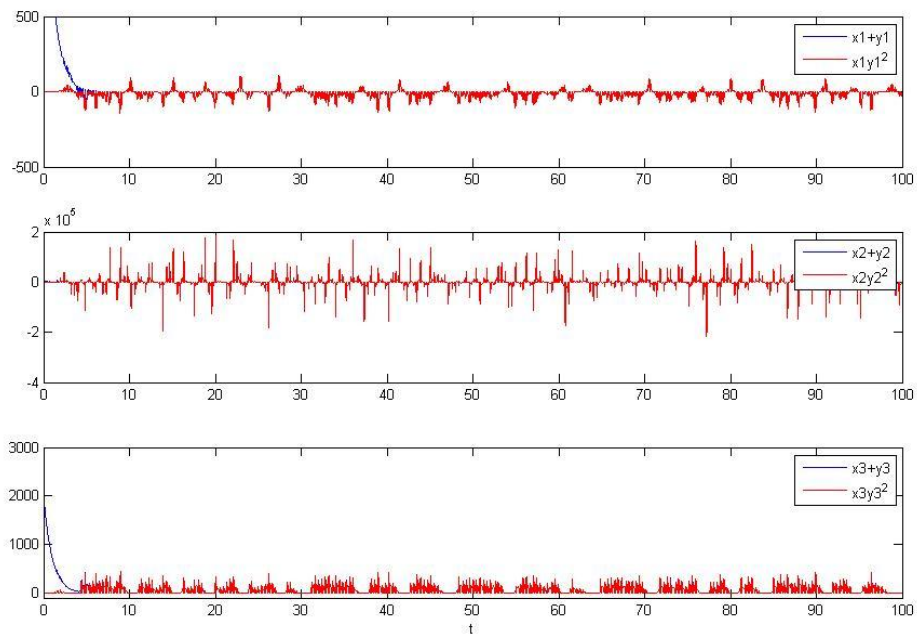
Fig. 4.14 Time histories of $x_i + y_i$ and $x_i y_i^2$ for Case 3
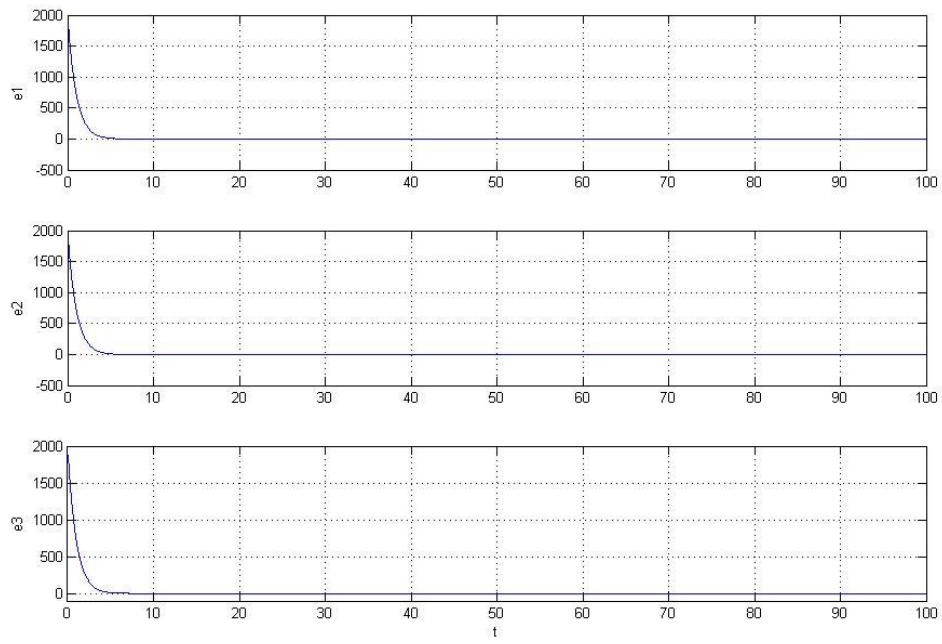
Fig. 4.15 Time histories of the state errors for Case 3.
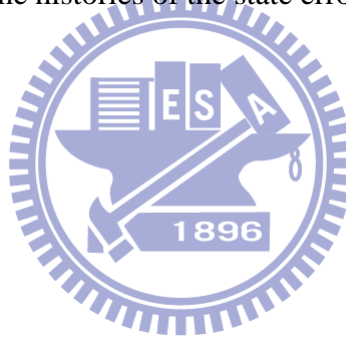
Chapter 5

Multiple Symplectic Synchronization for

Ge-Ku-Duffing System

5.1 Preliminary

In this Chapter, a new type of synchronization, multiple symplectic synchronization is studied. Symplectic synchronization and double symplectic synchronization are special cases of the multiple symplectic synchronization. When the double symplectic functions is extended to a more general form, $\mathbf{G}(x, y, z, ..., w, t) = \mathbf{F}(x, y, z, ..., w, t)$, it is called "multiple symplectic synchronization". The multiple symplectic synchronization may be applied to increase the security of secret communication due to the complexity of its synchronization form.

5.2 Multiple Symplectic Synchronization Scheme

Generalized synchronization refers to a functional relation between the state vectors of master and of slave, i.e. $y = \mathbf{F}(x, t)$, where x and y are the state vectors of master and slave. Recently[50], generalized synchronization is extended to a more general form, $y = \mathbf{F}(x, y, t)$. This means that the final desired state y of the "slave" system not only depends upon the "master" system state x but also depends upon the state y itself. Therefore the "slave" system is not traditional pure slave obeying the master system completely but plays a role to determine the final desired state of the "slave" system. This kind of synchronization, is called "symplectic synchronization", and the "master" system is called Partner A, the "slave" system is called Partner B.

Since the symplectic functions are presented at both the right hand side and the

left hand side of the equality, it is called double symplectic synchronization, $\mathbf{G}(x, y, t) = \mathbf{F}(x, y, t)$, where x, y are state vectors of Partner A and Partner B, respectively, $\mathbf{G}(x, y, t)$ and $\mathbf{F}(x, y, t)$ are given vector functions of x,y and time.

When the double symplectic functions is extended to a more general form, $\mathbf{G}(x, y, z, ..., w, t) = \mathbf{F}(x, y, z, ..., w, t)$, it is called "multiple symplectic synchronization", where $x, y, z, ..., w$ are state vectors of studied systems. $\mathbf{G}(x, y, z, ..., w, t)$ and $\mathbf{F}(x, y, z, ..., w, t)$ are given vector functions of $x, y, z, ..., w$ and time.

5.3 Synchronization of Three Different Chaotic Systems

Case 1.

Consider a new Ge-Ku-van der Pol(GKv)system is described by

$$
\begin{aligned}
\dot{x}_1 &= x_2, \\
\dot{x}_2 &= -ax_2 - x_3\left[b\left(c - x_1^2\right) + dx_3\right], \\
\dot{x}_3 &= -gx_3 - h\left(1 - x_3^2\right)x_2 + lx_1,
\end{aligned}
\tag{5.1}
$$

where $a = 0.08, b = -0.35, c = 100.56, d = -1000.02, g = 0.61, h = 0.08, l = 0.01$ and the initial condition is $x_1(0) = 0.01, x_2(0) = 0.01, x_3(0) = 0.01$. The chaotic attractor of the new Ge-Ku-van der Pol system is shown in Fig. 5.1.

The Chen system is described by

$$
\begin{aligned}
\dot{z}_1 &= a_1 z_2 - a_1 z_1, \\
\dot{z}_2 &= \left(c_1 - a_1\right) z_1 - z_1 z_3 + c_1 z_2, \\
\dot{z}_3 &= z_1 z_2 - b_1 z_3,
\end{aligned}
\tag{5.2}
$$

where $a_1 = 35, b_1 = 3, c_1 = 28$ and the initial condition is $z_1(0) = 0.5, z_2(0) = 0.26, z_3(0) = 0.35$. The chaotic attractor of the Chen system is shown in Fig. 5.2.

The controlled Ge-Ku-Duffing(GKD) system is described by

49

$$\dot{y}_1 = y_2 + u_1,$$
$$\dot{y}_2 = -ky_2 - y_1\left[m\left(r - y_1^2\right) + sy_3\right] + u_2, \tag{5.3}$$
$$\dot{y}_3 = -y_3 - y_3^3 - ny_2 + wy_1 + u_3,$$

where $k = 0.1, m = 11, r = 40, s = 54, n = 6, w = 30$, $\mathbf{u} = [u_1, u_2, u_3]^{\mathrm{T}}$ is the controller,

and the initial condition is $y_1(0) = 2$, $y_2(0) = 2.4$, $y_3(0) = 5$. The chaotic attractor of

uncontrolled Ge-Ku-Duffing system is shown in Fig. 5.3. The Lyapunov exponents

and the bifurcation diagram of uncontrolled GKD system are shown in Fig. 5.4 and

Fig. 5.5.

$$\text{Define } \mathbf{G}(x, y, z, t) = \begin{bmatrix} x_1 + y_1 + z_1 \\ x_2 + y_2 + z_2 \\ x_3 + y_3 + z_3 \end{bmatrix}, \quad \mathbf{F}(x, y, z, t) = \begin{bmatrix} x_1 y_1 z_1 + x_2 y_2 z_1 + x_3 y_3 z_1 \\ x_1 y_1 z_2 + x_2 y_2 z_2 + x_3 y_3 z_2 \\ x_1 y_1 z_3 + x_2 y_2 z_3 + x_3 y_3 z_3 \end{bmatrix},$$

and our goal is to achieve the multiple symplectic synchronization

$\mathbf{G}(x, y, z, t) = \mathbf{F}(x, y, z, t)$.

Define $\mathbf{e} = \mathbf{G}(x, y, z, t) - \mathbf{F}(x, y, z, t)$. Thus we design the controller as

$$
\begin{aligned}
u_1 = -\{&x_2 + y_2 + a_1 z_2 - a_1 z_1 - x_2 y_1 z_1 - x_1 y_2 z_1 - x_1 y_1 \left(a_1 z_2 - a_1 z_1\right) \\
&- \left(-ax_2 - x_3(b(c - x_1^2) + dx_3)\right) y_2 z_1 - \left(-ky_2 - y_1(m(r - y_1^2) + sy_3)\right) x_2 z_1 \\
&- (a_1 z_2 - a_1 z_1) x_2 y_2 - (-gx_3 + h(1 - x_3^2) x_2 + lx_2) y_3 z_1 \\
&- (-y_3 - y_3^3 - ky_2 + wy_1) x_3 z_1 - \left(a_1 z_2 - a_1 z_1\right) x_3 y_3 + x_1 + y_1 + z_1 - x_1 y_1 z_1 \\
&- x_2 y_2 z_1 - x_3 y_3 z_1\},
\end{aligned}
$$

$$
\begin{aligned}
u_2 = -\{&-ax_2 - x_3(b(c - x_1^2) + dx_3) + (-ky_2 - y_1(m(r - y_1^2) + sy_3)) \\
&+ ((c_1 - a_1) z_1 - z_1 z_3 + c_1 z_2) - x_2 y_1 z_2 - x_1 y_2 z_2 - x_1 y_1 \left((c_1 - a_1) z_1 - z_1 z_3 + c_1 z_2\right) \\
&- \left(-ax_2 - x_3(b(c - x_1^2) + dx_3)\right) y_2 z_2 - \left(-ky_2 - y_1(m(r - y_1^2) + sy_3)\right) x_2 z_2 \\
&- ((c_1 - a_1) z_1 - z_1 z_3 + c_1 z_2) x_2 y_2 - (-gx_3 + h(1 - x_3^2) x_2 + lx_2) y_3 z_2 \\
&- (-y_3 - y_3^3 - ky_2 + wy_1) x_3 z_2 - \left((c_1 - a_1) z_1 - z_1 z_3 + c_1 z_2\right) x_3 y_3 + x_2 + y_2 + z_2 \\
&- x_1 y_1 z_2 - x_2 y_2 z_2 - x_3 y_3 z_2\}
\end{aligned}
$$

$$u_3 = -\{(-gx_3 + h(1 - x_3^2)x_2 + lx_1) + (-y_3 - y_3^3 - ky_2 + wy_1)$$
$$+ (z_1 z_2 - b_1 z_3) - x_2 y_1 z_3 - x_1 y_2 z_3 - x_1 y_1 (z_1 z_2 - b_1 z_3)$$
$$- (-ax_2 - x_3(b(c - x_1^2) + dx_3)) y_2 z_3 - (-ky_2 - y_1(m(r - y_1^2) + sy_3)) x_2 z_3$$
$$- (z_1 z_2 - b_1 z_3)x_2 y_2 - (-gx_3 + h(1 - x_3^2)x_2 + lx_2) y_3 z_3$$
$$- (-y_3 - y_3^3 - ky_2 + wy_1)x_3 z_3 - (z_1 z_2 - b_1 z_3) x_3 y_3 + x_3 + y_3 + z_3 - x_1 y_1 z_3$$
$$- x_2 y_2 z_3 - x_3 y_3 z_3\}$$

When the multiple symplectic synchronization is achieved, the phase portrait of
the controlled Ge-Ku-Duffing system and the time histories of the state errors and the
time histories of $\mathbf{G}(x, y, z, t)$ and $\mathbf{F}(x, y, z, t)$ are shown in Fig. 5.6 and Fig. 5.7 and
Fig. 5.8, respectively.

Case 2.

Consider a new Ge-Ku-Mathieu(GKM) system is described by

$$\dot{x}_1 = x_2,$$
$$\dot{x}_2 = -ax_2 - x_1 \left[b(c - x_1^2) + dx_2 x_3 \right], \tag{5.4}$$
$$\dot{x}_3 = -(g + hx_1)x_3 + lx_2 + px_1 x_3,$$

where $a = -0.6, b = 5, c = 11, d = 0.3, g = 8, h = 10, l = 0.5, p = 0.2$, and the initial
conditions are $x_1(0) = 0.01$, $x_2(0) = 0.01$, $x_3(0) = 0.01$. The chaotic attractor of the
new Ge-Ku Mathieu system is shown in Fig. 5.9.

The *Rössler* system is described by

$$\dot{z}_1 = -z_2 - z_3,$$
$$\dot{z}_2 = z_1 + a_1 z_2, \tag{5.5}$$
$$\dot{z}_3 = b_1 + z_1 z_3 - c_1 z_3,$$

where $a_1 = 0.15$, $b_1 = 0.2$, $c_1 = 10$ and the initial condition is
$z_1(0) = 2, z_2(0) = 2.4, z_3(0) = 5$. The chaotic attractor of the *Rössler* system is
shown in Fig. 5.10.

The controlled Ge-Ku-Duffing(GKD) system is described by

$$\dot{y}_1 = y_2 + u_1,$$
$$\dot{y}_2 = -ky_2 - y_1 \left[m\left(r - y_1^2\right) + sy_3 \right] + u_2, \tag{5.6}$$
$$\dot{y}_3 = -y_3 - y_3^3 - ny_2 + wy_1 + u_3,$$

where $k = 0.1, m = 11, r = 40, s = 54, n = 6, w = 30$, $\mathbf{u} = [u_1, u_2, u_3]^{\mathrm{T}}$ is the controller,

and the initial condition is $y_1(0) = 2$, $y_2(0) = 2.4$, $y_3(0) = 5$. The chaotic attractor of

uncontrolled Ge-Ku-Duffing system is shown in Fig. 5.3. The Lyapunov exponents

and the bifurcation diagram of uncontrolled GKD system are shown in Fig. 5.4 and

Fig. 5.5.

$$\text{Define} \quad \mathbf{G}(x, y, z, t) = \begin{bmatrix} x_1 + y_1 + z_1 \\ x_2 + y_2 + z_2 \\ x_3 + y_3 + z_3 \end{bmatrix} \quad, \quad \mathbf{F}(x, y, z, t) = \begin{bmatrix} x_1 y_1 z_1^2 + x_2 y_2 z_1^2 + x_3 y_3 z_1^2 \\ x_1 y_1 z_2^2 + x_2 y_2 z_2^2 + x_3 y_3 z_2^2 \\ x_1 y_1 z_3^2 + x_2 y_2 z_3^2 + x_3 y_3 z_3^2 \end{bmatrix},$$

and our goal is to achieve the multiple symplectic synchronization

$$\mathbf{G}(x, y, z, t) = \mathbf{F}(x, y, z, t).$$

Define $\mathbf{e} = \mathbf{G}(x, y, z, t) - \mathbf{F}(x, y, z, t)$. Thus we design the controller as

$$
\begin{aligned}
u_1 = -\{ & x_2 + y_2 - z_2 - z_3 - x_2 y_1 z_1^2 - x_1 y_2 z_1^2 - 2x_1 y_1 z_1 (-z_2 - z_3) \\
& - \left(-ax_2 - x_1 \left[b\left(c - x_1^2\right) + dx_2 x_3 \right] \right) y_2 z_1^2 - \left(-ky_2 - y_1 (m(r - y_1^2) + sy_3) \right) x_2 z_1^2 \\
& - 2x_2 y_2 z_1 (-z_2 - z_3) - (-(g + hx_1) x_3 + lx_2 + px_1 x_3) y_3 z_1^2 \\
& - (-y_3 - y_3^3 - ky_2 + wy_1) x_3 z_1^2 - 2x_3 y_3 z_1 (-z_2 - z_3) + x_1 + y_1 + z_1 - x_1 y_1 z_1^2 \\
& - x_2 y_2 z_1^2 - x_3 y_3 z_1^2 \}
\end{aligned}
$$

,

$$
\begin{aligned}
u_2 = -\{ & (-ax_2 - x_1 \left[b\left(c - x_1^2\right) + dx_2 x_3 \right]) + (-ky_2 - y_1 (m(r - y_1^2) + sy_3)) \\
& + (z_1 + a_1 z_2) - x_2 y_1 z_2^2 - x_1 y_2 z_2^2 - 2x_1 y_1 z_2 (z_1 + a_1 z_2) \\
& - \left(-ax_2 - x_1 \left[b\left(c - x_1^2\right) + dx_2 x_3 \right] \right) y_2 z_2^2 \\
& - \left(-ky_2 - y_1 (m(r - y_1^2) + sy_3) \right) x_2 z_2^2 - 2x_2 y_2 z_2 (z_1 + a_1 z_2) \\
& - (-(g + hx_1) x_3 + lx_2 + px_1 x_3) y_3 z_2^2 - (-y_3 - y_3^3 - ky_2 + wy_1) x_3 z_2^2 \\
& - 2x_3 y_3 z_2 (z_1 + a_1 z_2) + x_2 + y_2 + z_2 - x_1 y_1 z_2^2 - x_2 y_2 z_2^2 - x_3 y_3 z_2^2 \}
\end{aligned}
$$

$$
\begin{aligned}
u_3 = -\{&(-\left(g+hx_1\right)x_3 + lx_2 + px_1x_3) + (-y_3 - y_3^3 - ky_2 + wy_1) \\
&+ (b_1 + z_1z_3 - c_1z_3) - x_2y_1z_3^2 - x_1y_2z_3^2 - 2x_1y_1z_3\left(b_1 + z_1z_3 - c_1z_3\right) \\
&- \left(-ax_2 - x_1\left[b\left(c - x_1^2\right) + dx_2x_3\right]\right)y_2z_3^2 - \left(-ky_2 - y_1(m(r - y_1^2) + sy_3)\right)x_2z_3^2 \\
&- 2x_2y_2z_3(b_1 + z_1z_3 - c_1z_3) - (-\left(g+hx_1\right)x_3 + lx_2 + px_1x_3)y_3z_3^2 \\
&- (-y_3 - y_3^3 - ky_2 + wy_1)x_3z_3^2 - 2x_3y_3z_3\left(b_1 + z_1z_3 - c_1z_3\right) + x_3 + y_3 + z_3 - x_1y_1z_3^2 \\
&- x_2y_2z_3^2 - x_3y_3z_3^2\}
\end{aligned}
$$

When the multiple symplectic synchronization is achieved, the phase portrait of the controlled Ge-Ku-Duffing system and the time histories of the state errors and the time histories of $\mathbf{G}(x, y, z, t)$ and $\mathbf{F}(x, y, z, t)$ are shown in Fig. 5.11 and Fig. 5.12 and Fig. 5.13, respectively.

Case 3.

Consider a new Double Ge-Ku system is described by

$$
\begin{aligned}
\dot{x}_1 &= x_2, \\
\dot{x}_2 &= -ax_2 - x_1\left[b\left(c - x_1^2\right) + dx_3\right], \\
\dot{x}_3 &= -ax_3 - x_3\left[b\left(c - x_3^2\right) + ex_1\right],
\end{aligned}
\tag{5.7}
$$

where $a = -0.5, b = -1.4, c = 1.9, d = 54, e = 6.2$ and the initial conditions are $x_1(0) = 0.01, x_2(0) = 0.01, x_3(0) = 0.01$. The chaotic attractor of the new Double Ge-Ku system is shown in Fig. 5.14.

The Li system is described by

$$
\begin{aligned}
\dot{z}_1 &= -a_1z_2 - a_1z_1, \\
\dot{z}_2 &= -z_1z_3 + c_1z_2, \\
\dot{z}_3 &= z_1z_2 - b_1z_3,
\end{aligned}
\tag{5.8}
$$

where $a_1 = 36, \ b_1 = 3, \ c_1 = 20$ and the initial condition is $z_1(0) = 0.2, z_2(0) = 0.35, z_3(0) = 0.2$. The chaotic attractor of the Li system is shown in Fig. 5.15.

The controlled Ge-Ku-Duffing(GKD) system is described by

$$\dot{y}_1 = y_2 + u_1,$$
$$\dot{y}_2 = -ky_2 - y_1\left[m\left(r - y_1^2\right) + sy_3\right] + u_2, \qquad (5.9)$$
$$\dot{y}_3 = -y_3 - y_3^3 - ny_2 + wy_1 + u_3,$$

where $k = 0.1, m = 11, r = 40, s = 54, n = 6, w = 30$, $\mathbf{u} = [u_1, u_2, u_3]^{\mathrm{T}}$ is the controller, and the initial condition is $y_1(0) = 2$, $y_2(0) = 2.4$, $y_3(0) = 5$. The chaotic attractor of uncontrolled Ge-Ku-Duffing system is shown in Fig. 5.3. The Lyapunov exponents and the bifurcation diagram of uncontrolled GKD system are shown in Fig. 5.4 and Fig. 5.5.

$$\text{Define} \quad \mathbf{G}(x,y,z,t) = \begin{bmatrix} x_1 + y_1 + z_1 \\ x_2 + y_2 + z_2 \\ x_3 + y_3 + z_3 \end{bmatrix}, \quad \mathbf{F}(x,y,z,t) = \begin{bmatrix} x_1^2 y_1 z_1 + x_2^2 y_2 z_1 + x_3^2 y_3 z_1 \\ x_1^2 y_1 z_2 + x_2^2 y_2 z_2 + x_3^2 y_3 z_2 \\ x_1^2 y_1 z_3 + x_2^2 y_2 z_3 + x_3^2 y_3 z_3 \end{bmatrix},$$

and our goal is to achieve the multiple symplectic synchronization

$$\mathbf{G}(x,y,z,t) = \mathbf{F}(x,y,z,t).$$

Define $\mathbf{e} = \mathbf{G}(x,y,z,t) - \mathbf{F}(x,y,z,t)$. Thus we design the controller as

$$
\begin{aligned}
u_1 = -\Big\{ & x_2 + y_2 - a_1 z_2 - a_1 z_1 - 2x_1 x_2 y_1 z_1 - x_1^2 y_2 z_1 - x_1^2 y_1 (-a_1 z_2 - a_1 z_1) \\
& - 2x_2 y_2 z_1 \left(-ax_2 - x_1\left[b\left(c - x_1^2\right) + dx_3\right]\right) - \left(-ky_2 - y_1(m(r - y_1^2) + sy_3)\right) x_2^2 z_1 \\
& - x_2^2 y_2 (-a_1 z_2 - a_1 z_1) - 2x_3 y_3 z_1 \left(-ax_3 - x_3\left[b\left(c - x_3^2\right) + ex_1\right]\right) \\
& - (-y_3 - y_3^3 - ky_2 + wy_1) x_3^2 z_1 - x_3^2 y_3 \left(-a_1 z_2 - a_1 z_1\right) + x_1 + y_1 + z_1 - x_1^2 y_1 z_1 \\
& - x_2^2 y_2 z_1 - x_3^2 y_3 z_1 \Big\}
\end{aligned}
\quad ,
$$

$$
\begin{aligned}
u_2 = -\Big\{ & \left(-ax_2 - x_1\left[b\left(c - x_1^2\right) + dx_3\right]\right) + \left(-ky_2 - y_1(m(r - y_1^2) + sy_3)\right) \\
& + (-z_1 z_3 + c_1 z_2) - 2x_1 x_2 y_1 z_2 - x_1^2 y_2 z_2 - x_1^2 y_1 \left(-z_1 z_3 + c_1 z_2\right) \\
& - 2x_2 y_2 z_2 \left(-ax_2 - x_1\left[b\left(c - x_1^2\right) + dx_3\right]\right) - \left(-ky_2 - y_1(m(r - y_1^2) + sy_3)\right) x_2^2 z_2 \\
& - x_2^2 y_2 (-z_1 z_3 + c_1 z_2) - 2x_3 y_3 z_2 \left(-ax_3 - x_3\left[b\left(c - x_3^2\right) + ex_1\right]\right) \\
& - (-y_3 - y_3^3 - ky_2 + wy_1) x_3^2 z_2 - x_3^2 y_3 \left(-z_1 z_3 + c_1 z_2\right) + x_2 + y_2 + z_2 - x_1^2 y_1 z_2 \\
& - x_2^2 y_2 z_2 - x_3^2 y_3 z_2 \Big\}
\end{aligned}
$$

$$u_3 = -\{(-ax_3 - x_3\left[b\left(c - x_3^2\right) + ex_1\right]) + (-y_3 - y_3^3 - ky_2 + wy_1)$$
$$+ (z_1 z_2 - b_1 z_3) - 2x_1 x_2 y_1 z_3 - x_1^2 y_2 z_3 - x_1^2 y_1\left(z_1 z_2 - b_1 z_3\right)$$
$$- 2x_2 y_2 z_3\left(-ax_2 - x_1\left[b\left(c - x_1^2\right) + dx_3\right]\right) - \left(-ky_2 - y_1(m(r - y_1^2) + sy_3)\right)x_2^2 z_3$$
$$- x_2^2 y_2(z_1 z_2 - b_1 z_3) - 2x_3 y_3 z_3(-ax_3 - x_3\left[b\left(c - x_3^2\right) + ex_1\right])$$
$$- (-y_3 - y_3^3 - ky_2 + wy_1)x_3^2 z_3 - x_3^2 y_3\left(z_1 z_2 - b_1 z_3\right) + x_3 + y_3 + z_3 - x_1^2 y_1 z_3$$
$$- x_2^2 y_2 z_3 - x_3^2 y_3 z_3\}$$

When the multiple symplectic synchronization is achieved, the phase portrait of the controlled Ge-Ku-Duffing system and the time histories of the state errors and the time histories of $\mathbf{G}(x, y, z, t)$ and $\mathbf{F}(x, y, z, t)$ are shown in Fig. 5.16 and Fig. 5.17 and Fig. 5.18, respectively.
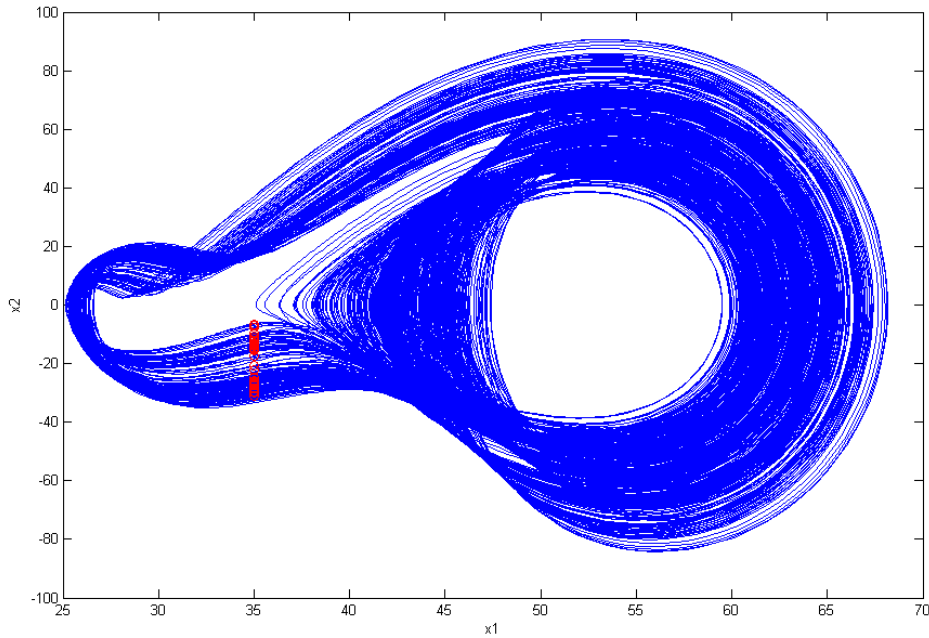
Fig. 5.1 The chaotic attractor of a new Ge-Ku-van der Pol system.
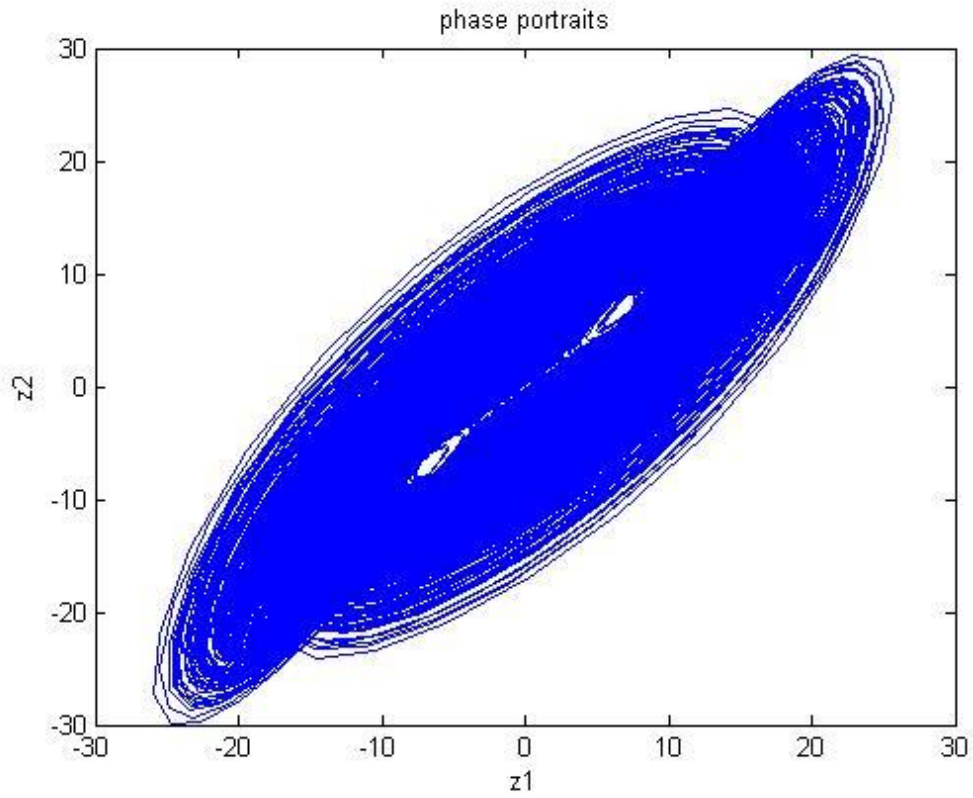
Fig. 5.2 The chaotic attractor of the Chen system.
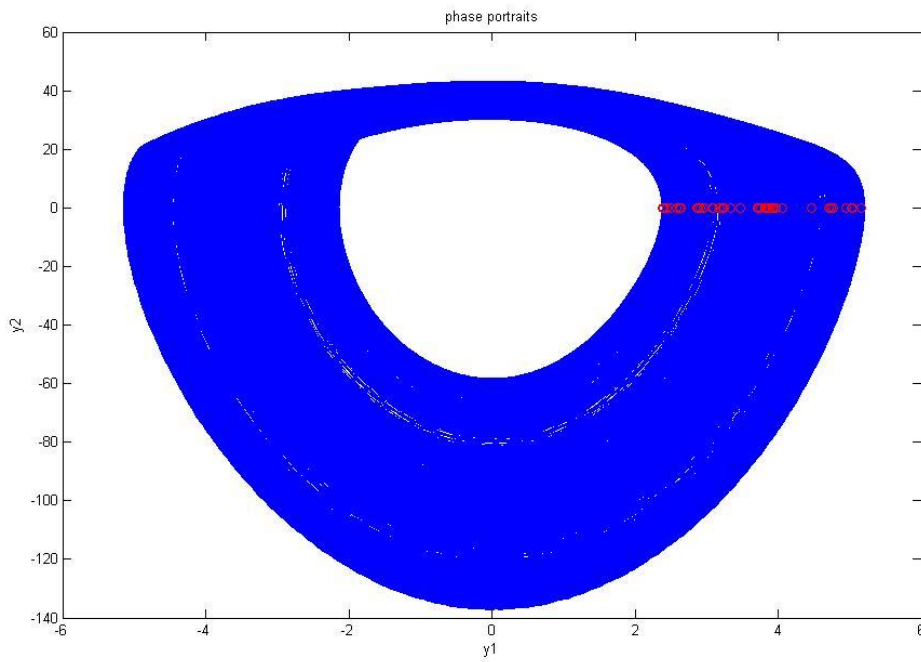
Fig. 5.3 The chaotic attractor of a uncontrolled new Ge-Ku-Duffing system.

Fig. 5.4 The Lyapunov exponents of a uncontrolled new Ge-Ku-Duffing system.

Fig. 5.5 The bifurcation diagram of a uncontrolled new Ge-Ku-Duffing system.
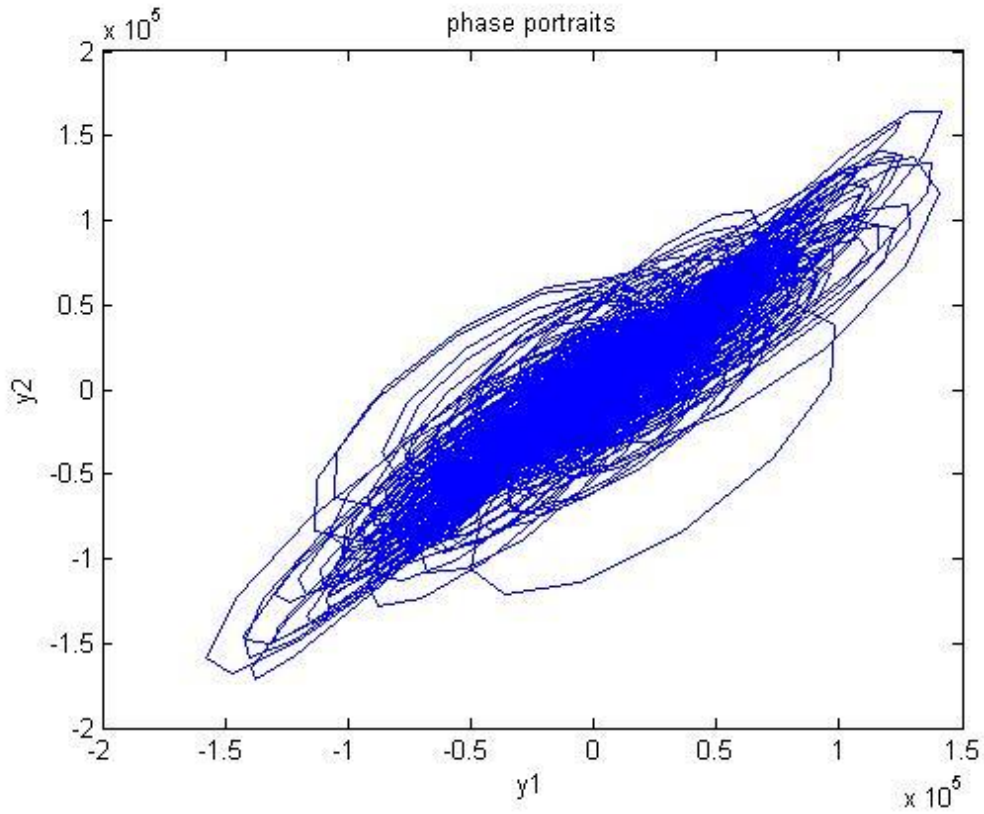
Fig. 5.6 Phase portrait of a controlled new Ge-Ku-Duffing system for Case 1.
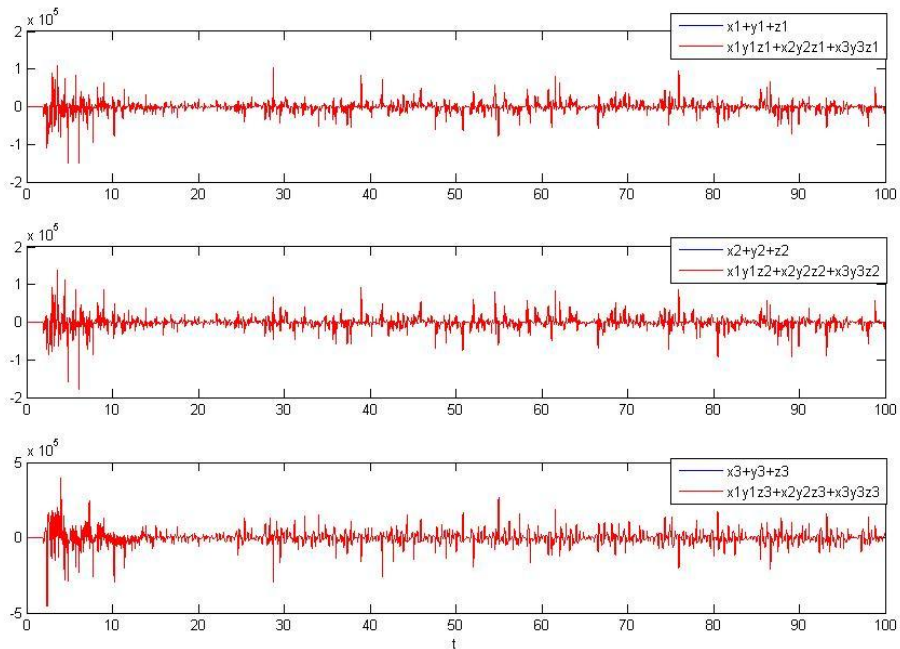
Fig. 5.7 Time histories of $\mathbf{G}(\mathbf{x}, \mathbf{y}, \mathbf{z}, t)$ and $\mathbf{F}(\mathbf{x}, \mathbf{y}, \mathbf{z}, t)$ for Case 1.
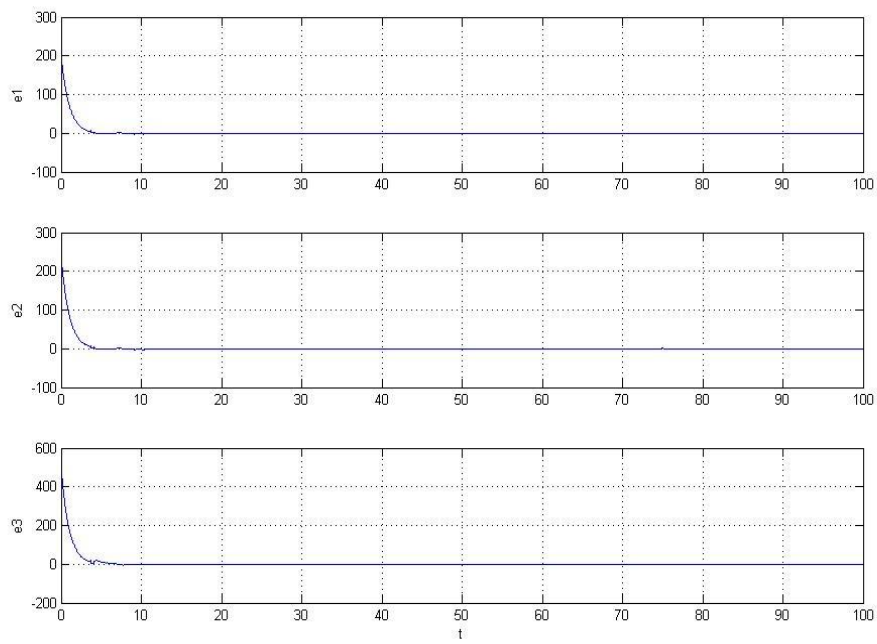
Fig. 5.8 Time histories of the state errors for Case 1.
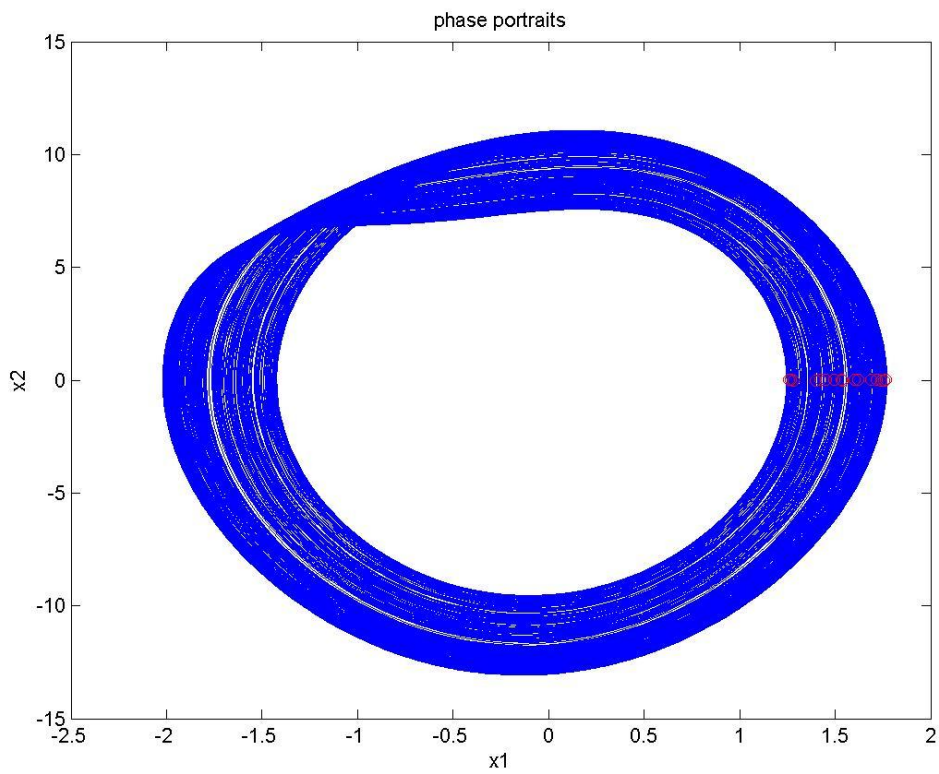
phase portraits

Fig. 5.9 The chaotic attractor of a new Ge-Ku-Mathieu system.
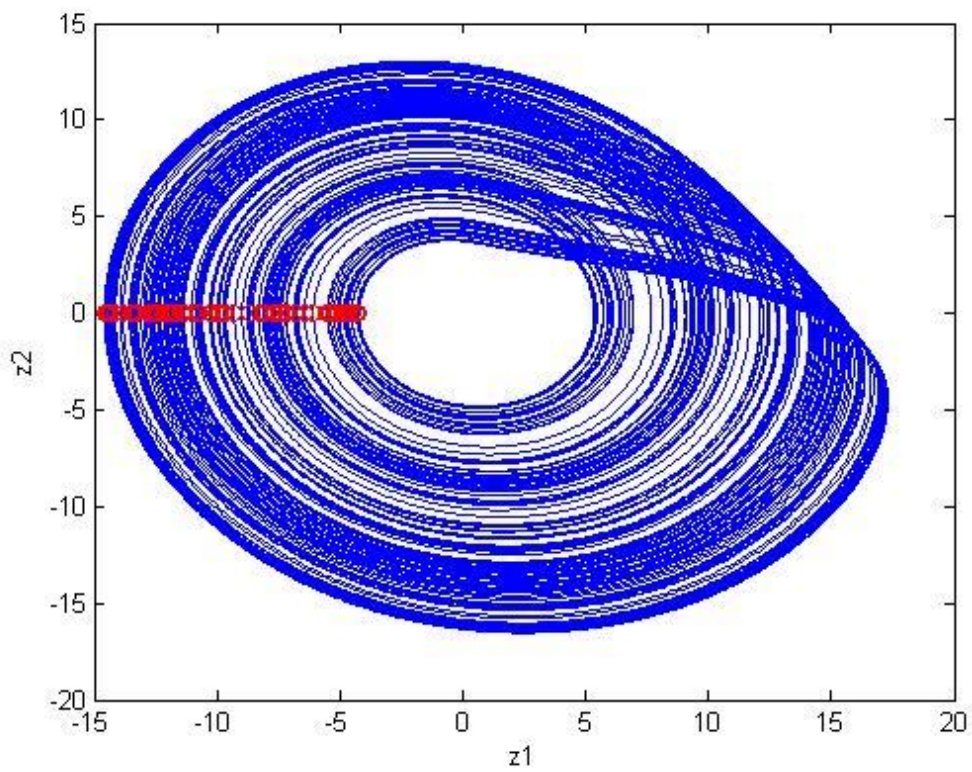
Fig. 5.10 The chaotic attractor of the *Rössler* system.
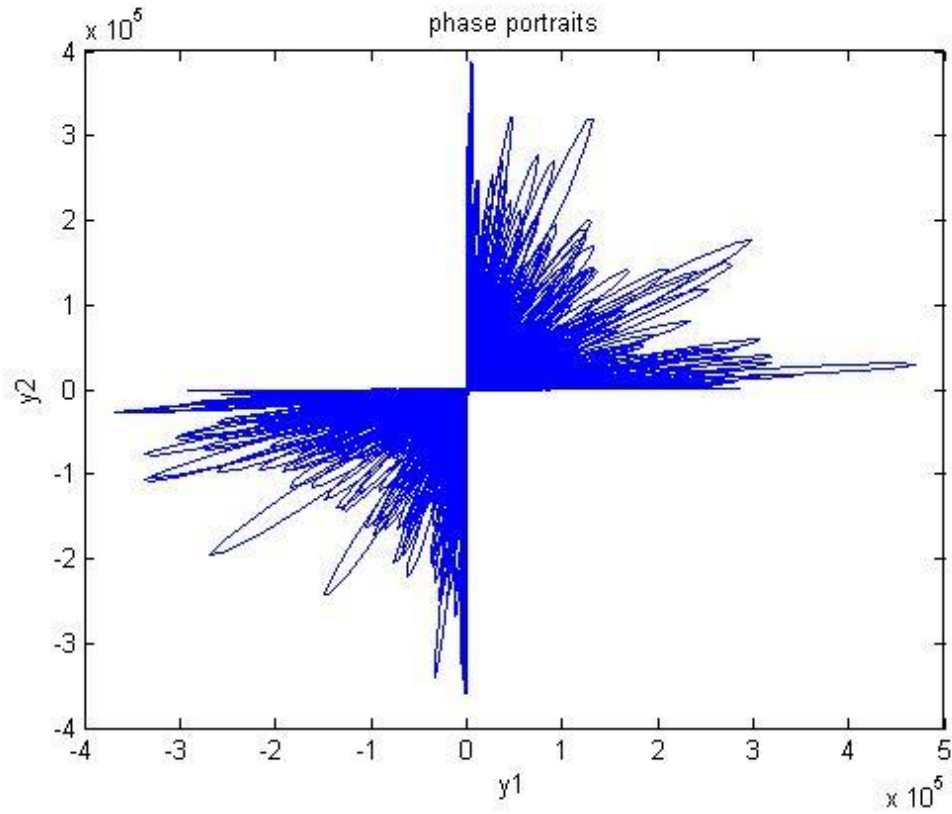
Fig. 5.11 Phase portrait of the controlled Ge-Ku-Duffing system for Case 2.
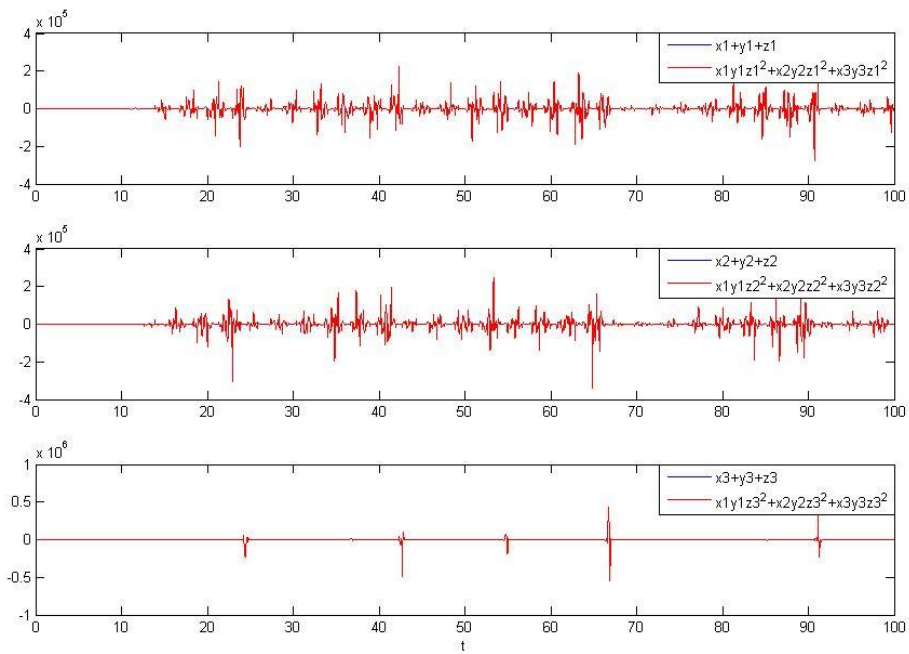
Fig. 5.12 Time histories of $\mathbf{G(x,y,z},t)$ and $\mathbf{F(x,y,z},t)$ for Case 2.

61
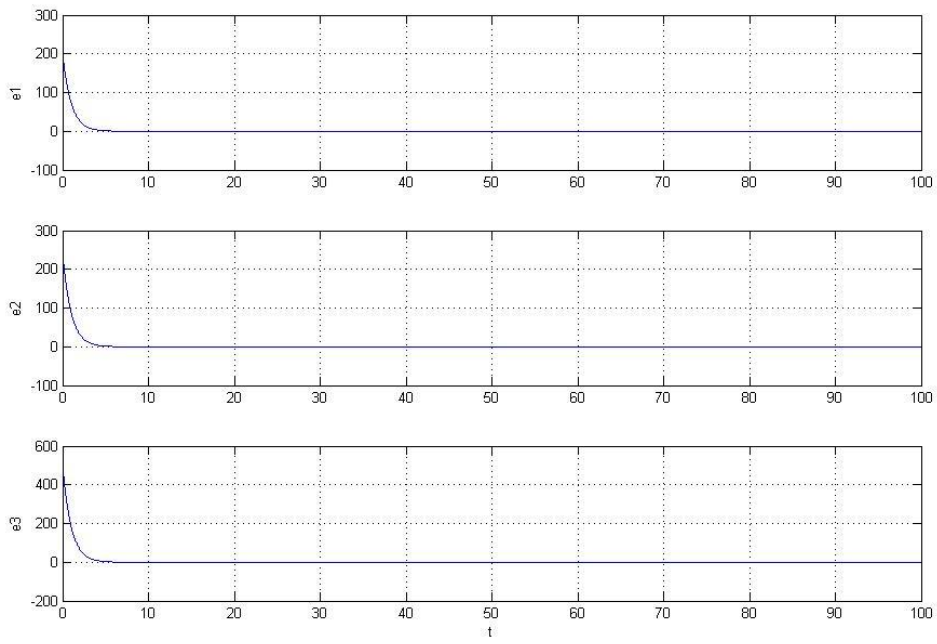
Fig. 5.13 Time histories of the state errors for Case 2.
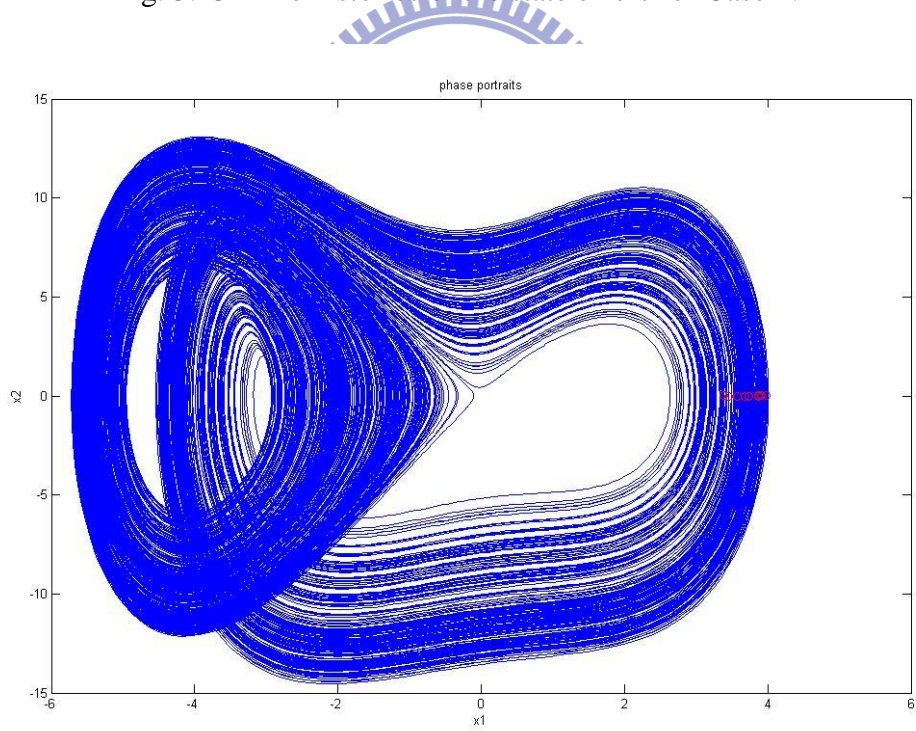
Fig. 5.14 The chaotic attractor of a new Double Ge-Ku system.
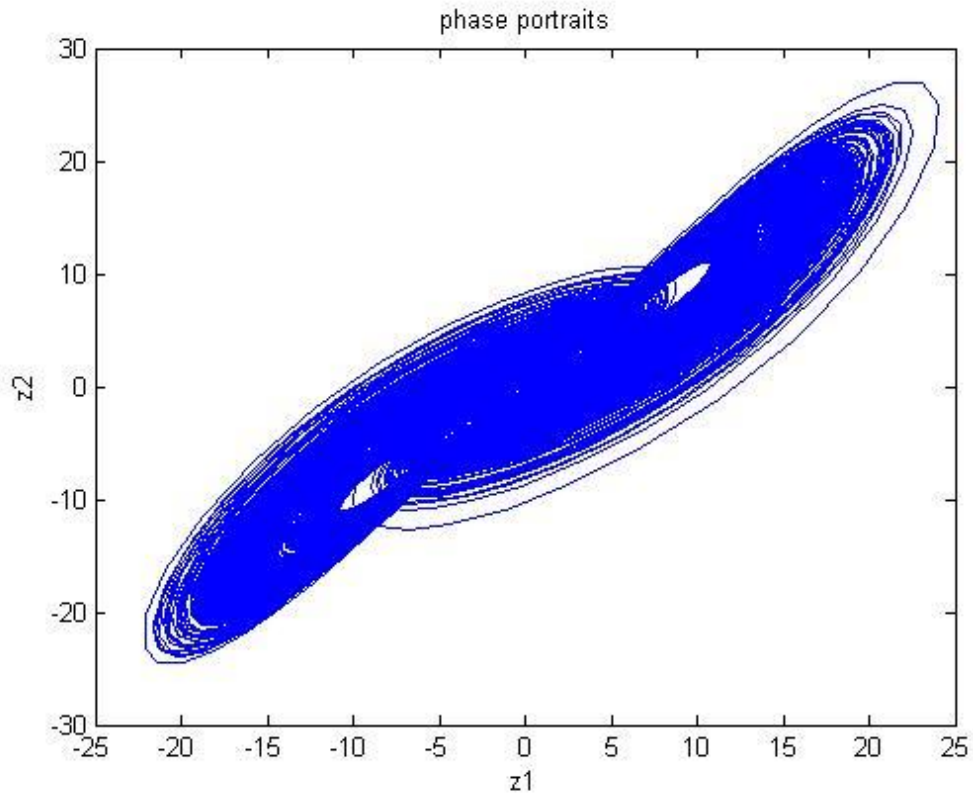
Fig. 5.15 The chaotic attractor of the *Lü* system.
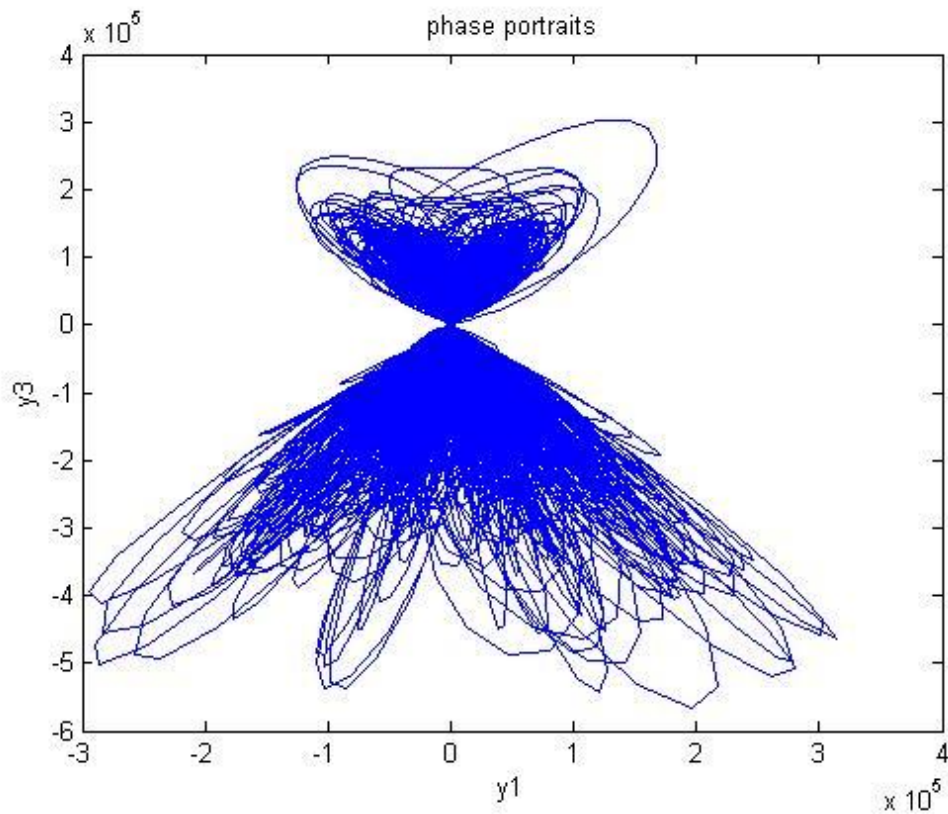
Fig. 5.16 Phase portrait of the controlled Ge-Ku-Duffing system for Case 3.
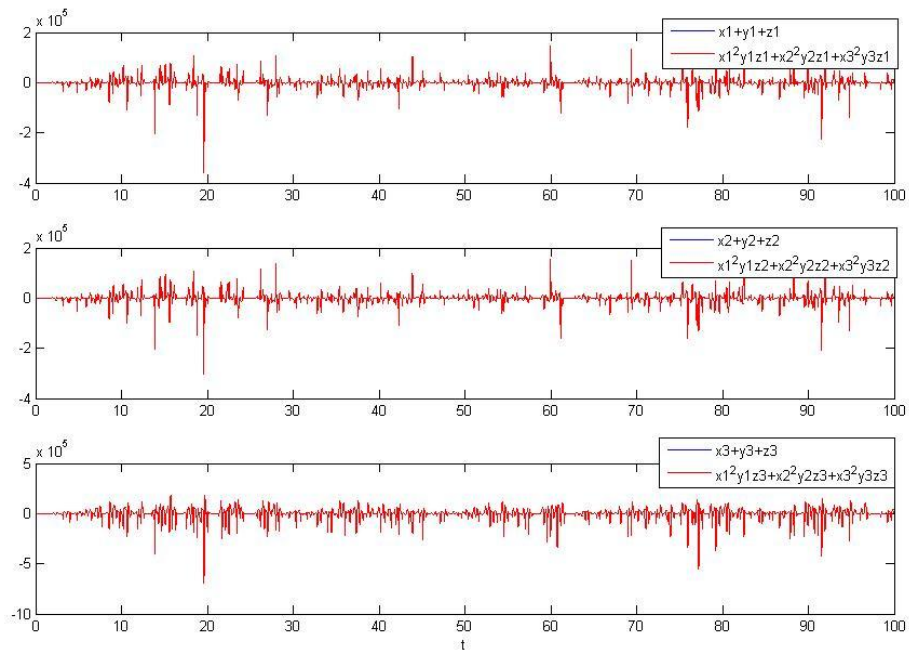
Fig. 5.17 Time histories of $\mathbf{G}(\mathbf{x}, \mathbf{y}, \mathbf{z}, t)$ and $\mathbf{F}(\mathbf{x}, \mathbf{y}, \mathbf{z}, t)$ for Case 3.
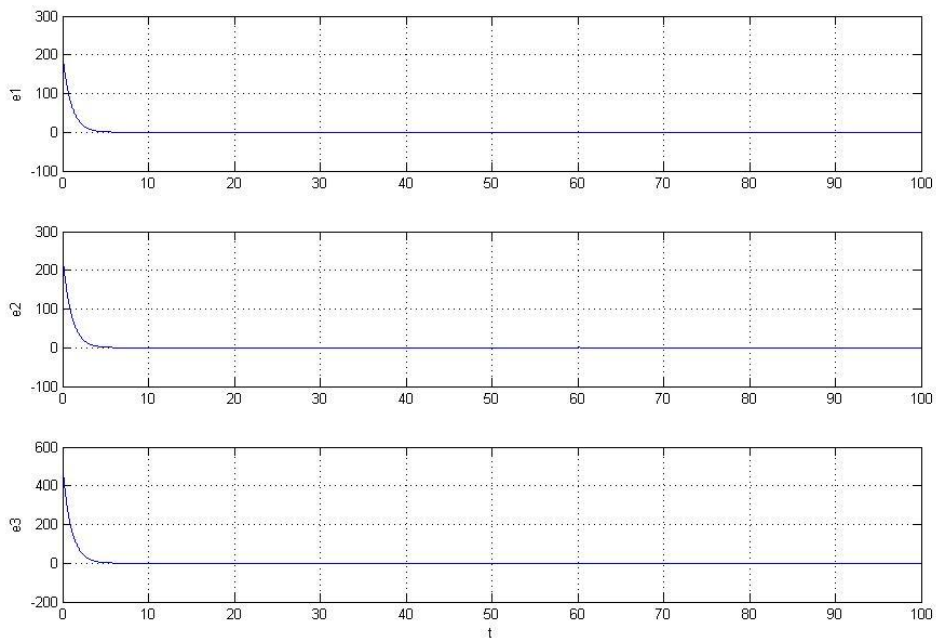
Fig. 5.18 Time histories of the state errors for Case 3.

Chapter 6

Fuzzy Modeling and Synchronization of Chaotic Systems via New Fuzzy Model

6.1 Preliminary

In this Chapter, a new fuzzy model [51] is used to simulate and synchronize two different chaotic systems. Via the new fuzzy model, a complicated nonlinear system is linearized to a simple form − linear coupling of only two linear subsystems and the numbers of fuzzy rules can be reduced from 2^N to $2 \times N$ (where N is the number of nonlinear terms). The fuzzy equations become much simpler.

6.2 New Fuzzy Model Theory

In system analysis and design, it is important to select an appropriate model representing a real system. As an expression model of a real plant, the fuzzy implications and the fuzzy reasoning method suggested by Takagi and Sugeno are traditionally used. The new fuzzy model is also described by fuzzy IF-THEN rules. The core of the new fuzzy model is that we express each nonlinear equation into two linear sub-equations by fuzzy IF-THEN rules and take all the first linear sub-equations to form one linear subsystem and all the second linear sub-equations to form another linear subsystem. The overall fuzzy model of the system is achieved by fuzzy blending of this two linear subsystem models. Consider a continuous-time nonlinear dynamic system as follows:

Equation i:

rule 1:

   IF $z_i(t)$ is M_{i1}

   THEN $\dot{x}_i(t) = A_{i1}x(t) + B_{i1}u(t)$,

65

rule 2:

IF $z_i(t)$ is M_{i2}

THEN $\dot{x}_i(t) = A_{i2}x(t) + B_{i2}u(t)$, (6.1)

where

$$x(t) = [x_1(t), x_2(t), ..., x_n(t)]^T,$$

$$u(t) = [u_1(t), u_2(t), ..., u_n(t)]^T,$$

$i = 1, 2 .. n$, where n is the number of nonlinear terms. $z_i(t)$ is the nonlinear term of $x(t)$, M_{i1}, M_{i2} are fuzzy sets, A_i, B_i are column vectors and $\dot{x}_i(t) = A_{ij}x(t) + B_{ij}u(t)$, $j = 1, 2$ is the output from the first and the second IF-THEN rules. Given a pair of $(\mathbf{x}(t), \mathbf{u}(t))$ and take all the first linear sub-equations to form one linear subsystem and all the second linear sub-equations to form another linear subsystem, the final output of the fuzzy system is inferred as follows:

$$\dot{x}(t) = M_1 \begin{bmatrix} A_{11}x(t) + B_{11}u(t) \\ A_{21}x(t) + B_{21}u(t) \\ \vdots \\ A_{i1}x(t) + B_{i1}u(t) \end{bmatrix} + M_2 \begin{bmatrix} A_{12}x(t) + B_{12}u(t) \\ A_{22}x(t) + B_{22}u(t) \\ \vdots \\ A_{i2}x(t) + B_{i2}u(t) \end{bmatrix}$$ (6.2)

where M_1 and M_2 are diagonal matrices as following:

$$\text{dia}(M_1) = \begin{bmatrix} M_{11} & M_{21} & ... & M_{i1} \end{bmatrix}, \text{dia}(M_2) = \begin{bmatrix} M_{12} & M_{22} & ... & M_{i2} \end{bmatrix}$$

Note that for each equation i:

$$\sum_{j=1}^{2} M_{ij}(z_i(t)) = 1,$$

$M_{ij}(z_i(t)) \geq 0$, $i = 1, 2, ..., n$ and $j = 1, 2$.

Via the new fuzzy model, the final form of the fuzzy model becomes very simple. The new model provides a much more convenient approach for fuzzy model research and fuzzy application. The simulation results of chaotic systems are

discussed in next Section.

6.3 New Fuzzy Model of Chaotic Systems

In this Section, the new fuzzy models of two different chaotic systems, Sprott C [52] and system Sprott E [52] system, are shown for Model 1 and Model 2.

Model system:

Sprott gave three dimensional ODE's with at most quadratic nonlinearities and found 19 distinct examples of chaotic flows with either five terms and two nonlinearities or six terms and one nonlinearity. Two of these 19 systems are used here.

Model 1: New fuzzy model of Sprott C system with uncertainty

The Sprott C system with uncertainty is:

$$\begin{cases} \dot{x}_1 = x_2 x_3 \\ \dot{x}_2 = x_1 - x_2 + \Delta_1 \\ \dot{x}_3 = 1 - x_1^2 \end{cases} \tag{6.3}$$

with initial states (0.8, 1, 0.01), and uncertainty Δ_1 is 0.1sin(t) . The chaotic attractor of the Sprott C system is shown in Fig. 6.1.

If T-S fuzzy model is used for representing local linear models of Sprott C system, 8 fuzzy rules and 8 linear subsystems are need. The process of modeling is shown as follows:

T-S fuzzy model:

Assume that:

(1) $x_2 \in [-Z_1, Z_1]$ and $Z_1 > 0$

(2) $\Delta_1 \in [-Z_2, Z_2]$ and $Z_2 > 0$

(3) $x_1 \in [-Z_3, Z_3]$ and $Z_3 > 0$

Then we have the following T-S fuzzy rules:

Rule 1: IF x_2 is M_{11} , Δ_1 is M_{21} and x_1 is M_{31} THEN $\dot{X} = A_1 X$,

Rule 2: IF x_2 is M_{11} , Δ_1 is M_{21} and x_1 is M_{32} THEN $\dot{X} = A_2 X$,

Rule 3: IF x_2 is M_{11} , Δ_1 is M_{22} and x_1 is M_{31} THEN $\dot{X} = A_3 X$,

Rule 4: IF x_2 is M_{11} , Δ_1 is M_{22} and x_1 is M_{32} THEN $\dot{X} = A_4 X$,

Rule 5: IF x_2 is M_{12} , Δ_1 is M_{21} and x_1 is M_{31} THEN $\dot{X} = A_5 X$,

Rule 6: IF x_2 is M_{12} , Δ_1 is M_{21} and x_1 is M_{32} THEN $\dot{X} = A_6 X$,

Rule 7: IF x_2 is M_{12} , Δ_1 is M_{22} and x_1 is M_{31} THEN $\dot{X} = A_7 X$,

Rule 8: IF x_2 is M_{12} , Δ_1 is M_{22} and x_1 is M_{32} THEN $\dot{X} = A_8 X$,

Then the final output of the Sprott C system can be composed by fuzzy linear subsystems mentioned above. It is obviously an inefficient and complicated work.

New fuzzy model:

By using the new fuzzy model, Sprott C system can be linearized as simple linear equations. The steps of fuzzy modeling are shown as follows:

Steps of fuzzy modeling:

Step 1:

Assume that $x_2 \in [-Z_1, Z_1]$ and $Z_1 > 0$, then the first equation of (6.3) can be exactly represented by new fuzzy model as following:

Rule 1: IF x_2 is M_{11} , THEN $\dot{x}_1 = x_3 Z_1$, $\qquad(6.4)$

Rule 2: IF x_2 is M_{12} , THEN $\dot{x}_1 = -x_3 Z_1$ $\qquad(6.5)$

where

$$M_{11} = \frac{1}{2}(1 + \frac{x_2}{Z_1}), \quad M_{12} = \frac{1}{2}(1 - \frac{x_2}{Z_1}),$$

and $Z_1 = 8$ from Fig. 6.2 . M_{11} and M_{12} are fuzzy sets of the first equation of (6.3) and $M_{11} + M_{12} = 1$.

Step 2:

Assume that $\Delta_1 \in [-Z_2, Z_2]$ and $Z_2 > 0$, then the second equation of (6.3) can be exactly represented by new fuzzy model as following:

Rule 1: IF Δ_1 is M_{21}, THEN $\dot{x}_2 = x_1 - x_2 + Z_2$, $\qquad$ (6.6)

Rule 2: IF Δ_1 is M_{22}, THEN $\dot{x}_2 = x_1 - x_2 - Z_2$ $\qquad$ (6.7)

where

$$M_{21} = \frac{1}{2}(1 + \frac{\Delta_1}{Z_2}), \quad M_{22} = \frac{1}{2}(1 - \frac{\Delta_1}{Z_2}),$$

and $Z_2 = 2$ from Fig. 6.2. M_{21} and M_{22} are fuzzy sets of the second equation of (6.3) and $M_{21} + M_{22} = 1$.

Step 3:

Assume that $x_1 \in [-Z_3, Z_3]$ and $Z_3 > 0$, then the third equation of (6.3) can be exactly represented by new fuzzy model as following:

Rule 1: IF x_1 is M_{31}, THEN $\dot{x}_3 = 1 - x_1 Z_3$, $\qquad$ (6.8)

Rule 2: IF x_1 is M_{32}, THEN $\dot{x}_3 = 1 + x_1 Z_3$ $\qquad$ (6.9)

where

$$M_{31} = \frac{1}{2}(1 + \frac{x_1}{Z_3}), \quad M_{32} = \frac{1}{2}(1 - \frac{x_1}{Z_3}),$$

and $Z_3 = 8$ from Fig. 6.2. M_{31} and M_{32} are fuzzy sets of the third equation of (6.3) and $M_{31} + M_{32} = 1$.

Here, we call Eqs.(6.4), (6.6) and (6.8) the first linear subsystem under the fuzzy rules, and Eqs.(6.5), (6.7) and (6.9) the second linear subsystem under the fuzzy rules.

The first linear subsystem is

$$\begin{cases} \dot{x}_1 = x_3 Z_1 \\ \dot{x}_2 = x_1 - x_2 + Z_2 \\ \dot{x}_3 = 1 - x_1 Z_3 \end{cases} \qquad (6.10)$$

The second linear subsystem is

$$\begin{cases} \dot{x}_1 = -\, x_3\, Z_1 \\ \dot{x}_2 = \, x_1 -\, x_2 -\, Z \\ \dot{x}_3 = 1 +\, x_1\, Z_3 \end{cases} \tag{6.11}$$

The final output of the fuzzy Sprott C system is inferred as follows and the chaotic behavior of fuzzy system is shown in Fig. 6.3. Now we have:

$$\begin{bmatrix} \dot{x}_1 \\ \dot{x}_2 \\ \dot{x}_3 \end{bmatrix} = \begin{bmatrix} M_{11} & 0 & 0 \\ 0 & M_{21} & 0 \\ 0 & 0 & M_{31} \end{bmatrix} \begin{bmatrix} x_3 Z_1 \\ x_1 - x_2 + Z_2 \\ 1 - x_1 Z_3 \end{bmatrix}$$
$$+ \begin{bmatrix} M_{12} & 0 & 0 \\ 0 & M_{22} & 0 \\ 0 & 0 & M_{32} \end{bmatrix} \begin{bmatrix} -x_3 Z_1 \\ x_1 - x_2 + Z_2 \\ 1 + x_1 Z_3 \end{bmatrix} \tag{6.12}$$

Eq. (6.12) can be rewritten as a simple mathematical expression:

$$\dot{X}(t) = \sum_{i=1}^{2} \Psi_i (A_i X(t) + \tilde{b}_i) \tag{6.13}$$

where Ψ_i are diagonal matrices as follows:

$$dia(\Psi_1) = \begin{bmatrix} M_{11} & M_{21} & M_{31} \end{bmatrix}, \quad dia(\Psi_2) = \begin{bmatrix} M_{12} & M_{22} & M_{32} \end{bmatrix}$$

$$A_1 = \begin{bmatrix} 0 & 0 & Z_1 \\ 1 & -1 & 0 \\ -Z_3 & 0 & 0 \end{bmatrix}, \quad \tilde{b}_1 = \begin{bmatrix} 0 \\ Z_2 \\ 1 \end{bmatrix}$$

$$A_2 = \begin{bmatrix} 0 & 0 & -Z_1 \\ 1 & -1 & 0 \\ Z_3 & 0 & 0 \end{bmatrix}, \quad \tilde{b}_2 = \begin{bmatrix} 0 \\ -Z_2 \\ 1 \end{bmatrix}$$

Via new fuzzy model, the number of fuzzy rules can be greatly reduced. Just two linear subsystems are enough to express such complex chaotic behaviors. The simulation results are similar the original chaotic behavior of the Sprott C system as shown in Fig. 6.3.

Model 2: New fuzzy model of stochastic Sprott E system

The stochastic Sprott E system is:

$$\begin{cases} \dot{y}_1 = y_2 y_3 \\ \dot{y}_2 = y_1^2 - y_2 \\ \dot{y}_3 = 1 - 4y_1 + \Delta_2 \end{cases} \tag{6.14}$$

where Δ_2 is Rayleigh noise and initial conditions are chosen as (0.2, 0.063, 0.01),

the stochastic Sprott E model exhibits chaotic motion which is shown in Fig. 6.4.

New fuzzy model:

Assume that:

(1) $y_2 \in [-Z_4, Z_4]$ and $Z_4 > 0$,

(2) $\Delta_2 \in [-Z_5, Z_5]$ and $Z_5 > 0$,

(3) $y_1 \in [-Z_6, Z_6]$ and $Z_6 > 0$,

then we have the following new fuzzy rules:

Rule 1: IF y_2 is N_{11}, THEN $\dot{y}_1 = y_2 Z_4$, (6.15)

Rule 2: IF y_2 is N_{12}, THEN $\dot{y}_1 = -y_2 Z_4$, (6.16)

where

$$N_{11} = \frac{1}{2}(1 + \frac{y_2}{Z_4}), \quad N_{12} = \frac{1}{2}(1 - \frac{y_2}{Z_4})$$

and

Rule 1: IF y_1 is N_{21}, THEN $\dot{y}_2 = Z_5 y_1 - y_2$, (6.17)

Rule 2: IF y_1 is N_{22}, THEN $\dot{y}_2 = -Z_5 y_1 - y_2$, (6.18)

where

$$N_{21} = \frac{1}{2}(1 + \frac{y_1}{Z_5}), \quad N_{22} = \frac{1}{2}(1 - \frac{y_1}{Z_5}).$$

and

Rule 1: IF Δ_2 is N_{31}, THEN $\dot{y}_3 = 1 - 4y_1 + Z_6$, (6.19)

Rule 2: IF Δ_2 is N_{32}, THEN $\dot{y}_3 = 1 - 4y_1 - Z_6$, (6.20)

where

$$N_{31} = \frac{1}{2}(1 + \frac{\Delta_2}{Z_6}), \quad N_{32} = \frac{1}{2}(1 - \frac{\Delta_2}{Z_6}).$$

in Eqs. (3-13)~(3-18), $Z_4 = 8$, $Z_5 = 6$ and $Z_5 = 5$ from Fig. 6.5. $N_{11}, N_{12}, N_{21}, N_{22}$, N_{31} and N_{32} are fuzzy sets of Eq.(6.14) and $N_{11} + N_{12} = 1$, $N_{21} + N_{22} = 1$ and $N_{31} + N_{32} = 1$

Here, we call (6.15), (6.17) and (6.19) the first liner subsystem under the fuzzy rules and (6.16), (6.18) and (6.20) the second linear subsystem under the fuzzy rules. The first linear subsystem is

$$\begin{cases} \dot{y}_1 = Z_4 y_3 \\ \dot{y}_2 = Z_5 y_1 - y_2 \\ \dot{y}_3 = 1 - 4y_1 + Z_6 \end{cases} \tag{6.21}$$

The second linear subsystem is

$$\begin{cases} \dot{y}_1 = -Z_4 y_3 \\ \dot{y}_2 = -Z_5 y_1 - y_2 \\ \dot{y}_3 = 1 - 4y_1 - Z_6 \end{cases} \tag{6.22}$$

The final output of the fuzzy Sprott E system is inferred as follows and the chaotic behavior of fuzzy system is shown in Fig. 6.6.

$$\begin{bmatrix} \dot{y}_1 \\ \dot{y}_2 \\ \dot{y}_3 \end{bmatrix} = \begin{bmatrix} N_{11} & 0 & 0 \\ 0 & N_{21} & 0 \\ 0 & 0 & N_{31} \end{bmatrix}^T \begin{bmatrix} Z_4 y_3 \\ Z_5 y_1 - y_2 \\ 1 - 4y_1 + Z_6 \end{bmatrix}$$
$$+ \begin{bmatrix} N_{12} & 0 & 0 \\ 0 & N_{22} & 0 \\ 0 & 0 & N_{32} \end{bmatrix}^T \begin{bmatrix} -Z_4 y_3 \\ -Z_5 y_1 - y_2 \\ 1 - 4y_1 - Z_6 \end{bmatrix} \tag{6.23}$$

Eq. (6.23) can be rewritten as a simple mathematical expression:

$$\dot{Y}(t) = \sum_{i=1}^{2} \Gamma_i (C_i Y(t) + \tilde{c}_i) \tag{6.24}$$

where

$$dia(\Gamma_1) = \begin{bmatrix} N_{11} & N_{21} & N_{31} \end{bmatrix}, \quad dia(\Gamma_2) = \begin{bmatrix} N_{12} & N_{22} & N_{32} \end{bmatrix}$$

$$C_1 = \begin{bmatrix} 0 & 0 & Z_4 \\ Z_5 & -1 & 0 \\ -4 & 0 & 0 \end{bmatrix}, \quad \tilde{c}_1 = \begin{bmatrix} 0 \\ 0 \\ 1 + Z_6 \end{bmatrix}$$

$$C_2 = \begin{bmatrix} 0 & 0 & -Z_4 \\ -Z_5 & -1 & 0 \\ -4 & 0 & 0 \end{bmatrix}, \quad \tilde{c}_2 = \begin{bmatrix} 0 \\ 0 \\ 1 - Z_6 \end{bmatrix}$$

Via new fuzzy model, two linear subsystems are enough to express such complex chaotic behaviors. The simulation results are similar to the original chaotic behavior of the Sprott E system.

6.4 Fuzzy Synchronization Scheme

In this Section, we derive the new fuzzy synchronization scheme based on our new fuzzy model to synchronize two different fuzzy chaotic systems. The following fuzzy systems as the master and slave systems are given:

master system:

$$\dot{X}(t) = \sum_{i=1}^{2} \Psi_i (A_i X(t) + \tilde{b}_i) \tag{6.25}$$

slave system:

$$\dot{Y}(t) = \sum_{i=1}^{2} \Gamma_i (C_i Y(t) + \tilde{c}_i) + BU(t) \tag{6.26}$$

Eq. (6.25) and Eq. (6.26) represent the two different chaotic systems, and in Eq. (6.26) there is control input U(t). Define the error signal as $e(t) = X(t) - Y(t)$, we have:

$$\dot{e}(t) = \dot{X}(t) - \dot{Y}(t) = \sum_{i=1}^{2} \Psi_i (A_i X(t) + \tilde{b}_i) - \sum_{i=1}^{2} \Gamma_i (C_i Y(t) + \tilde{c}_i) - BU(t) \tag{6.27}$$

The fuzzy controllers are designed as follows:

$$U(t) = u_1(t) + u_2(t) \tag{6.28}$$

where

$$u_1(t) = \sum_{i=1}^{2} \Psi_i F_i X(t) - \sum_{i=1}^{2} \Gamma_i P_i Y(t),$$

73

$$u_2(t) = \sum_{i=1}^{2} \Psi_i \tilde{b}_i - \sum_{i=1}^{2} \Gamma_i \tilde{c}_i$$

such that $\|e(t)\| \to 0$ as $t \to \infty$. Our design is to determine the feedback gains F_i and P_i.

By substituting $U(t)$ into Eq.(6.27), we obtain:

$$\dot{e}(t) = \sum_{i=1}^{2} \Psi_i \{(A_i - BF_i)X(t)\} - \sum_{i=1}^{2} \Gamma_i \{(C_i - BP_i)Y(t)\} \tag{6.29}$$

Theorem 1: The error system in Eq. (6.29) is asymptotically stable and the slave system in Eq. (6.26) can synchronize the master system in Eq. (6.25) under the fuzzy controller in Eq. (6.28) if the following conditions below can be satisfied:

$$G = (A_i - BF_i) = (C_i - BP_i) < 0 , \quad i = 1 \sim 2 . \tag{6.30}$$

Proof:

The errors in Eq. (6.29) can be exactly linearized via the fuzzy controllers in Eq. (4-4) if there exist the feedback gains F_i such that

$$(A_1 - BF_1) = (A_2 - BF_2) = (C_1 - BP_1) = (C_2 - BP_2) < 0 . \tag{6.31}$$

Then the overall control system is linearized as

$$\dot{e}(t) = Ge(t), \tag{6.32}$$

where $G = (A_1 - BF_1) = (A_2 - BF_2) = (C_1 - BP_1) = (C_2 - BP_2) < 0$.

As a consequence, the zero solution of the error system (6.32) linearized via the fuzzy controller (6.28) is asymptotically stable.

6.5 Simulation Results

There are two examples in this Section to investigate the effectiveness and feasibility of our new fuzzy model.

Example 1: Synchronization of identical master and slave Sprott C system

The fuzzy Sprott C system in Eq. (6.13) is chosen as the master system and the fuzzy slave Sprott C system, with fuzzy controllers is as follows:

$$\dot{Y}(t) = \sum_{i=1}^{2} \Gamma_i (C_i Y(t) + \tilde{c}_i) + BU(t) \tag{6.33}$$

where Γ_i are diagonal matrices

$$dia(\Gamma_1) = \begin{bmatrix} N_{11} & N_{21} & N_{31} \end{bmatrix}, \quad dia(\Gamma_2) = \begin{bmatrix} N_{12} & N_{22} & N_{32} \end{bmatrix}$$

and

$$C_1 = \begin{bmatrix} 0 & 0 & Z_1 \\ 1 & -1 & 0 \\ -Z_3 & 0 & 0 \end{bmatrix}, \quad \tilde{c}_1 = \begin{bmatrix} 0 \\ Z_2 \\ 1 \end{bmatrix}$$

$$C_2 = \begin{bmatrix} 0 & 0 & -Z_1 \\ 1 & -1 & 0 \\ Z_3 & 0 & 0 \end{bmatrix}, \quad \tilde{c}_2 = \begin{bmatrix} 0 \\ Z_2 \\ 1 \end{bmatrix}.$$

Therefore, the error and error dynamics are:

$$\begin{bmatrix} e_1 \\ e_2 \\ e_3 \end{bmatrix} = \begin{bmatrix} x_1 - y_1 \\ x_2 - y_2 \\ x_3 - y_3 \end{bmatrix},$$

$$\begin{bmatrix} \dot{e}_1 \\ \dot{e}_2 \\ \dot{e}3 \end{bmatrix} = \begin{bmatrix} \dot{x}_1 - \dot{y}_1 \\ \dot{x}_2 - \dot{y}_2 \\ \dot{x}_3 - \dot{y}_3 \end{bmatrix} = \sum_{i=1}^{2} \Psi_i (A_i X(t) + \tilde{b}_i) - \sum_{i=1}^{2} \Gamma_i (C_i Y(t) + \tilde{c}_i) - BU(t) \tag{6.34}$$

B is chosen as an identity matrix and the fuzzy controllers in Eq. (6.28) are used:

$$\begin{bmatrix} \dot{e}_1 \\ \dot{e}_2 \\ \dot{e}3 \end{bmatrix} = \Psi_1 [A_1 - BF_1]_{3\times3} \begin{bmatrix} x_1 \\ x_2 \\ x_3 \end{bmatrix} + \Psi_2 [A_2 - BF_2]_{3\times3} \begin{bmatrix} x_1 \\ x_2 \\ x_3 \end{bmatrix}$$

$$-\Gamma_1 [C_1 - BP_1]_{3\times3} \begin{bmatrix} y_1 \\ y_2 \\ y_3 \end{bmatrix} - \Gamma_2 [C_2 - BP_2]_{3\times3} \begin{bmatrix} y_1 \\ y_2 \\ y_3 \end{bmatrix} \tag{6.35}$$

According to Eq.(6.30) , we have $G = [A_1 - BF_1] = [A_2 - BF_2] = [C_1 - BP_1]$

$= [C_2 - BP_2] < 0$. G is chosen as:
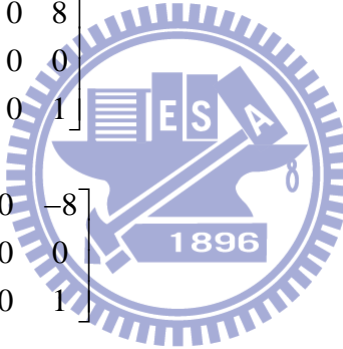
$$G = \begin{bmatrix} -1 & 0 & 0 \\ 0 & -1 & 0 \\ 0 & 0 & -1 \end{bmatrix} \tag{6.36}$$

Thus, the feedback gains F_1, F_2, P_1 and P_2 can be determined by the following equation:

$$F_1 = B^{-1}[A_1 - G] = \begin{bmatrix} 1 & 0 & 8 \\ 1 & 0 & 0 \\ -8 & 0 & 1 \end{bmatrix}$$

$$F_2 = B^{-1}[A_2 - G] = \begin{bmatrix} 1 & 0 & -8 \\ 1 & 0 & 0 \\ 8 & 0 & 1 \end{bmatrix} \tag{6.37}$$

$$P_1 = B^{-1}[C_1 - G] = \begin{bmatrix} 1 & 0 & 8 \\ 1 & 0 & 0 \\ -8 & 0 & 1 \end{bmatrix}$$

$$P_2 = B^{-1}[C_2 - G] = \begin{bmatrix} 1 & 0 & -8 \\ 1 & 0 & 0 \\ 8 & 0 & 1 \end{bmatrix}$$

The synchronization errors are shown in Fig. 6.7.

Example 2: Synchronization of Sprott C system and Sprott E system.

The fuzzy Sprott C system in Eq. (6.13) is chosen as the master system and the fuzzy slave Sprott E system, with fuzzy controllers is as follows:

$$\dot{Y}(t) = \sum_{i=1}^{2} \Gamma_i (C_i Y(t) + \tilde{c}_i) + BU(t) \tag{6.38}$$
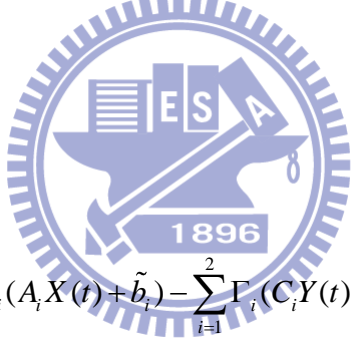
where Γ_i are diagonal matrices

$$dia(\Gamma_1) = \begin{bmatrix} N_{11} & N_{21} & N_{31} \end{bmatrix}, \quad dia(\Gamma_2) = \begin{bmatrix} N_{12} & N_{22} & N_{32} \end{bmatrix}$$

and

$$C_1 = \begin{bmatrix} 0 & 0 & Z_4 \\ Z_5 & -1 & 0 \\ -4 & 0 & 0 \end{bmatrix}, \quad \tilde{c}_1 = \begin{bmatrix} 0 \\ 0 \\ 1+Z_6 \end{bmatrix}$$

$$C_1 = \begin{bmatrix} 0 & 0 & -Z_4 \\ -Z_5 & -1 & 0 \\ -4 & 0 & 0 \end{bmatrix}, \quad \tilde{c}_1 = \begin{bmatrix} 0 \\ 0 \\ 1-Z_6 \end{bmatrix}$$

Therefore, the error and error dynamics are:

$$\begin{bmatrix} e_1 \\ e_2 \\ e_3 \end{bmatrix} = \begin{bmatrix} x_1 - y_1 \\ x_2 - y_2 \\ x_3 - y_3 \end{bmatrix},$$

$$\begin{bmatrix} \dot{e}_1 \\ \dot{e}_2 \\ \dot{e}3 \end{bmatrix} = \begin{bmatrix} \dot{x}_1 - \dot{y}_1 \\ \dot{x}_2 - \dot{y}_2 \\ \dot{x}_3 - \dot{y}_3 \end{bmatrix} = \sum_{i=1}^{2} \Psi_i (A_i X(t) + \tilde{b}_i) - \sum_{i=1}^{2} \Gamma_i (C_i Y(t) + \tilde{c}_i) - BU(t) \qquad (6.39)$$

B is chosen as an identity matrix and the fuzzy controllers in Eq. (6.28) are used:

$$\begin{bmatrix} \dot{e}_1 \\ \dot{e}_2 \\ \dot{e}3 \end{bmatrix} = \Psi_1 [A_1 - BF_1]_{3\times 3} \begin{bmatrix} x_1 \\ x_2 \\ x_3 \end{bmatrix} + \Psi_2 [A_2 - BF_2]_{3\times 3} \begin{bmatrix} x_1 \\ x_2 \\ x_3 \end{bmatrix}$$

$$-\Gamma_1 [C_1 - BP_1]_{3\times 3} \begin{bmatrix} y_1 \\ y_2 \\ y_3 \end{bmatrix} - \Gamma_2 [C_2 - BP_2]_{3\times 3} \begin{bmatrix} y_1 \\ y_2 \\ y_3 \end{bmatrix} \qquad (6.40)$$

According to Eq.(6.30) , we have $G = [A_1 - BF_1] = [A_2 - BF_2] = [C_1 - BP_1]$

$= [C_2 - BP_2] < 0$. G is chosen as:

$$G = \begin{bmatrix} -1 & 0 & 0 \\ 0 & -1 & 0 \\ 0 & 0 & -1 \end{bmatrix} \qquad (6.41)$$

Thus, the feedback gains F_1, F_2, P_1 and P_2 can be determined by the following equation:

$$F_1 = B^{-1}\left[A_1 - G\right] = \begin{bmatrix} 1 & 0 & 8 \\ 1 & 0 & 0 \\ -8 & 0 & 1 \end{bmatrix}$$

$$F_2 = B^{-1}\left[A_2 - G\right] = \begin{bmatrix} 1 & 0 & -8 \\ 1 & 0 & 0 \\ 8 & 0 & 1 \end{bmatrix} \tag{6.42}$$

$$P_1 = B^{-1}\left[C_1 - G\right] = \begin{bmatrix} 1 & 0 & 8 \\ 6 & 0 & 0 \\ -4 & 0 & 1 \end{bmatrix}$$

$$P_2 = B^{-1}\left[C_2 - G\right] = \begin{bmatrix} 1 & 0 & -8 \\ -6 & 0 & 0 \\ -4 & 0 & 1 \end{bmatrix}$$

The synchronization errors are shown in Fig. 6.8.
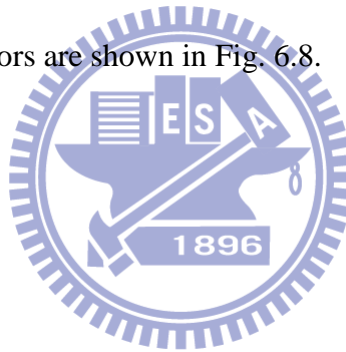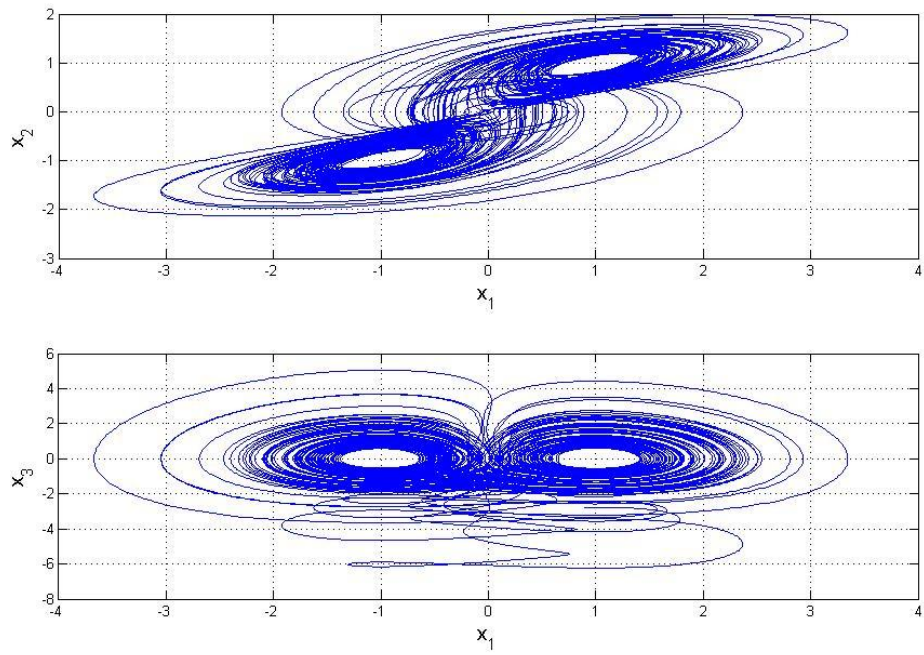
Fig. 6.1. Chaotic behavior of Sprott C system with uncertainty.
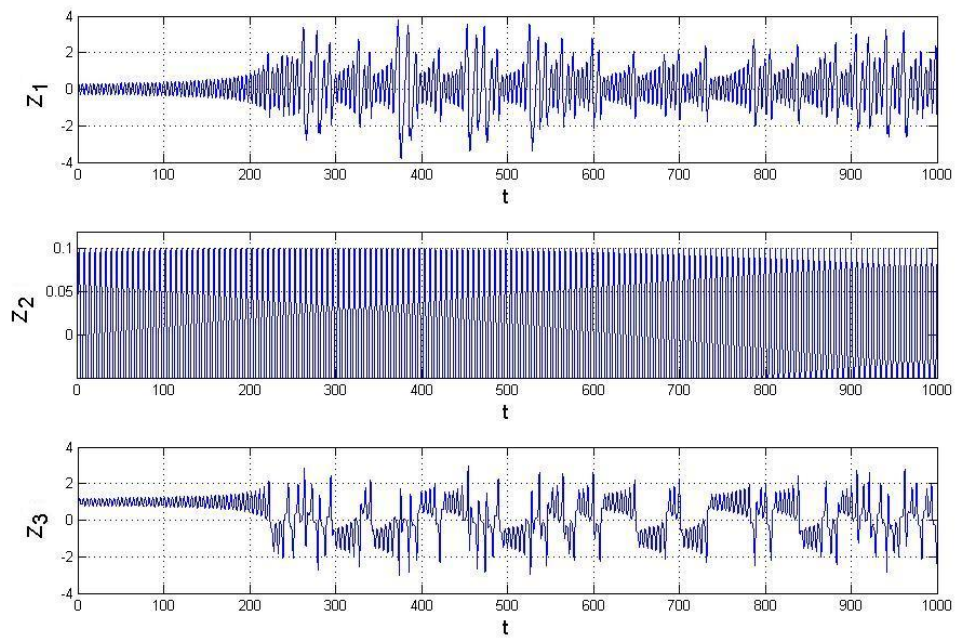
Fig. 6.2. Time histories of Z_1, Z_2 and Z_3 for Sprott C system.
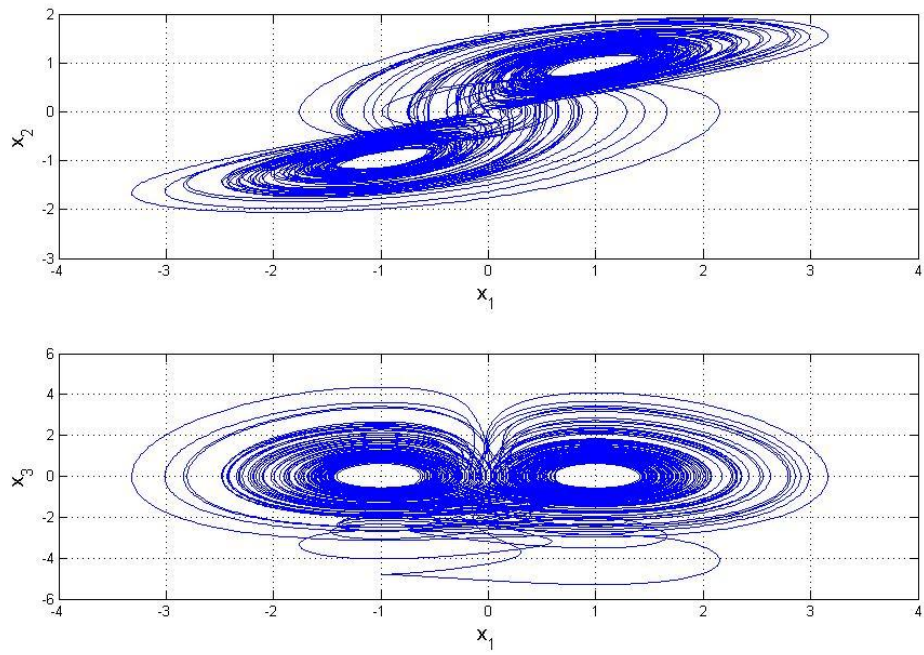
Fig. 6.3. Chaotic behavior of new fuzzy Sprott C system with uncertainty.
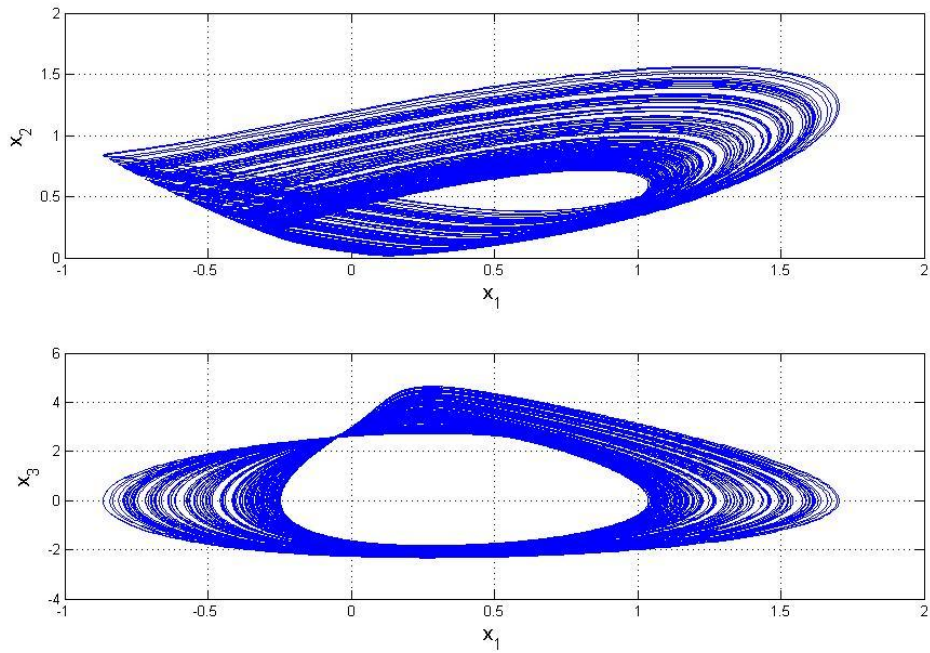
Fig. 6.4. Chaotic behavior of stochastic Sprott E system.
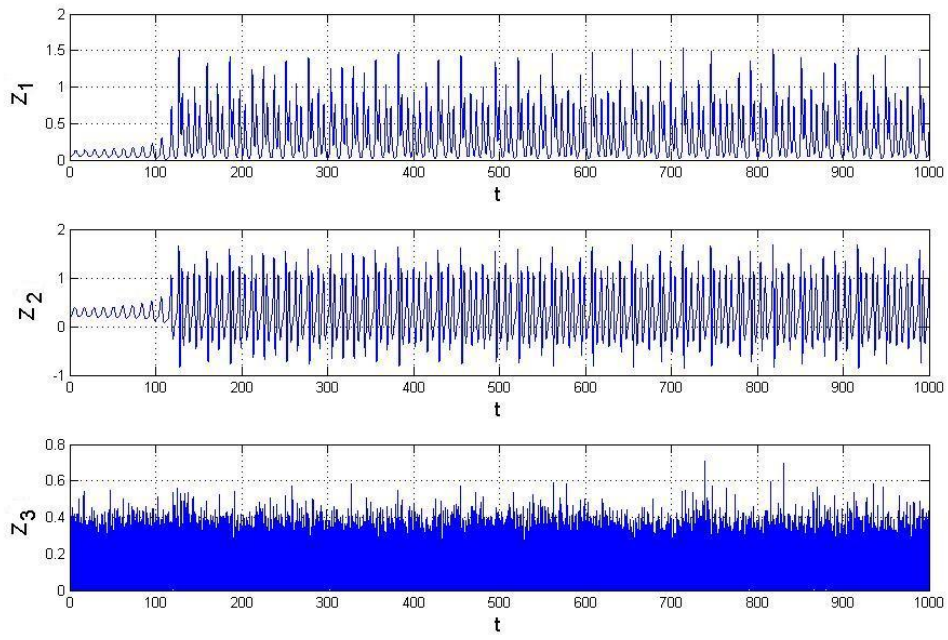
Fig. 6.5. Time histories of Z_1, Z_2 and Z_3 for Sprott E system.
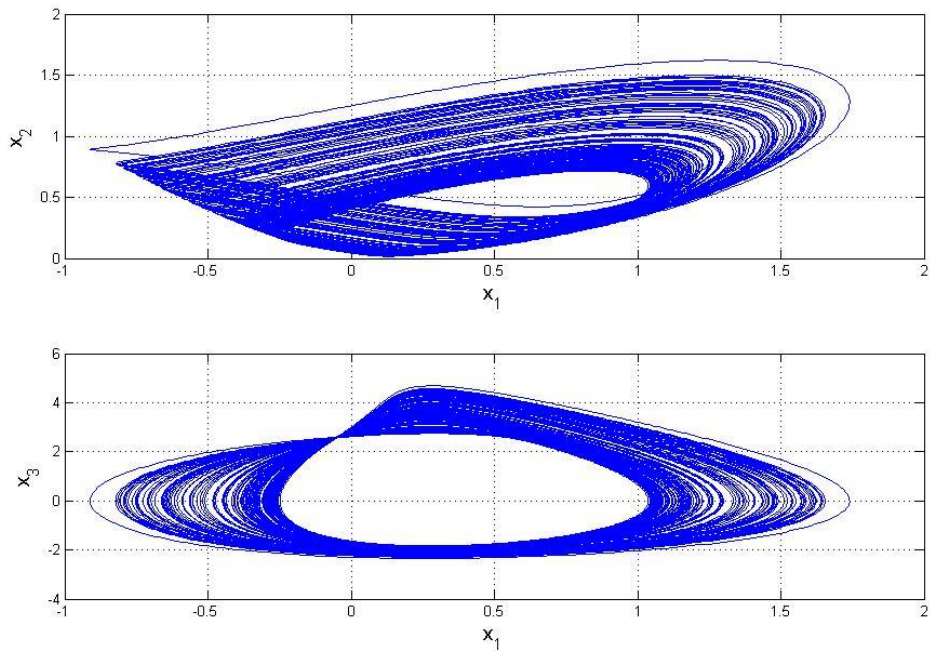
Fig. 6.6. Chaotic behavior of new fuzzy stochastic Sprott E system.
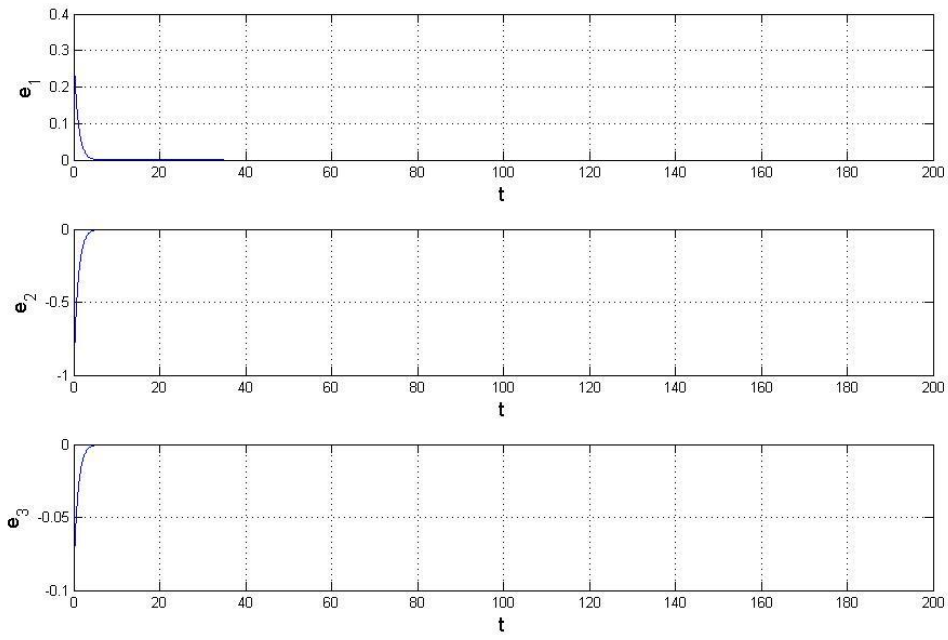
Fig. 6.7. Time histories of errors for Example 1.
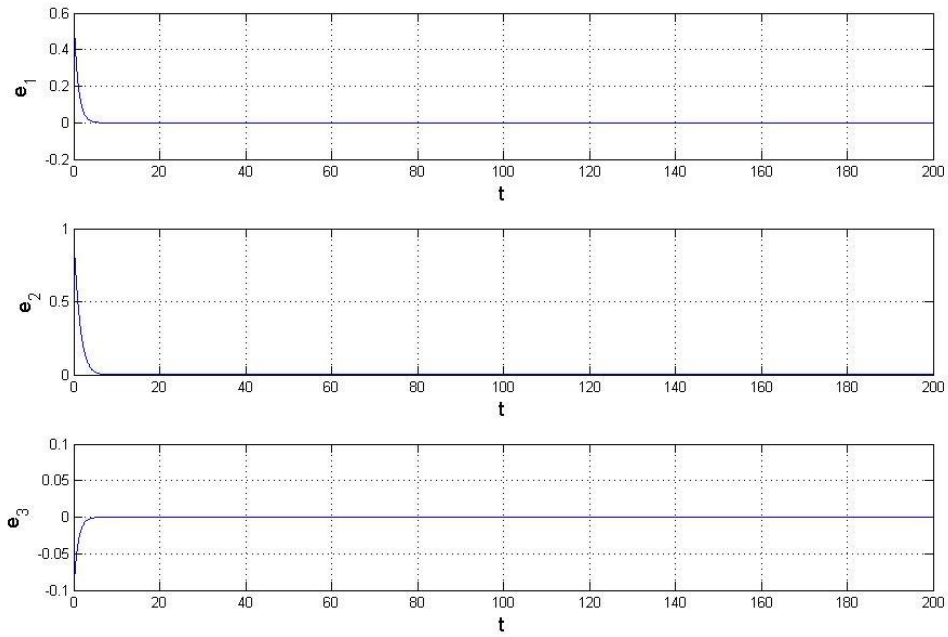
Fig. 6.8. Time histories of errors for Example 2.

Chapter 7

Projective Synchronization by Fuzzy Logic Constant Controller and Its Application to Different Chaotic Systems with Deterministic and Stochastic Uncertainties

7.1 Preliminary

In this Chapter, a simplest controller, the fuzzy logic constant controller (FLCC) ,which are derived via fuzzy logic design and Lyapunov direct method, are presented for projective synchronization of non-autonomous chaotic systems with deterministic and stochastic uncertainties.

7.2 Projective Chaos Synchronization by FLCC Scheme

Consider the following master chaotic system

$$\dot{\mathbf{x}} = \mathbf{A}\mathbf{x} + f(x) + \Delta \tag{7.1}$$

where $\mathbf{x} = [x_1, x_2, \cdots x_n]^T \in R^n$ denotes a state vector, $\mathbf{A}$ is an $n \times n$ constant coefficient matrix , f is a nonlinear vector function and Δ is a stochastic disturbance.

The slave system which can be either identical or different from the master system, is

$$\dot{\mathbf{y}} = B\mathbf{y} + g(y) + u \tag{7.2}$$

where $\mathbf{y} = [y_1, y_2, \cdots y_n]^T \in R^n$ denotes a state vector, B is an $n \times n$ constant coefficient matrix, g is a nonlinear vector function., and $u = [u_1, u_2, \cdots, u_n]^T \in R^n$ is the fuzzy logic controller vector needed to be designed.

In order to make the chaos state $\mathbf{y}$ approaching the projective master state $\alpha\mathbf{x}$,

define $\mathbf{e} = \alpha\mathbf{x} - \mathbf{y}$ as the state error. The chaos control is accomplished in the sense that :

$$\lim_{t \to \infty} \mathbf{e} = \lim_{t \to \infty} (\alpha\mathbf{x} - \mathbf{y}) = 0 \tag{7.3}$$

where

$$\mathbf{e} = \boldsymbol{\alpha}\mathbf{x} - \mathbf{y} = [e_1, ..., e_n] \tag{7.4}$$

From Eq. (7.1)~(7.3) we have the following error dynamics:

$$\dot{\mathbf{e}} = \alpha\dot{\mathbf{x}} - \dot{\mathbf{y}} = \alpha[A\mathbf{x} + f(\mathbf{x}) + \Delta] + B\mathbf{u} + g(t) \tag{7.5}$$

According to Lyapunov direct method, we have the following Lyapunov function to derive the fuzzy logic controller for projective synchronization:

$$V = f(e_1, .. e_m, .. e_n) = \frac{1}{2}(e_1^2 + ... + e_m^2 + .. e_n^2) > 0 \tag{7.6}$$

The derivative of the Lyapunov function is:

$$\dot{V} = e_1\dot{e}_1 + ... + e_m\dot{e}_m + ...e_n\dot{e}_n \tag{7.7}$$

If the controllers included in $\dot{e}_1...\dot{e}_m...\dot{e}_n$ can be suitably designed to achieve $\dot{V} < 0$, then the zero solution $\mathbf{e} = 0$ is asymptotically stable and the projective synchronization is accomplished. The design process of FLCC is introduced as follows.

We use one vector signal, error derivatives $\dot{\mathbf{e}}(t) = \begin{bmatrix} \dot{e}_1, \dot{e}_2 \cdots \dot{e}_m, \cdots \dot{e}_n \end{bmatrix}^T$ as the antecedent part of the proposed FLCC to design the control input u which will be used in the consequent part of the proposed FLCC :

$$u = \begin{bmatrix} u_1, u_2 \cdots u_m, \cdots u_n \end{bmatrix}^T \tag{7.8}$$

where u is a constant column vector and the FLCC accomplishes the objective to stabilize the error dynamics (7.5).

The strategy of the FLCC designing is proposed as follow and the configuration of the strategy is shown in Fig. 7.1.

Assume the upper bound and lower bound of $\dot{e}_m$ are Z_m and $-Z_m$, then the FLCC can be design step by step as follows:

(1) If e_m is detected as positive ($e_m > 0$), we have to design a controller for $\dot{e}_m < 0$, then $\dot{V} = e_m \dot{e}_m < 0$ can be achieved. Therefore we have the following i-th if–then fuzzy rule as:

$$Rule\ 1 : IF\ \dot{e}_m\ is\ M_1\ THEN\ u_{m1} = Z_m \tag{7.9}$$

$$Rule\ 2 : IF\ \dot{e}_m\ is\ M_2\ THEN\ u_{m2} = Z_m \tag{7.10}$$

$$Rule\ 3 : IF\ \dot{e}_m\ is\ M_3\ THEN\ u_{m3} = e_m \tag{7.11}$$

(2) If e_m is detected as negative ($e_m < 0$), we have to design a controller for $\dot{e}_m > 0$, then $\dot{V} = e_m \dot{e}_m < 0$ can be achieved. Therefore we have the following i-th if–then fuzzy rule as:

$$Rule\ 1 : IF\ \dot{e}_m\ is\ M_1\ THEN\ u_{m1} = -Z_m \tag{7.12}$$

$$Rule\ 2 : IF\ \dot{e}_m\ is\ M_2\ THEN\ u_{m2} = -Z_m \tag{7.13}$$

$$Rule\ 3 : IF\ \dot{e}_m\ is\ M_3\ THEN\ u_{m3} = e_m \tag{7.14}$$

(3) If e_m approaches to zero, then the projective synchronization is nearly achieved. Therefore we have the following i-th if–then fuzzy rule as:

$$Rule\ 1 : IF\ \dot{e}_m\ is\ M_1\ THEN\ u_{m1} = e_m \approx 0 \tag{7.15}$$

$$Rule\ 2 : IF\ \dot{e}_m\ is\ M_2\ THEN\ u_{m2} = e_m \approx 0 \tag{7.16}$$

$$Rule\ 3 : IF\ \dot{e}_m\ is\ M_3\ THEN\ u_{m3} = e_m \approx 0 \tag{7.17}$$

where $M_1 = \dfrac{|\dot{e}_m|}{Z_m}$, $M_2 = \dfrac{|\dot{e}_m|}{Z_m}$ and $M_3 = \text{sgn}(\dfrac{Z_m - \dot{e}_m}{Z_m}) + \text{sgn}(\dfrac{\dot{e}_m - Z_m}{Z_m})$, M_1, M_2 and M_3

refer to the membership functions of positive (P), negative (N) and zero (Z) separately which are presented in Fig. 7.2. For each case, u_{mi}, $i = 1\sim3$ is the i-th output of $\dot{e}_m$ which is a constant controller. The centriod defuzzifier which evaluates the output of all rules, is

$$u_m = \frac{\sum\limits_{i=1}^{3} M_i \times u_{mi}}{\sum\limits_{i=1}^{3} M_i} \tag{7.18}$$

The fuzzy rule base is listed in Table 1, in which the input variables in the antecedent part of the rules are $\dot{e}_m$ and the output variable in the consequent part is u_{mi}.

Table 7.1 Rule-table of FLCC

Rule	Antecedent	Consequent Part
	$\dot{e}_m$	u_{mi}
1	Negative (N)	u_{m1}
2	Positive (P)	u_{m2}
3	Zero (Z)	u_{m3}

After designing appropriate fuzzy logic constant controllers and being substituted into Eq. (7.7), a negative definite of derivatives of Lyapunov function $\dot{V}$ can be obtained and the asymptotically stability of Lyapunov theorem can be achieved.

Consequently, the processes of FLCC designing to control the error system following the trajectory of error dynamics is by getting the upper bounds and lower bounds of the error derivatives without any controller, i.e. $-Z_m \leq \dot{e}_m \leq Z_m$. Through the fuzzy logic system which follows the rules of Eqs. (7.9) ~ (7.17), a negative definite of derivatives of Lyapunov function $\dot{V}$ can be obtained and the asymptotically stability of Lyapunov theorem can be achieved.

7.3 Simulation Results

There are two case in this Section to show the effectiveness of our new method.

7.3.1 Projective Synchronization of   Sprott C and Sprott E system by new FLCC

The master Sprott C system [52]with disturbance is:

$$
\begin{cases}
\dfrac{dx_1(t)}{dt} = x_2(t)x_3(t) + \Delta_1 \\[2mm]
\dfrac{dx_2(t)}{dt} = x_1(t) - x_2(t) + \Delta_2 \\[2mm]
\dfrac{dx_3(t)}{dt} = 1 - x_1^2(t) + \Delta_3
\end{cases}
\tag{7.19}
$$

when initial condition $(x_{10}, x_{20}, x_{30}) = (0.8,\ 1,\ 0.01)$ and disturbance Δ_1 is $0.01\cos(5t)$, Δ_2 is $0.05\cos(5t)$ and Δ_3 is $0.1\cos(5t)$. The chaotic attractor of the Sprott C system is shown in Fig. 7.3.

The slave Sprott E system[52] is:

$$
\begin{cases}
\dfrac{dy_1(t)}{dt} = y_2(t)y_3(t) + u_1 \\[2mm]
\dfrac{dy_2(t)}{dt} = y_1^2(t) - y_2(t) + u_2 \\[2mm]
\dfrac{dy_3(t)}{dt} = y_1(t) - 4y_1(t) + u_3
\end{cases}
\tag{7.20}
$$

when initial condition $(y_{10}, y_{20}, y_{30}) = (0.2,\ 0.063,\ 0.01)$, the Sprott E system exhibits chaotic motion which is shown in Fig. 7.4. u_1, u_2 and u_3 are FLCC to synchronize projectively the slave system to master one, i.e.,

$$
\lim_{t \to \infty} \mathbf{e} = 0
\tag{7.21}
$$

The projective synchronization error vector is

$$
\mathbf{e} = \begin{bmatrix} e_1(t) \\ e_2(t) \\ e_3(t) \end{bmatrix} = \alpha \begin{bmatrix} x_1(t) \\ x_2(t) \\ x_3(t) \end{bmatrix} - \begin{bmatrix} y_1(t) \\ y_2(t) \\ y_3(t) \end{bmatrix}
\tag{7.22}
$$

where the projective constant is $\alpha = 4$.

From Eq. (7.22), we have the following error dynamics:

$$\begin{cases} \dot{e}_1 = \alpha(x_2 x_3 + \Delta_1) - (y_2 y_3 + u_1) \\ \dot{e}_2 = \alpha(x_1 - x_2 + \Delta_2) - (y_1^2 - y_2 + u_2) \\ \dot{e}_3 = \alpha(1 - x_1^2 + \Delta_3) - (y_1 - 4y_1 + u_3) \end{cases} \tag{7.23}$$

Choosing Lyapunov function as:

$$V = \frac{1}{2}(e_1^2 + e_2^2 + e_3^2) \tag{7.24}$$

Its time derivative is:

$$\begin{aligned} \dot{V} &= e_1 \dot{e}_1 + e_2 \dot{e}_2 + e_3 \dot{e}_3 \\ &= e_1(\alpha(x_2 x_3 + \Delta_1) - (y_2 y_3 + u_1)) \\ &\quad + e_2(\alpha(x_1 - x_2 + \Delta_2) - (y_1^2 - y_2 + u_2) \\ &\quad + e_3(\alpha(1 - x_1^2 + \Delta_3) - (y_1 - 4y_1 + u_3) \end{aligned} \tag{7.25}$$

In order to design FLCC, we divide Eq. (7.25) into three parts as follows:

Assume $V = \frac{1}{2}(e_1^2 + e_2^2 + e_3^2) = V_1 + V_2 + V_3$, then $\dot{V} = e_1\dot{e}_1 + e_2\dot{e}_2 + e_3\dot{e}_3 = \dot{V}_1 + \dot{V}_2 + \dot{V}_3$,

where $V_1 = \frac{1}{2}e_1^2$, $V_2 = \frac{1}{2}e_2^2$ and $V_3 = \frac{1}{2}e_3^2$.

Part 1: $\dot{V}_1 = e_1\dot{e}_1 = e_1(\alpha(x_2 x_3 + \Delta_1) - (y_2 y_3 + u_1))$

Part 2: $\dot{V}_2 = e_2\dot{e}_2 = e_2(\alpha(x_1 - x_2 + \Delta_2) - (y_1^2 - y_2 + u_2))$

Part 3: $\dot{V}_3 = e_3\dot{e}_3 = e_3(\alpha(1 - x_1^2 + \Delta_3) - (y_1 - 4y_1 + u_3))$

FLCC in *Part 1, 2 and 3* can be obtained via the fuzzy rules in Table 7.1 as follows and the maxima value and minima value of $\dot{e}_1$, $\dot{e}_2$, $\dot{e}_3$ (without any controller) can be observed in time history of error derivatives drawn in Fig 7.5.

The projective synchronization scheme is proposed according to *Part 1,2* and *3* as $\dot{V}_1 = e_1\dot{e}_1 < 0$, $\dot{V}_2 = e_2\dot{e}_2 < 0$ and $\dot{V}_3 = e_3\dot{e}_3 < 0$. Hence, we have

$\dot{V} = \dot{V}_1 + \dot{V}_2 + \dot{V}_3 < 0$. It is clear that all of the rules in our FLCC can lead the Lyapunov theorem for asymptotical stability is satisfied and the simulation results are shown in Fig. 7.6 and 7.7.

7.3.2 Projective Synchronization of Ge-Ku-Duffing and Double Ge-Ku system by new FLCC

Consider the master Ge-Ku-Duffing system[43] with uncertainty is described by

$$
\begin{cases}
\dfrac{dx_1(t)}{dt} = x_2(t) + \Delta_1 \\[2mm]
\dfrac{dx_2(t)}{dt} = -ax_2(t) - x_1(t)(b(c - x_1^2(t)) + dx_3(t)) + \Delta_2 \\[2mm]
\dfrac{dx_3(t)}{dt} = -x_3(t) - x_3^3(t) - fx_2(t) + gx_1(t) + \Delta_3
\end{cases}
\tag{7.26}
$$

Let initial states be $x_1(0) = 2, x_2(0) = 2.4, x_3(0) = 5$ and system parameters $a = 0.1, b = 11, c = 40, \ d = 54, f = 6, g = 30$ and uncertainty $\Delta_1 = 0.1\cos(3t)$, $\Delta_2 = Rayleigh \ noise$ shown in Fig. 7.8 and $\Delta_3 = 0.1\sin(2t)$. The chaotic attractor of the Ge-Ku-Duffing system is shown in Fig. 7.9.

The slave Double Ge-Ku system[43] is:

$$
\begin{cases}
\dfrac{dy_1(t)}{dt} = y_2(t) + u_1 \\[2mm]
\dfrac{dy_2(t)}{dt} = -ly_2(t) - y_1(t)(m(n - y_1^2(t)) + py_3(t)) + u_2 \\[2mm]
\dfrac{dy_3(t)}{dt} = -ly_3(t) - y_3(t)(m(n - y_3^2(t)) + ry_1(t)) + u_3
\end{cases}
\tag{7.27}
$$

when initial condition $y_1(0) = 0.1, y_2(0) = 0.1, y_3(0) = 0.1$, and system parameters $l = -0.5, m = -14, n = 1.9, p = 54, r = 6.2$ .The Double Ge-Ku system exhibits chaotic motion which is shown in Fig. 7.10. u_1, u_2 and u_3 are FLCC to synchronize projectively the slave system to master one, i.e.,

$$
\lim_{t \to \infty} \mathbf{e} = 0
\tag{7.28}
$$

The projective synchronization error vector is

$$
\mathbf{e} = \begin{bmatrix} e_1(t) \\ e_2(t) \\ e_3(t) \end{bmatrix} = \alpha \begin{bmatrix} x_1(t) \\ x_2(t) \\ x_3(t) \end{bmatrix} - \begin{bmatrix} y_1(t) \\ y_2(t) \\ y_3(t) \end{bmatrix}
\tag{7.29}
$$

where the projective constant is $\alpha = 2$.

From Eq. (7.29), we have the following error dynamics:

$$\begin{cases} \dot{e}_1 = \alpha(x_2(t)+\Delta_1)-(y_2(t)+u_1) \\ \dot{e}_2 = \alpha(-ax_2(t)-x_1(t)(b(c-x_1^2(t))+dx_3(t))+\Delta_2)-(-ly_2(t)-y_1(t)(m(n-y_1^2(t))+py_3(t))+u_2) \\ \dot{e}_3 = \alpha(-x_3(t)-x_3^3(t)-fx_2(t)+gx_1(t)+\Delta_3)-(-ly_3(t)-y_3(t)(m(n-y_3^2(t))+ry_1(t))+u_3) \end{cases} \qquad (7.30)$$

Choosing Lyapunov function as:

$$V = \frac{1}{2}(e_1^2 + e_2^2 + e_3^2) \qquad (7.31)$$

Its time derivative is:

$$\begin{aligned} \dot{V} &= e_1\dot{e}_1 + e_2\dot{e}_2 + e_3\dot{e}_3 \\ &= e_1(\alpha(x_2(t)+\Delta_1)-(y_2(t)+u_1)) \\ &\quad + e_2(\alpha(-ax_2(t)-x_1(t)(b(c-x_1^2(t))+dx_3(t)) \\ &\quad -((-ly_2(t)-y_1(t)(m(n-y_1^2(t))+py_3(t)) \\ &\quad + e_3(\alpha(-x_3(t)-x_3^3(t)+f_2x(t)+gx(t)+\Delta_3) \\ &\quad -(-ly_3(t)-y_3(t)(m(n-y_3^2(t))+u_3)) \end{aligned} \qquad (7.32)$$

In order to design FLCC, we divide Eq. (7.32) into three parts as follows:

Assume $V = \frac{1}{2}(e_1^2 + e_2^2 + e_3^2) = V_1 + V_2 + V_3$, then $\dot{V} = e_1\dot{e}_1 + e_2\dot{e}_2 + e_3\dot{e}_3 = \dot{V}_1 + \dot{V}_2 + \dot{V}_3$,

where $V_1 = \frac{1}{2}e_1^2$, $V_2 = \frac{1}{2}e_2^2$ and $V_3 = \frac{1}{2}e_3^2$.

Part 1:

$$\dot{V}_1 = e_1\dot{e}_1 = e_1(\alpha(x_2(t)+\Delta_1)-(y_2(t)+u_1))$$

Part 2:

$$\begin{aligned} \dot{V}_2 = e_2\dot{e}_2 &= e_2(\alpha(-ax_2(t)-x_1(t)(b(c-x_1^2(t))+dx_3(t))+\Delta_2) \\ &\quad -(-ly_2(t)-y_1(t)(m(n-y_1^2(t))+py_3(t))+u_2)) \end{aligned}$$

Part 3:

$$\begin{aligned} \dot{V}_3 = e_3\dot{e}_3 &= e_3(\alpha(-x_3(t)-x_3^3(t)-fx_2(t)+gx_1(t)+\Delta_3) \\ &\quad -(-ly_3(t)-y_3(t)(m(n-y_3^2(t))+ry_1(t))+u_3)) \end{aligned}$$

FLCC in *Part 1, 2 and 3* can be obtained via the fuzzy rules in Table 7.1 as follows and the maximum value and minimum values of $\dot{e}_1$, $\dot{e}_2$, $\dot{e}_3$ (without any

controller) can be observed in time history of error derivatives drawn in Fig. 7.11.

The synchronizatio*n* scheme is proposed in *Part 1, 2* and *3* and as $\dot{V}_1 = e_1\dot{e}_1 < 0$,

$\dot{V}_2 = e_2\dot{e}_2 < 0$ and $\dot{V}_3 = e_3\dot{e}_3 < 0$. Hence, we have $\dot{V} = \dot{V}_1 + \dot{V}_2 + \dot{V}_3 < 0$. It is clear that

all of the rules in our FLCC can lead the Lyapunov theorem of asymptotical stability

is satisfied and the simulation results are shown in Fig. 7.12 and 7.13.

If the traditional method is used in this case. We choose a positive definite

Lyapunov function for e_1, e_2, e_3:

$$V = \frac{1}{2}(e_1^2 + e_2^2 + e_3^2) \tag{7.33}$$

Its time derivative is

$$
\begin{aligned}
\dot{V} &= e_1\dot{e}_1 + e_2\dot{e}_2 + e_3\dot{e}_3 \\
&= e_1(\alpha(x_2(t) + \Delta_1) - (y_2(t) + u_1')) \\
&\quad + e_2(\alpha(-ax_2(t) - x_1(t)(b(c - x_1^2(t)) + dx_3(t)) + \Delta_2) \\
&\quad - ((-ly_2(t) - y_1(t)(m(n - y_1^2(t)) + py_3(t)) + u_2')) \\
&\quad + e_3(\alpha(-x_3(t) - x_3^3(t) - fx_2(t) + gx_1(t) + \Delta_3) \\
&\quad - (-ly_3(t) - y_3(t)(m(n - y_3^2(t)) + ry_1(t)) + u_3'))
\end{aligned}
\tag{7.34}
$$

Choose

$$
\begin{aligned}
u_1' &= \alpha(x_2(t) + \Delta_1) - y_2(t) + \alpha x_1(t) - y_1(t) \\
u_2' &= \alpha(-ax_2(t) - x_1(t)(b(c - x_1^2(t)) + dx_3(t)) + \Delta_2) \\
&\quad - ((-ly_2(t) - y_1(t)(m(n - y_1^2(t)) + py_3(t))) + \alpha x_2 - y_2 \\
u_3' &= \alpha(-x_3(t) - x_3^3(t) - fx_2(t) + gx_1(t) + \Delta_3) \\
&\quad - (-ly_3(t) - y_3(t)(m(n - y_3^2(t)) + ry_1(t))) + \alpha x_3 - y_3
\end{aligned}
\tag{7.35}
$$

We obtain

$$\dot{V} = -e_1^2 - e_2^2 - e_3^2 < 0 \tag{7.36}$$

Comparing with FLCC in Table 7.2, we see that traditional controllers are more

complex than that of FLCC. The manipulation is the same as that in Subsection 7.3.1.

Table 7.2. The controllers of FLCC and of traditional method.

Subsection 7.3.1:	
Traditional	FLCC

$$\begin{cases} u_1^{'} = \alpha(x_2 x_3 + \Delta_1) - (y_2 y_3 + u_1) + \alpha x_1 - y_1 \\ u_2^{'} = \alpha(x_1 - x_2 + \Delta_2) - (y_1^2 - y_2 + u_2) + \alpha x_2 - y_2 \\ u_3^{'} = \alpha(1 - x_1^2 + \Delta_3) - (y_1 - 4y_1 + u_3) + \alpha x_3 - y_3 \end{cases} \qquad \begin{cases} Z_1 = 20, \quad e_1 \to 0 \\ Z_2 = 20, \quad e_2 \to 0 \\ Z_3 = 20, \quad e_3 \to 0 \end{cases}$$

Subsection 7.3.2:	
Traditional	FLCC

$$\begin{cases} u_1^{'} = \alpha(x_2(t) + \Delta_1) - y_2(t) + \alpha x_1(t) - y_1(t) \\ u_2^{'} = \alpha(-ax_2(t) - x_1(t)(b(c - x_1^2(t)) + dx_3(t)) + \Delta_2) \\ \qquad - ((-ly_2(t) - y_1(t)(m(n - y_1^2(t)) + py_3(t)))) + \alpha x_2 - y_2 \\ u_3^{'} = \alpha(-x_3(t) - x_3^3(t) - fx_2(t) + gx_1(t) + \Delta_3) \\ \qquad - (-ly_3(t) - y_3(t)(m(n - y_3^2(t)) + ry_1(t))) + \alpha x_3 - y_3 \end{cases} \qquad \begin{cases} Z_1 = 200, \quad e_1 \to 0 \\ Z_2 = 3000, \quad e_2 \to 0 \\ Z_3 = 500, \quad e_3 \to 0 \end{cases}$$

7.4 Comparison of Simulations of New Strategy and of Traditional Method

The FLCC are simpler than that of traditional controllers and will give less simulation errors. This conclusion can be proved by the following simulation results.

In Fig. 7.7 and 7.14, it is presented clearly that the FLCC is faster than traditional controller to achieve projective synchronization. In Fig. 7.13 and 7.15, the results are similar.

Furthermore, in Table 7.3, comparison between error data is given. All data are picked from 35.01 to 35.05s with sampling time 0.01s. From these data, the superiority of new strategy is obvious.

Table 7.3. Error data at 35.01, 35.02, 35.03, 35.04,35.05s after the action of controllers

Error for new strategy	Error for traditional method

Subsection 7.3.1: e_1

0.000000000000721	*0.026467294618436*
0.000000000000714	*0.026203940636773*
0.000000000000707	*0.02594320707101*
0.000000000000700	*0.025685067847574*
0.000000000000693	*0.025429497152326*

Subsection 7.3.1: e_2

-0.000000000000032	*0.029170713652016*
-0.000000000000032	*0.028880460201524*
-0.000000000000032	*0.028593094821119*
-0.000000000000031	*0.028308588774023*
-0.000000000000031	*0.028026913609395*

Subsection 7.3.1: e_3

0.000000000000044	*-0.009388571342601*
0.000000000000044	*-0.009295153496884*
0.000000000000043	*-0.009202665174263*
0.000000000000043	*-0.009111097125828*
0.000000000000042	*-0.009020440194699*
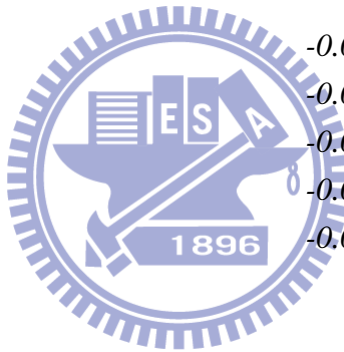
Subsection 7.3.2: e_1

-0.000000000000055	*-0.024478766106521*
-0.000000000000054	*-0.024235198314146*
-0.000000000000053	*-0.023994054061798*
-0.000000000000053	*-0.023755309234852*
-0.000000000000052	*-0.023518939958626*

Subsection 7.3.2: e_2

0.000000000025608	*0.313445617992862*
0.000000000025437	*0.310326781983228*
0.000000000025381	*0.307238978910405*
0.000000000025409	*0.304181899991505*
0.000000000025452	*0.301155239516092*

Subsection 7.3.2: e_3

0.000000000022935	*-0.094135747156624*

0.000000000023133	*-0.09319908082227*
0.000000000023270	*-0.092271734473663*
0.000000000023322	*-0.091353615375398*
0.000000000023274	*-0.090444631714798*
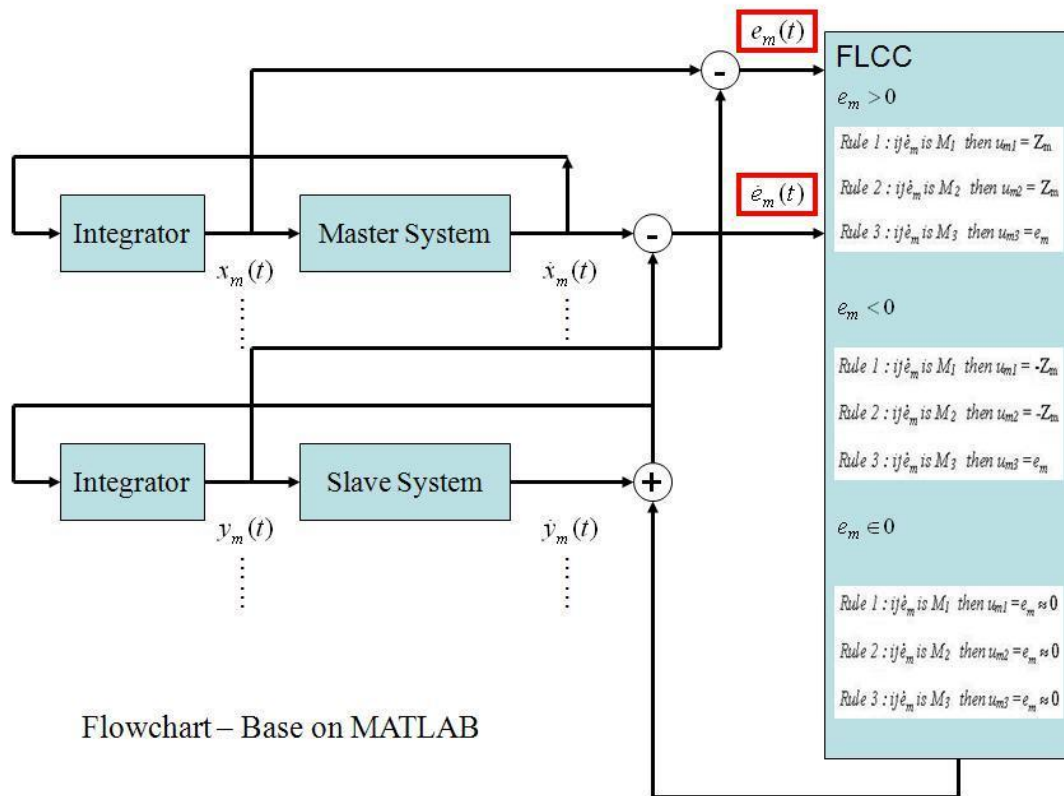
Fig. 7.1. The block diagram sketch of fuzzy logic controller.

M
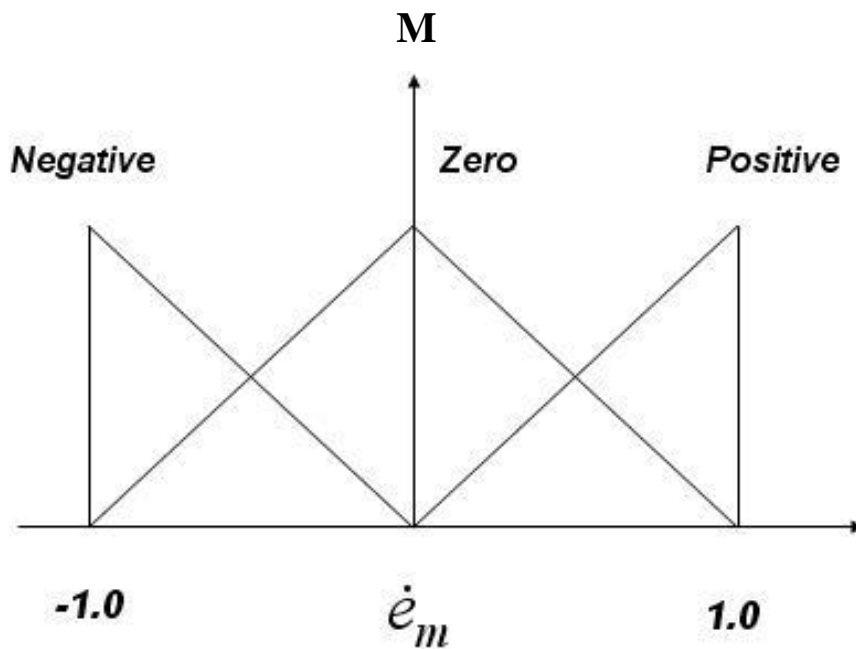
Fig. 7.2. Membership functions.
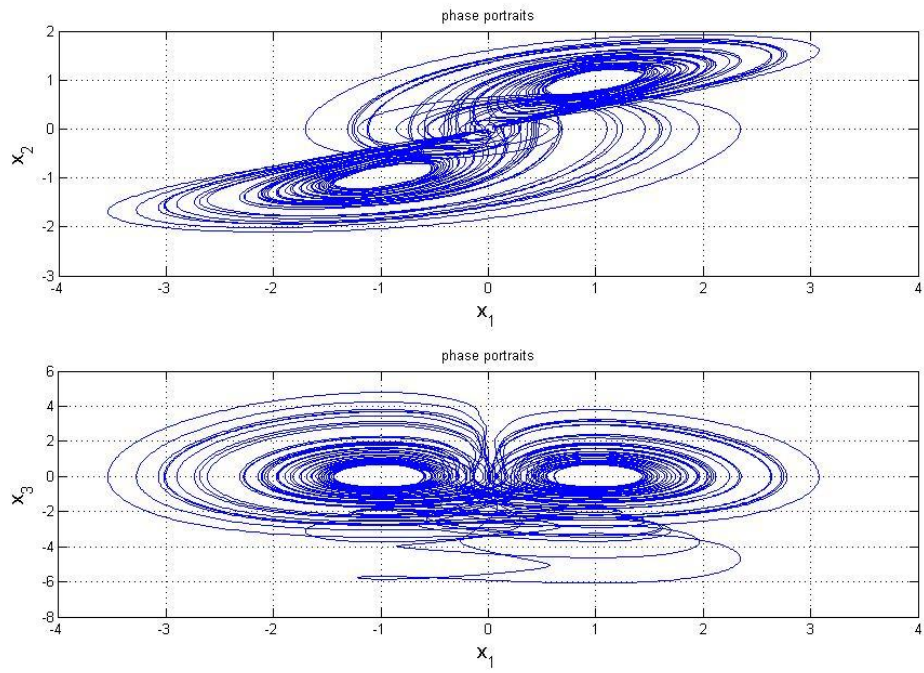
Fig. 7.3. Phase portrait of Master system for *Subsection 7.3.1*.
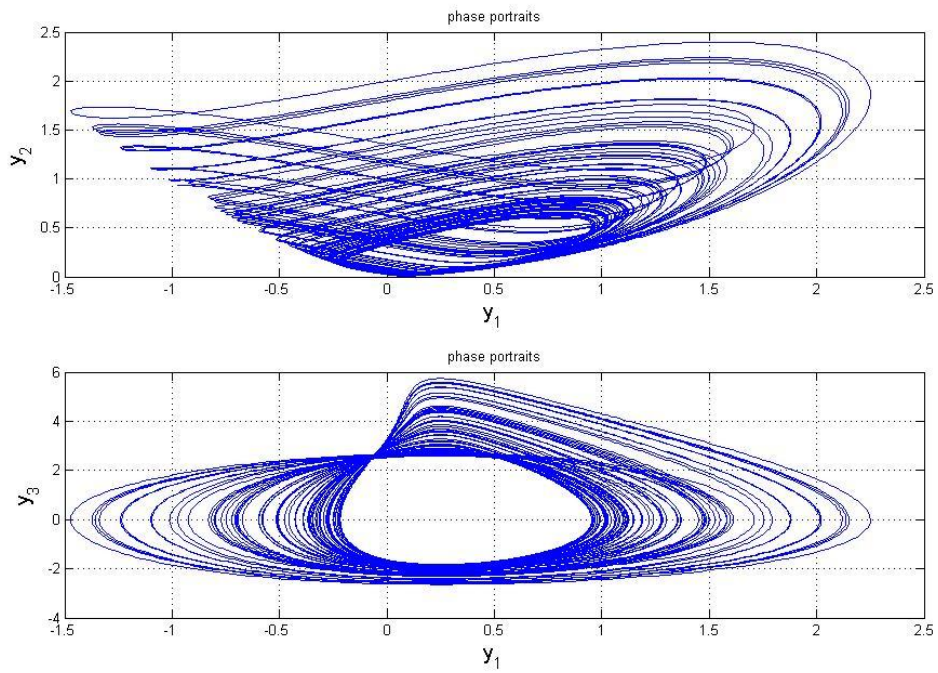
Fig. 7.4. Phase portrait of Slave system for *Subsection 7.3.1*.
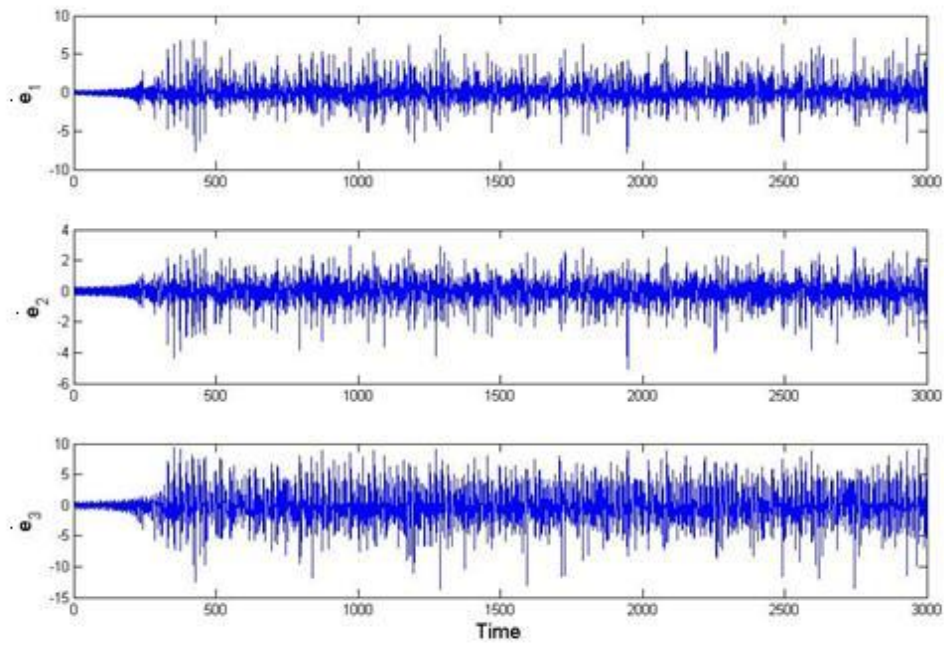
Fig. 7.5. Time histories of error derivatives for *Subsection 7.3.1* without controllers.
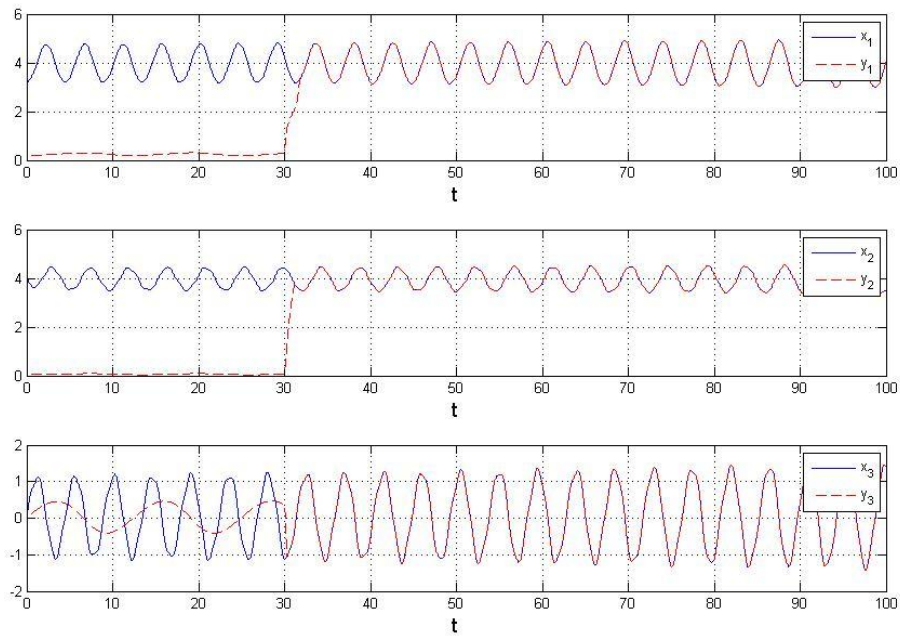
Fig. 7.6. Time histories of states for *Subsection 7.3.1* where the FLCC is added after

30s.

97
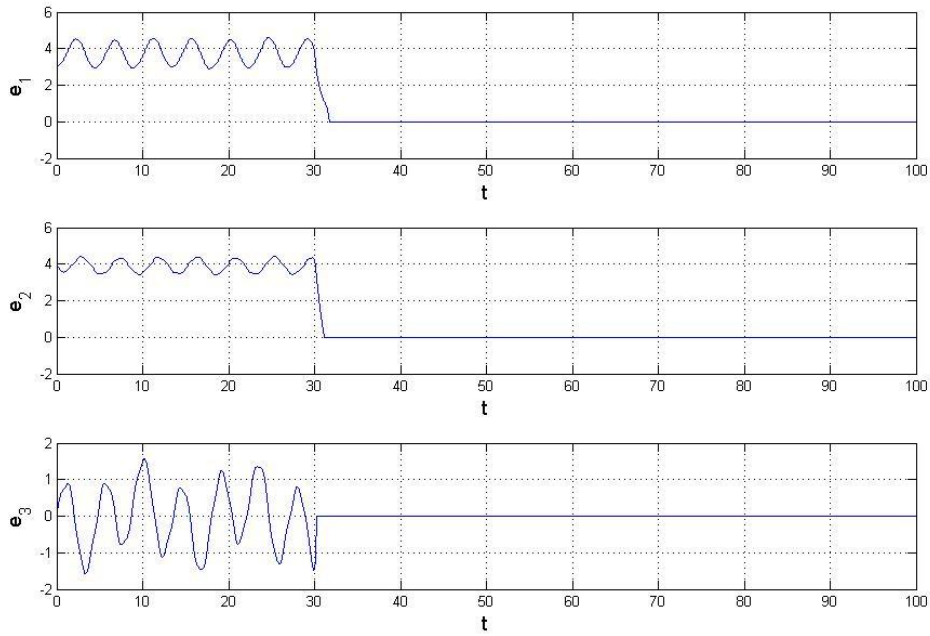
Fig. 7.7. Time histories of errors for *Subsection 7.3.1* where the FLCC is added after

30s.
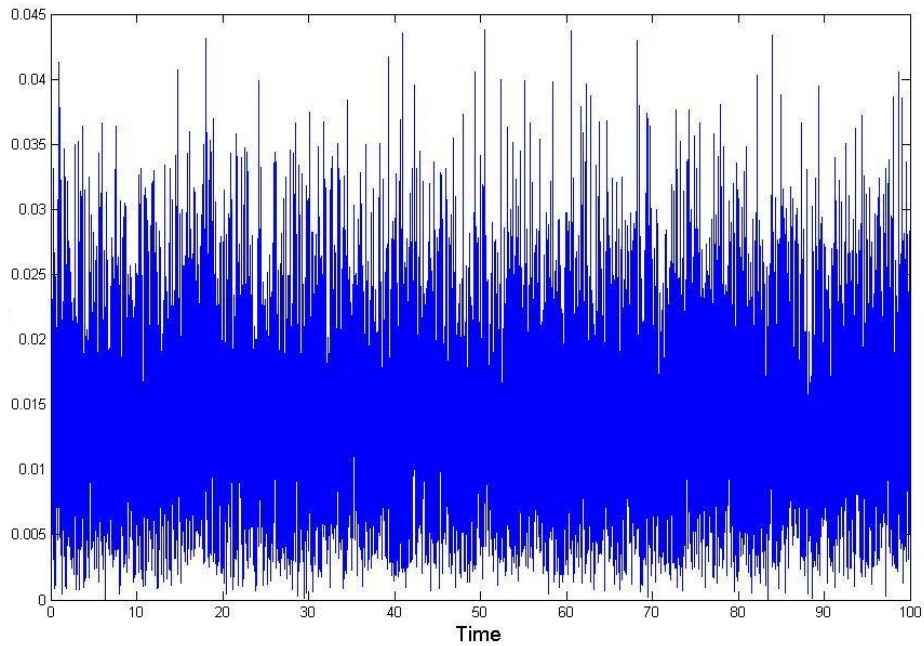
Fig. 7.8. The stochastic signal of $\Delta_2 =$ Rayleigh noise
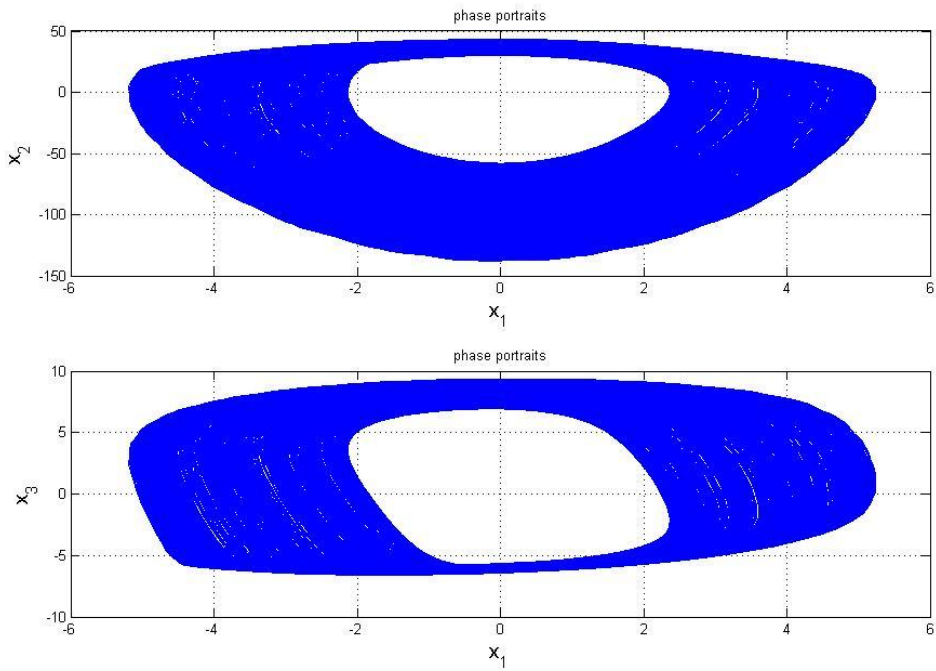
Fig. 7.9. Phase portrait of Master system for *Subsection 7.3.2*.
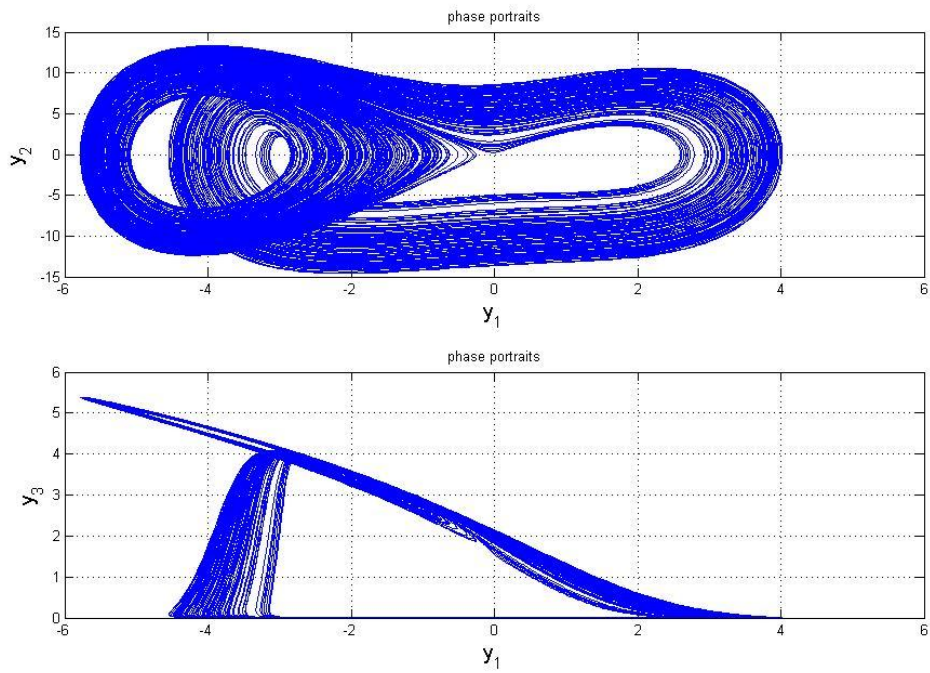
Fig. 7.10. Phase portrait of Slave system for *Subsection 7.3.2*.
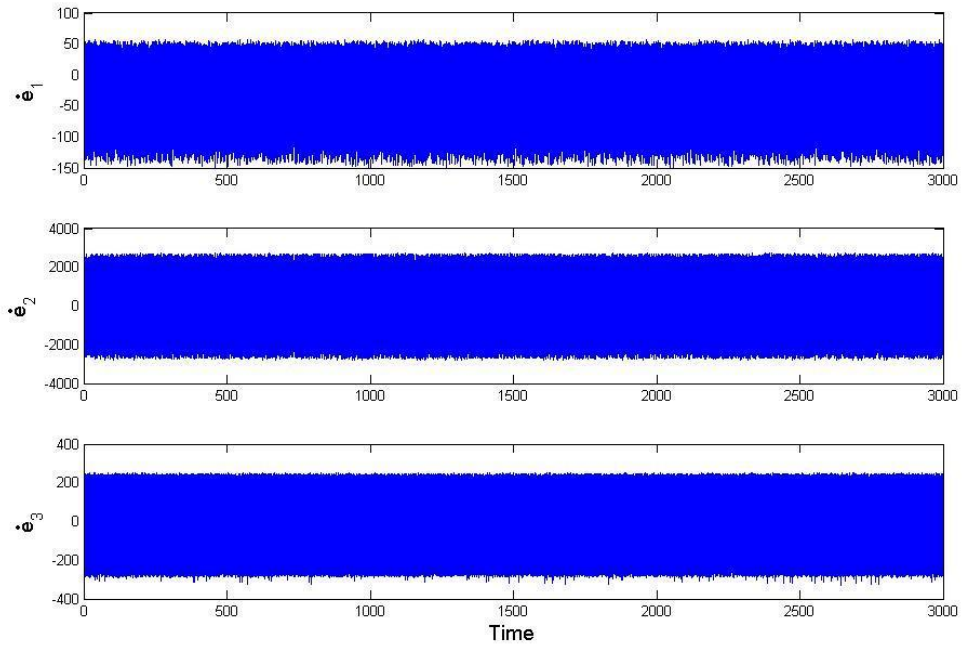
Fig. 7.11. Time histories of error derivatives for *Subsection 7.3.2* without controllers.
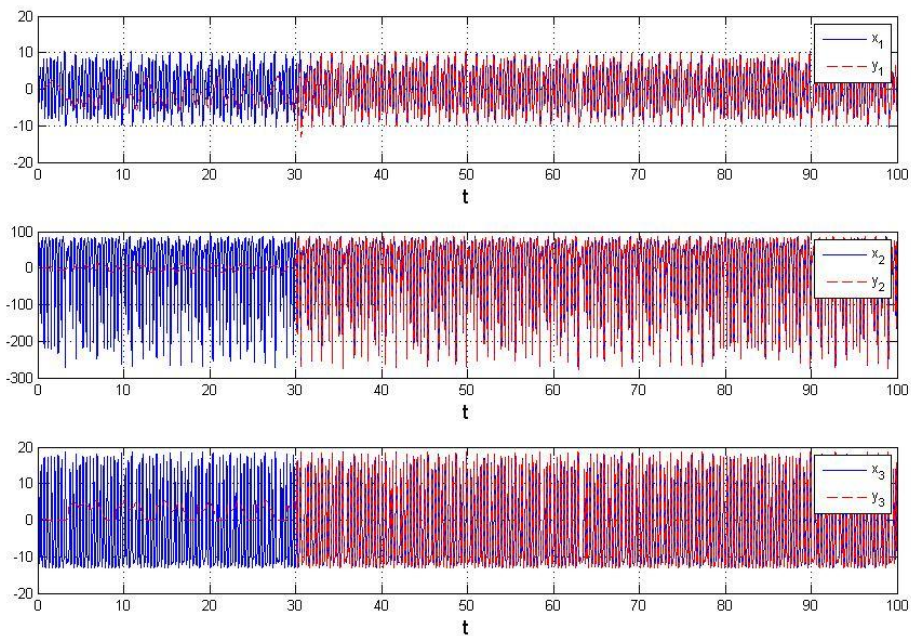
Fig. 7.12. Time histories of states for *Subsection 7.3.2* where the FLCC is added after

30s.
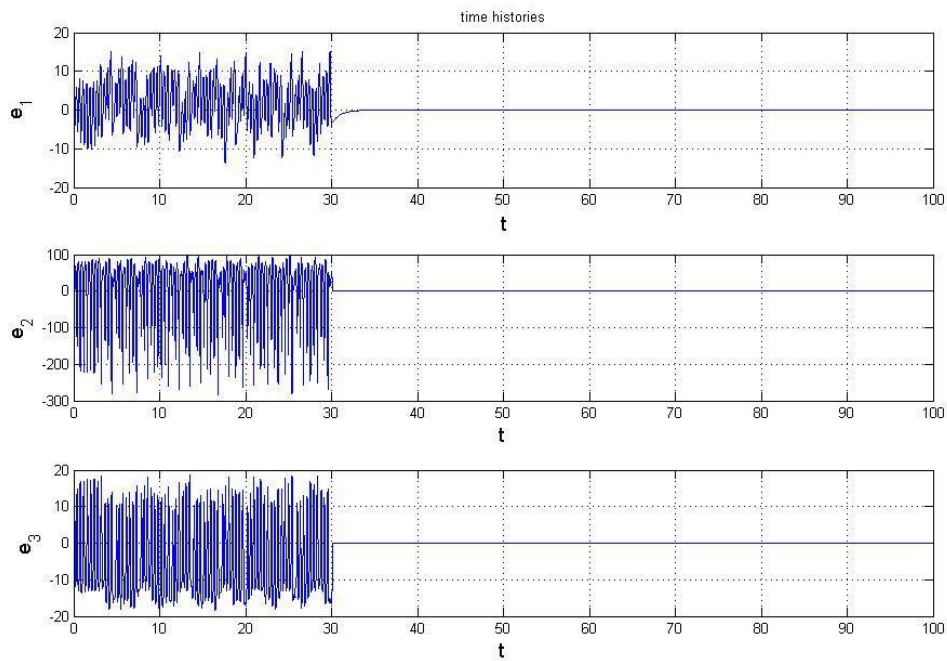
Fig. 7.13. Time histories of errors for *Subsection 7.3.2* where the FLCC is added after 30s.
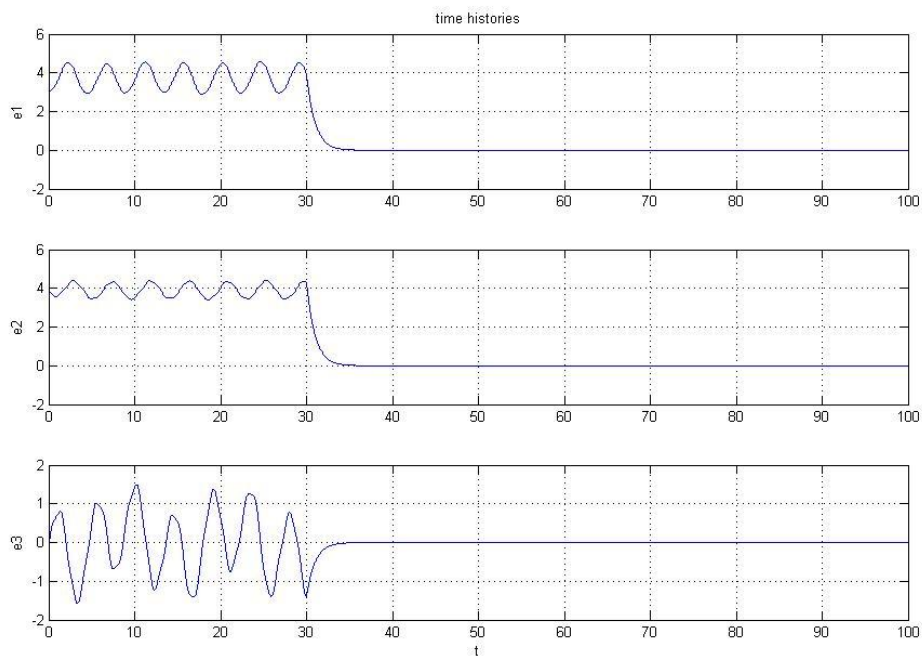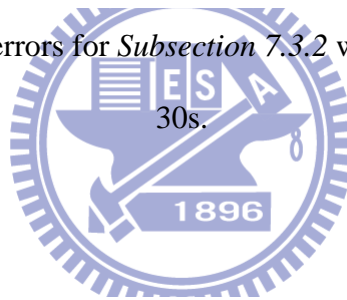
Fig. 7.14. Time histories of errors of using traditional controller design method for

101

Fig. 7.15. Time histories of errors of using traditional controller design method for
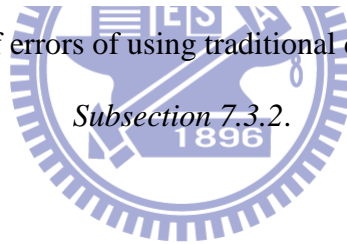
Subsection 7.3.2.

Chapter 8

Conclusions

In this thesis, chaos and various chaos synchronizations of Ge-Ku-Duffing system and Sprott C, E system are studied. In Chapter 2, the chaotic behavior in new Ge-Ku-Duffing system is studied by phase portraits, time history, Poincaré maps, Lyapunov exponent and bifurcation diagrams.

In Chapter 3, a new strategy to achieve chaos synchronization by the different translation pragmatical synchronization using partial region stability theory is proposed. By using the partial region stability theory , the Lyapunov function of error states becomes a simple linear homogeneous function , the controllers are more simple since they are in lower degree than that of traditional controllers. Furthermore, according to the pragmatical asymptotically stability theorem, error vector e approaches zero and the estimated parameters also approach the uncertain parameters. The equilibrium point is pragmatically asymptotically stable. It is important to note that k_1, k_2 are not arbitrary , two proper value must chosen to make that the error dynamics always in first quadrant, so give two more insurances for secret communication than other synchronization methods.

In Chapter 4, a new type of synchronization, double symplectic synchronization, is studied in this Chapter. It is an extension of symplectic synchronization. By applying active control, the double symplectic synchronization is achieved. The simulation results show that the proposed scheme is effective and feasible. Furthermore, the double symplectic synchronization of chaotic systems can be used to increase the security of secret communication.

In Chapter 5, a new type of synchronization, multiple symplectic synchronization, is studied in this Chapter. It is an extension of double symplectic

synchronization. By applying active control, the multiple symplectic synchronization is achieved. The simulation results show that the proposed scheme is effective and feasible. Furthermore, the multiple symplectic synchronization of chaotic systems can be used to increase the security of secret communication.

In Chapter 6, a new strategy to achieve chaos synchronization via the new fuzzy model is proposed. By using the new fuzzy model, a complicated nonlinear system can be linearized to a simple form, linear coupling of only two linear subsystems and the numbers of fuzzy rules can be reduced from 2^N to $2 \times N$. The simulation results show that the proposed scheme is effective and feasible.

In Chapter 7, we propose a new fuzzy logic constant controller (FLCC), which constructs fuzzy rules subject to Lyapunov direct method. Error derivatives are used according to the upper and lower bounds. The fuzzy rules and the simplest corresponding constant controllers are obtained while complicated and nonlinear controllers would no longer appear. Simulation results in synchronization show that FLCC has high performance of the convergence of error states and good robustness for the chaotic systems with deterministic and stochastic uncertainties.

Appendix A

GYC Partial Region Stability Theory [53-55]

A.1 Definition of the Stability on Partial Region

Consider the differential equations of disturbed motion of a nonautonomous system in the normal form

$$\frac{dx_s}{dt} = X_s(t, x_1, \cdots, x_n), \qquad (s = 1, \cdots, n) \tag{A.1}$$

where the function X_s is defined on the intersection of the partial region Ω (shown in Fig. A1) and

$$\sum_s x_s^2 \leq H \tag{A.2}$$

and $t > t_0$, where t_0 and H are certain positive constants. X_s which vanishes when the variables x_s are all zero, is a real valued function of t, $x_1, \cdots, x_n$. It is assumed that X_s is smooth enough to ensure the existence, uniqueness of the solution of the initial value problem. When X_s does not contain t explicitly, the system is autonomous.

Obviously, $x_s = 0$ $(s = 1, \cdots n)$ is a solution of Eq.(A.1). We are interested to the asymptotical stability of this zero solution on partial region Ω (including the boundary) of the neighborhood of the origin which in general may consist of several subregions (Fig. A1).

Definition 1:

For any given number $\varepsilon > 0$, if there exists a $\delta > 0$, such that on the closed given partial region Ω when

$$\sum_s x_{s0}^2 \leq \delta, \quad (s = 1, \cdots, n) \tag{A.3}$$

for all $t \geq t_0$, the inequality

$$\sum_s x_s^2 < \varepsilon, \quad (s = 1, \cdots, n) \tag{A.4}$$

is satisfied for the solutions of Eq.(A.1) on Ω, then the disturbed motion $x_s = 0$ $(s = 1, \cdots n)$ is stable on the partial region Ω.

Definition 2:

If the undisturbed motion is stable on the partial region Ω, and there exists a $\delta' > 0$, so that on the given partial region Ω when

$$\sum_s x_{s0}^2 \leq \delta', \quad (s = 1, \cdots, n) \tag{A.5}$$

The equality

$$\lim_{t \to \infty} \left(\sum_s x_s^2 \right) = 0 \tag{A.6}$$

is satisfied for the solutions of Eq.(A.1) on Ω, then the undisturbed motion $x_s = 0$ $(s = 1, \cdots n)$ is asymptotically stable on the partial region Ω.

The intersection of Ω and region defined by Eq.(A.5) is called the region of attraction.

Definition of Functions $V(t, x_1, \cdots, x_n)$:

Let us consider the functions $V(t, x_1, \cdots, x_n)$ given on the intersection Ω_1 of the partial region Ω and the region

$$\sum_s x_s^2 \leq h, \quad (s = 1, \cdots, n) \tag{A.7}$$

for $t \geq t_0 > 0$, where t_0 and h are positive constants. We suppose that the functions are single-valued and have continuous partial derivatives and become zero when $x_1 = \cdots = x_n = 0$.

Definition 3:

If there exists $t_0 > 0$ and a sufficiently small $h > 0$, so that on partial region Ω_1 and $t \geq t_0$, $V \geq 0$ (or ≤ 0), then V is a positive (or negative) semidefinite, in general semidefinite, function on the Ω_1 and $t \geq t_0$.

Definition 4:

If there exists a positive (negative) definitive function $W(x_1 \ldots x_n)$ on Ω_1, so that on the partial region Ω_1 and $t \geq t_0$

$$V - W \geq 0 \ (or -V - W \geq 0), \tag{A.8}$$

then $V(t, x_1, \ldots, x_n)$ is a positive definite function on the partial region Ω_1 and $t \geq t_0$.

Definition 5:

If $V(t, x_1, \ldots, x_n)$ is neither definite nor semidefinite on Ω_1 and $t \geq t_0$, then $V(t, x_1, \ldots, x_n)$ is an indefinite function on partial region Ω_1 and $t \geq t_0$. That is, for any small $h > 0$ and any large $t_0 > 0$, $V(t, x_1, \ldots, x_n)$ can take either positive or negative value on the partial region Ω_1 and $t \geq t_0$.

Definition 6: Bounded function V

If there exist $t_0 > 0$, $h > 0$, so that on the partial region Ω_1, we have

$$\left| V(t, x_1, \ldots, x_n) \right| < L$$

where L is a positive constant, then V is said to be bounded on Ω_1.

Definition 7: Function with infinitesimal upper bound

If V is bounded, and for any $\lambda > 0$, there exists $\mu > 0$, so that on Ω_1 when $\sum_s x_s^2 \leq \mu$, and $t \geq t_0$, we have

$$\left| V(t, x_1, \ldots, x_n) \right| \leq \lambda$$

then V admits an infinitesimal upper bound on Ω_1.

A.2 GYC Theorem of Stability and of Asymptotical Stability on Partial Region

Theorem 1

If there can be found a definite function $V(t, x_1, \ldots, x_n)$ on the partial region for Eq. (A.1), and the derivative with respect to time based on these equations are:

$$\frac{dV}{dt} = \frac{\partial V}{\partial t} + \sum_{s=1}^{n} \frac{\partial V}{\partial x_s} X_s \qquad (A.9)$$

Then, it is a semidefinite function on the partial region whose sense is opposite to that of V, or if it becomes zero identically, then the undisturbed motion is stable on the partial region.

Proof:

Let us assume for the sake of definiteness that V is a positive definite function. Consequently, there exists a sufficiently large number t_0 and a sufficiently small number $h < H$, such that on the intersection Ω_1 of partial region Ω and

$$\sum_s x_s^2 \le h, \quad (s = 1, \dots, n)$$

and $t \ge t_0$, the following inequality is satisfied

$$V(t, x_1, \dots, x_n) \ge W(x_1, \dots, x_n),$$

where W is a certain positive definite function which does not depend on t. Besides that, Eq. (A.9) may assume only negative or zero value in this region.

Let ε be an arbitrarily small positive number. We shall suppose that in any case $\varepsilon < h$. Let us consider the aggregation of all possible values of the quantities $x_1, \dots, x_n$, which are on the intersection ω_2 of Ω_1 and

$$\sum_s x_s^2 = \varepsilon, \qquad (A.10)$$

and let us designate by $l > 0$ the precise lower limit of the function W under this condition. By virtue of Eq. (A.8), we shall have

$$V(t, x_1, \dots, x_n) \ge l \quad \text{for} \quad (x_1, \dots, x_n) \quad \text{on} \quad \omega_2. \qquad (A.11)$$

We shall now consider the quantities x_s as functions of time which satisfy the differential equations of disturbed motion. We shall assume that the initial values x_{s0} of these functions for $t = t_0$ lie on the intersection Ω_2 of Ω_1 and the region

$$\sum_s x_s^2 \le \delta, \qquad (A.12)$$

108

where δ is so small that

$$V(t_0, x_{10}, \ldots, x_{n0}) < l \tag{A.13}$$

By virtue of the fact that $V(t_0, 0, \ldots, 0) = 0$, such a selection of the number δ is obviously possible. We shall suppose that in any case the number δ is smaller than ε. Then the inequality

$$\sum_s x_s^2 < \varepsilon, \tag{A.14}$$

being satisfied at the initial instant will be satisfied, in the very least, for a sufficiently small $t - t_0$, since the functions $x_s(t)$ very continuously with time. We shall show that these inequalities will be satisfied for all values $t > t_0$. Indeed, if these inequalities were not satisfied at some time, there would have to exist such an instant $t=T$ for which this inequality would become an equality. In other words, we would have

$$\sum_s x_s^2(T) = \varepsilon,$$

and consequently, on the basis of Eq. (A.11)

$$V(T, x_1(T), \ldots, x_n(T)) \geq l \tag{A.15}$$

On the other hand, since $\varepsilon < h$, the inequality (Eq.(A.7)) is satisfied in the entire interval of time [t_0, T], and consequently, in this entire time interval $\dfrac{dV}{dt} \leq 0$. This yields

$$V(T, x_1(T), \ldots, x_n(T)) \leq V(t_0, x_{10}, \ldots, x_{n0}),$$

which contradicts Eq. (A.14) on the basis of Eq. (A.13). Thus, the inequality (Eq.(A.4)) must be satisfied for all values of $t > t_0$, hence follows that the motion is stable.

Finally, we must point out that from the view-point of mathenatics, the stability on partial region in general does not be related logically to the stability on whole region. If an undisturbed solution is stable on a partial region, it may be either stable

109

or unstable on the whole region and vice versa. In specific practical problems, we do not study the solution starting within Ω_2 and running out of Ω.

Theorem 2

If in satisfying the conditions of Theorem 1, the derivative $\dfrac{dV}{dt}$ is a definite function on the partial region with opposite sign to that of V and the function V itself permits an infinitesimal upper limit, then the undisturbed motion is asymptotically stable on the partial region.

Proof:

Let us suppose that V is a positive definite function on the partial region and that consequently, $\dfrac{dV}{dt}$ is negative definite. Thus on the intersection Ω_1 of Ω and the region defined by Eq. (A.7) and $t \geq t_0$ there will be satisfied not only the inequality (Eq.(A.8)), but the following inequality as well:

$$\frac{dV}{dt} \leq -W_1(x_1, \ldots x_n), \tag{A.16}$$

where W_1 is a positive definite function on the partial region independent of t.

Let us consider the quantities x_s as functions of time which satisfy the differential equations of disturbed motion assuming that the initial values $x_{s0} = x_s(t_0)$ of these quantities satisfy the inequalities (Eq. (A.12)). Since the undisturbed motion is stable in any case, the magnitude δ may be selected so small that for all values of $t \geq t_0$ the quantities x_s remain within Ω_1. Then, on the basis of Eq. (A.16) the derivative of function $V(t, x_1(t), \ldots, x_n(t))$ will be negative at all times and, consequently, this function will approach a certain limit, as t increases without limit, remaining larger than this limit at all times. We shall show that this limit is equal to some positive quantity different from zero. Then for all values of $t \geq t_0$ the following inequality will be satisfied:

$$V(t, x_1(t), \ldots, x_n(t)) > \alpha \tag{A.17}$$

where $\alpha > 0$.

Since V permits an infinitesimal upper limit, it follows from this inequality that

$$\sum_{s} x_s^2(t) \geq \lambda, \quad (s = 1, \ldots, n), \tag{A.18}$$

where λ is a certain sufficiently small positive number. Indeed, if such a number λ did not exist, that is , if the quantity $\sum_{s} x_s(t)$ were smaller than any preassigned number no matter how small, then the magnitude $V(t, x_1(t), \ldots, x_n(t))$, as follows from the definition of an infinitesimal upper limit, would also be arbitrarily small, which contradicts Eq. (A.17).

If for all values of $t \geq t_0$ the inequality (Eq. (A.18)) is satisfied, then Eq. (A.16) shows that the following inequality will be satisfied at all times:

$$\frac{dV}{dt} \leq -l_1,$$

where l_1 is positive number different from zero which constitutes the precise lower limit of the function $W_1(t, x_1(t), \ldots, x_n(t))$ under condition (Eq. (A.18)). Consequently, for all values of $t \geq t_0$ we shall have:

$$V(t, x_1(t), \ldots, x_n(t)) = V(t_0, x_{10}, \ldots, x_{n0}) + \int_{t_0}^{t} \frac{dV}{dt} dt \leq V(t_0, x_{10}, \ldots, x_{n0}) - l_1(t - t_0),$$

which is, obviously, in contradiction with Eq.(A.17). The contradiction thus obtained shows that the function $V(t, x_1(t), \ldots, x_n(t))$ approached zero as t increase without limit. Consequently, the same will be true for the function $W(x_1(t), \ldots, x_n(t))$ as well, from which it follows directly that

$$\lim_{t \to \infty} x_s(t) = 0, \quad (s = 1, \ldots, n),$$

which proves the theorem.
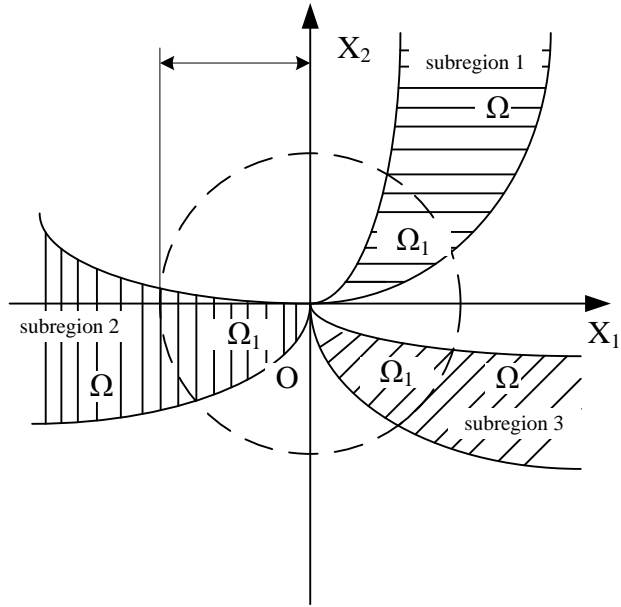
Fig. A.1. Partial regions Ω and Ω_1

Appendix B

Pragmatical Asymptotical Stability Theory

The stability for many problems in real dynamical systems is actual asymptotical stability, although may not be mathematical asymptotical stability. The mathematical asymptotical stability demands that trajectories from all initial states in the neighborhood of zero solution must approach the origin as $t \to \infty$. If there are only a small part or even a few of the initial states from which the trajectories do not approach the origin as $t \to \infty$, the zero solution is not mathematically asymptotically stable. However, when the probability of occurrence of an event is zero, it means the event does not occur actually. If the probability of occurrence of the event that the trajectries from the initial states are that they do not approach zero when $t \to \infty$, is zero, the stability of zero solution is actual asymptotical stability though it is not mathematical asymptotical stability. In order to analyze the asymptotical stability of the equilibrium point of such systems, the pragmatical asymptotical stability theorem is used.

Let X and Y be two manifolds of dimensions m and n (m<n), respectively, and φ be a differentiable map from X to Y, then $\varphi(X)$ is subset of Lebesque measure 0 of Y [56]. For an autonomous system

$$\frac{dx}{dt} = f(x_1, \cdots, x_n) \tag{B-1}$$

where $x = [x_1, \cdots, x_n]^T$ is a state vector, the function $f = [f_1, \cdots, f_n]^T$ is defined on $D \subset R^n$ and $\|x\| \le H > 0$. Let x=0 be an equilibrium point for the system (B-1). Then

$$f(0) = 0 \tag{B-2}$$

For a nonautonomous systems,

$$\dot{x} = f(x_1,...,x_{n+1}) \tag{B-3}$$

where $x = [x_1,...,x_{n+1}]^T$, the function $f = [f_1,...,f_n]^T$ is define on $D \subset R^n \times R_+$, here $t = x_{n+1} \subset R_+$. The equilibrium point is

$$f(0,x_{n+1}) = . \tag{B-4}$$

Definition The equilibrium point for the system (B-1) is pragmatically asymptotically stable provided that with initial points on C which is a subset of Lebesque measure 0 of D, the behaviors of the corresponding trajectories cannot be determined, while with initial points on D$-$C, the corresponding trajectories behave as that agree with traditional asymptotical stability [57,58].

Theorem Let $V = [x_1, \cdots, x_n]^T$: D→R$_+$ be positive definite and analytic on D, where $x_1, x_2,...,x_n$ are all space coordinates such that the derivative of V through Eq. (A-1)or(A-3), $\dot{V}$, is negative semi-definite of $[x_1, x_2, \cdots, x_n]^T$.

For autonomous system, Let X be the m-manifold consisted of point set for which $\forall x \neq 0$, $\dot{V}(x) = 0$ and D is a n-manifold. If m+1<n, then the equilibrium point of the system is pragmatically asymptotically stable.

For nonautonomous system, let X be the $m+1$-manifold consisting of point set of which $\forall x \neq 0, \dot{V}(x_1, x_2,..., x_n) = 0$ and D is $n+1$-manifold. If $m+1+1<n+1$, i.e. $m+1<n$ then the equilibrium point of the system is pragmatically asymptotically stable. Therefore, for both autonomous and nonautonomous system the formula $m+1<n$ is universal. So the following proof is only for autonomous system. The proof for nonautonomous system is similar.

Proof Since every point of X can be passed by a trajectory of Eq. (B-1), which is one- dimensional, the collection of these trajectories, A, is a (m+1)-manifold [59,

60].

If m+1＜n, then the collection C is a subset of Lebesque measure 0 of D. By the above definition, the equilibrium point of the system is pragmatically asymptotically stable.

If an initial point is ergodicly chosen in D, the probability of that the initial point falls on the collection C is zero. Here, equal probability is assumed for every point chosen as an initial point in the neighborhood of the equilibrium point. Hence, the event that the initial point is chosen from collection C does not occur actually. Therefore, under the equal probability assumption, pragmatical asymptotical stability becomes actual asymptotical stability. When the initial point falls on $D-C$, $\dot{V}(x)<0$, the corresponding trajectories behave as that agree with traditional asymptotical stability because by the existence and uniqueness of the solution of initial-value problem, these trajectories never meet C.

In Eq. (3.8) V is a positive definite function of n variables, i.e. p error state variables and n-p=m differences between unknown and estimated parameters, while $\dot{V}=e^{T}Ce$ is a negative semi-definite function of n variables. Since the number of error state variables is always more than one, p>1, m+1<n is always satisfied, by pragmatical asymptotical stability theorem we have

$$\lim_{t\to\infty}e=0 \tag{B-5}$$

and the estimated parameters approach the uncertain parameters. The pragmatical adaptive control theorem is obtained. Therefore, the equilibrium point of the system is pragmatically asymptotically stable. Under the equal probability assumption, it is actually asymptotically stable for both error state variables and parameter variables.

References

1. Pecora, L.M., Carroll, T.L., "Synchronization in chaotic systems", Phys Rev Lett. 64 (1990) 821.

2. Han, S. K., Kerrer, C. and Kuramoto, Y., "Dephasing and bursting in coupled neural oscillators", Phys. Rev. Lett. 75 (1995) 3190.

3. Blasius, B., Huppert, A. and Stone, L., "Complex dynamics and phase synchronization in spatially extended ecological systems", Nature 399 (1999) 354.

4. Cuomo, K. M. and Oppenheim, V., "Circuit implementation of synchronized chaos with application to communication", Phys. Rev. Lett. 71 (1993) 65.

5. Kocarev, L. and Parlitz, U., "General approach for chaotic synchronization with application to communication", Phys. Rev. Lett. 74 (1995) 5028.

6. Wang, C. and Ge, S. S., "Adaptive synchronization of uncertain chaotic systems cia backstepping design", Chaos, Solitons and Fractals 12 (2001) 119.

7. Femat, R., Ramirze, J. A. and Anaya, G. F., "Adaptive synchronization of high-order chaotic systems: a feedback with low-order parameterization", Physica D 139 (2000) 231.

8. Mei Sun, Lixin Tian and Shumin Jiang, Jun Xu, "Feedback control and adaptive control of thr energy resource chaotic system", Chaos, Solitons and Fractals 32 (2007) 1725.

9. Femat, R. and perales, G. S., "On the chaotic synchronization phenomenon", Phus., letters A 262 (1999) 50.

10. Abarbaned, H. D. I., Rulkov, N. F. snd Sushchik, M. M., "Generalized synchronization of chaos: the auxiliary systems", Phy. Rev E, 53 (1996) 4528.

11. Yang, S. S. and Duan, C. K., "Generalized synchronization in chaotic systems", Chaos, Solitons and Fractals 9 (1998) 1703.

12. Yang, X. S., "Concepts of synchronization in dynamic systems", Phys., letters A 260 (1999) 340.

13. Wu, X., Chen, G. and Cai, J., "Chaos synchronization of the master–slave generalized Lorenz systems via linear state error feedback control", Physica D 229 (2007) 52.

14. Wu, X., Cai, J. and Wang, M., "Global chaos synchronization of the parametrically excited Duffing oscillators by linear state error feedback control", Chaos Solitons Fractals 36 (2008) 121.

15. Yassen ,M. T., "Chaos synchronization between two different chaotic system using active control", Chaos Solitons Fractals **23 (2005)** 131**.**

16. Tang, F. and Wang, L., "An adaptive active control for the modified Chua's circuit", Phys Lett A 346 (2005) 342.

17. Pecora, L. M. and Carroll, T. L., "Synchronization in chaotic system", Phys. Rev. Lett. 64 (1990) 821.

18. Rosenblum, M. G., Pikovsky, A. S. and Kurths, J., "Phase synchronization of chaotic oscillators", Phys. Rev. Lett. 76 (1996) 1805.

19. Rosenblum, M. G., Pikovsky, A. S. and Kurths, J., "From phase to lag synchronization in coupled chaotic oscillators", Phys. Rev. Lett. 78 (1997) 4193.

20. Peng, C. C. and Chen, C. L., "Robust chaotic control of Lorenz system by backstepping design", Chaos Solitons Fractals 37 (2008) 598.

21. Zhang, J., Li, C., Zhang, H. and Yu, J., "Chaos synchronization using single variable feedback based on backstepping method", Chaos Solitons Fractals 21 (2004) 1183.

22. Rulkov, N. F., Sushchik, M. M., Tsimring, L. S. and Abarbanel,H. D. I., "Generalized synchronization of chaos in directionally coupled chaotic systems", Phys. Rev. E 51 (1995) 980.

23. Ge, Z. M., Yang, C. H., "Pragmatical generalized synchronization of chaotic systems with uncertain parameters by adaptive control", Physica D: Nonlinear Phenomena 231 (2007) 87.

24. Yang, S. S., Duan, C. K., "Generalized synchronization in chaotic systems", Chaos, Solitons & Fractals 9 (1998) 1703.

25. Krawiecki, A., Sukiennicki, A., "Generalizations of the concept of marginal synchronization of chaos", Chaos, Solitons & Fractals 11 (2000) 1445.

26. Ge, Z. M., Yang, C. H., Chen, H. H., Lee, S. C., "Non-linear dynamics and chaos control of a physical pendulum with vibrating and rotation support", J Sound Vib 242 (2001) 247.

27. Chen, M. Y., Han, Z. Z., Shang, Y., "General synchronization of Genesio–Tesi system", Int J Bifurcat Chaos 14 (2004) 347.

28. Narimani, M. and Lam, H. K., "Relaxed LMI-Based stability conditions for Takagi–Sugeno fuzzy control systems using regional-membership-function -shape-dependent analysis approach", IEEE Trans. Fuzzy Syst. 17 (2009) 1221.

29. Du, H. and Zhang, N., "Fuzzy control for nonlinear uncertain electrohydraulic

active suspensions with Input constraint", IEEE Trans. Fuzzy Syst. 17 (2009) 343.

30. Yang, Y., "Direct robust adaptive fuzzy control (DRAFC) for uncertain nonlinear systems using small gain theorem", Fuzzy Sets and Syst. 151 (2005) 79.

31. Han, H. and Su, C. Y., "Robust fuzzy control of nonlinear systems using shape-adaptive radial basis functions", Fuzzy Sets and Syst. 125 (2002) 23.

32. Lian, K. Y., Tu, H. W. and Liou, J. J., "Stability conditions for LMI-Based fuzzy control from viewpoint of membership functions", IEEE Trans. Fuzzy Syst. 14 (2006) 874.

33. Tong ,S. C., Li, Q. and Chai, T., "Fuzzy adaptive control for a class of nonlinear systems", Fuzzy Sets and Systems 101 (1999) 31.

34. Chiu, C. S., "Mixed feedforward/feedback based adaptive fuzzy control for a class of MIMO nonlinear systems", IEEE Trans. Fuzzy Syst. 14 (2006) 716.

35. Gao, H. and Chen, T., "Stabilization of nonlinear systems under variable sampling: a fuzzy control approach", IEEE Trans. Fuzzy Syst. 15 (2007) 972.

36. Zadeh, L. A., "Fuzzy logic", IEEE Comput. 21 (1988) 83.

37. Takagi, T. and Sugeno, M., "Fuzzy identification of systems and its applications to modelling and control," IEEE Trans. Syst., Man., Cybern. 15 (1985) 116.

38. Luoh, L., "New stability analysis of T–S fuzzy system with robust approach", Math Comput Simul. 59 (2002) 335.

39. Wu, X. J., Zhu, X. J., Cao, G. Y. and Tu, H. Y., "Dynamic modeling of SOFC based on a T–S fuzzy model", Simul Model Prac Theory 16 (2008) 494.

40. Liu, X. and Zhong, S., "T–S fuzzy model-based impulsive control of chaotic systems with exponential decay rate", Phys Lett A 370 (2007) 260.

41. Kim, J. H., Park, C. W., Kim, E. and Park, M., "Adaptive synchronization of T–S fuzzy chaotic systems with unknown parameters", Chaos Solitons & Fractals 24 (2005) 1353.

42. Chiu, C. S. and Chiang, T. S., "Robust output regulation of T-S Fuzzy systems with multiple time-varying state and input delays", IEEE Trans. Fuzzy Syst. 17 (2009) 962.

43. Ge ,Z.M. and Ku ,F.N., 1997, "Stability, bifurcation and chaos of a pendulum on rotating arm", Jpn. J. Appl. Phys. 36 (1997) 7052.

44. Park, J.H., "Adaptive synchronization of hyperchaotic chen system with uncertain parameters", Chaos Solitons Fractals 26 (2005) 959.

45. Park, J.H., "Adaptive synchronization of rossler system with uncertain parameters", Chaos Solitons Fractals 25 (2005) 333.

46. Elabbasy, E.M., Agiza,H.N. and El-Desoky,M.M., "Adaptive synchronization of a hyperchaotic system with uncertain parameter", Chaos Solitons Fractals 30 (2006) 1133.

47. Wu, X., Guan, Z.H., Wu, Z. and Li, T., "Chaos synchronization between Chen system and Genesio system", Phys. Lett. A 364 (2007) 315.

48. Hu, M., Xu, Z., Zhang, R. and Hu, A., "Adaptive full state hybrid projective synchronization of chaotic systems with the same and different order", Phys. Lett. 365 (2007) 315

49. Khalil, H. K., *Nonlinear Systems*, 3rd edition, Prentice Hall, New Jersey, 2002.

50. Ge, Z. M. and Yang, C. H., "Symplectic synchronization of different chaotic systems", Chaos, Solitons & Fractals 40 (2009) 2532

51. Ge, Z. M. and Li, S. Y., "Fuzzy modeling and synchronization of chaotic two-cells quantum cellular neural networks nano system via a novel fuzzy model" accepted by Journal of Computational and Theoretical Nanoscience 2009.

52. Sprott, J. C., "Some simple chaotic flows", Phys. Rev. E 50 (1993) 647.

53. Ge, Z.M., Yao C.W. and Chen, H.K., "Stability on partial region in dynamics", Journal of Chinese Society of Mechanical Engineer 15 (1994) 140.

54. Ge, Z.M. and Chen, H.K., "Three asymptotical stability theorems on partial region with applications", Japanse Journal of Applied Physics 37 (1998) 2762.

55. Ge, Z.M., "Necessary and sufficient conditions for the stability of a sleeping top described by three forms of dynamic equations", Physical Review E 77 (2008) 046606.

56. Matsushima,Y., *Differentiable Manifolds*, Marcel Dekker, City, 1972

57. Ge ,Z.M., Yu, J.K. and Chen, Y.T., "Pragmatical asymptotical stability theorem with application to satellite system", Jpn. J. Appl. Phys. 38 (1999) 6178.

58. Ge, Z.M. and Yu, J.K., "Pragmatical asymptotical stability theorem partial region and for partial variable with applications to gyroscopic systems", the Chinese Journal of Mechanics 16 (2000) 179.

59. Jiang, G.P., Chen, G., Tang, W.K.S., "A new criterion for chaos synchronization using linear state feedback control", Int J Bifurcat Chaos 13 (2003) 2343.

60. Rafikov, M., Balthazar, J.M., "On a optimal control design for Rossler system",

Phys Rev Lett A 64 (1990) 821.